

CONTENTS

Magnox Graphite Core Decommissioning and Disposal Issues.....	1
<i>M.E. Pick</i>	
Graphite Waste Treatment and Disposal – A UK Perspective on the Current Opportunities and Issues	15
<i>J. McKinney, S. Barlow</i>	
Current Status and Future Objectives for Graphite and Radium-bearing Waste Disposal Studies in France	23
<i>O. Ozanam</i>	
Aspects of Graphite Disposal and the Relationship to Risk: A Socio-Technical Problem	27
<i>G.B. Neighbour, M.A. McGuire</i>	
Radiation Damage in Graphite — a New Model.....	39
<i>M.I. Heggie, I. Suarez-Martinez, G. Savini, G.L. Haffenden, J.M. Campanera</i>	
Thermodynamic Modelling of an Irradiated Reactor Graphite Thermochemical Treatment Process	47
<i>S.A. Dmitriev, O.K. Karlina, V.L. Klimov, G.Yu. Pavlova, M.I. Ojovan</i>	
Current Status of the Radiological Characterization of the Irradiated Graphite from RBMK-1500 Reactor in Lithuania	57
<i>V. Remeikis, D. Ancius, A. Plukis, R. Plukiene, D. Ridikas, A. Smaizys, E. Narkunas, P. Poskas</i>	
Decontamination of Nuclear Graphite by Thermal Methods	77
<i>J. Fachinger</i>	
GLEEP Graphite Core Removal and Disposal	83
<i>M. Grave</i>	
Review of the Characterization of Nuclear Graphites in UK Reactors Scheduled for Decommissioning.....	99
<i>A. Jones, L. McDermott, B. Marsden and T.J. Marrow</i>	
Graphite Dust Explosibility in Decommissioning: A Demonstration of Minimal Risk.....	109
<i>A. Wickham and L. Rahmani</i>	

Magnox graphite core decommissioning and disposal issues

M.E. Pick

Magnox South, Gloucester, United Kingdom

Abstract. Graphite core dismantling and disposal will be a key issue for the decommissioning of the United Kingdom (UK) Magnox reactors. The irradiated graphite arisings from the UK gas cooled reactor programme represent a significant proportion of the radioactive wastes currently destined for the UK geological repository. Data on the graphite and radionuclide inventory of the Magnox reactor graphite cores are presented together with data on the core designs. Magnox reactor cores represent a significant fraction of the worldwide irradiated graphite inventory and the paper recognizes that there may be alternatives to geological disposal. Sources and arisings of carbon-14, which is one of the major long lived radionuclides of concern, are discussed along with wider aspects of the arisings and behaviour of carbon-14 in the environment. Indubitably, core graphite disposal and the technical challenges it poses is one of the major issues to address in achieving final site clearance in a cost effective manner and reducing the liability cost associated with disposal of graphite.

1. Introduction

The major large volume irradiated materials at final dismantling of Magnox reactors are:

- Graphite
- Steels
- Concrete

Each has particular challenges; irradiated graphite represents one of the largest volumes of irradiated materials and poses particular technical challenges. It is also a material for which there are a range of possible treatment and disposal options.

The United Kingdom (UK) NDA (Nuclear Decommissioning Authority) Business Plan, 2008–2011, (Ref.[1]) states that “We believe that, due to the absence of a solution for the disposition of activated graphite, it is not yet possible to make a business case for accelerating Magnox decommissioning. Nevertheless, we will complete work on the business case in line with our Strategy for discussion with Government and, subject to availability of funding and viable waste disposal routes, will continue to explore the option of identifying a lead Magnox site to act as ‘test site’ for reactor decommissioning”. This statement reflects the fact that the NDA has expressed the aspirational goal to achieve site clearance in 25 years, i.e. one generation [2]. This will pose additional challenges through the reduction in the period of radioactive decay before dismantling takes place, which will result in wastes of higher unit activity being handled.

The current strategy for the core graphite at final site clearance is to remove the graphite blocks and place in baskets in 4 m stainless steel containers with the option of encapsulation in cement. This will of course result in an increase in the overall volume of waste. Current Lifecycle Baseline (LCBL) plans envisage that final site clearance involving dismantling of the core will not be until approximately 85 years after reactor shutdown.

2. Inventory

In total there are 26 Magnox reactors in the UK situated on 11 sites (Fig. 1). All of these are now shut down with the exception of Oldbury (due to close 2008) and Wylfa (due to close 2012). The size and mass of the graphite cores underwent a progressive increase from ~1100 t on the earliest reactor cores at Calder Hall and Chapelcross to 5500 t on Wylfa reactor cores. Arisings of core graphite from individual Magnox reactor cores are shown in Fig. 2.



FIG. 1. Magnox reactor sites in the UK.

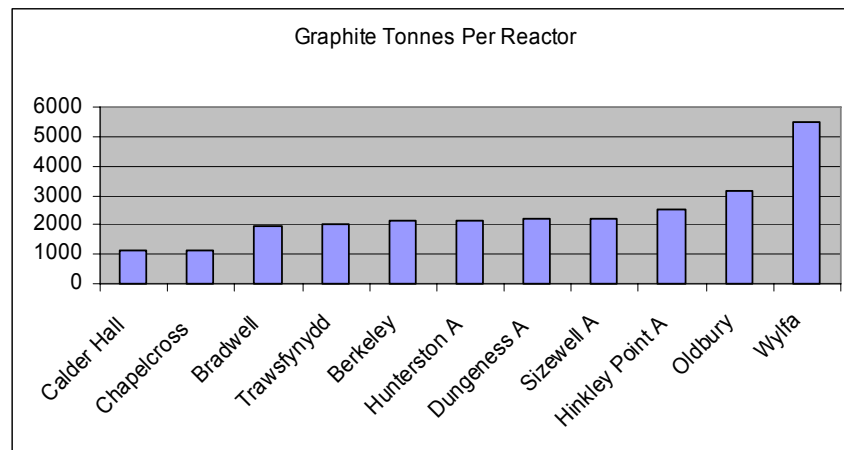


FIG. 2. Graphite core inventory of UK Magnox reactors.

The total arisings of Magnox reactor core graphite in the UK are of the order 45 600 m³, which equates to around 57 000 t using a bulk density of 1.25 t m⁻³. The core graphite arisings are given in the UK Radioactive Waste Inventory [3] which quotes the radionuclide inventory at 100 years after shutdown as this corresponds to the assumed dismantling date. In addition, there are about 2300 t of graphite fuel struts and sleeves which were employed on the Berkeley and Hunterston A reactors; these arisings are stored in vaults on these sites.

The core graphite is a mixture of Intermediate Level Waste (ILW) and Low Level Waste (LLW) depending on the core region from which it arose and the neutron flux it has been exposed to. The Magnox core graphite may be divided into the following components:

Moderator	- Typically ILW
Side Reflector	- LLW/ILW
Bottom Reflector	- Typically LLW
Top Reflector	- LLW/ILW

The Magnox core graphite was termed Pile Grade and was manufactured from petroleum coke by a synthetic route. Pile Grade A (PGA) graphite with a density of 1.70 g cm^{-3} was used for the moderator cores while Pile Grade B (PGB) graphite with a density of 1.64 g cm^{-3} was used for the reflectors. The graphite produced for the AGRs (Advanced Gas Cooled Reactors) in the UK was a higher density gilsocarbon with a density of 1.85 g cm^{-3} and used naturally occurring graphite as the filler source material and petroleum coke as the binder.

3. Radioactive inventory

In the context of disposal, the major radionuclides of concern due to their long half-life are carbon-14 and chlorine-36. At shutdown of the reactors tritium is the predominant radionuclide in terms of Bq of radioactivity, but as this decays with a 12.3 year half-life after 30 years post-shutdown, carbon-14, which has a half-life of 5730 years, becomes the predominant radionuclide in terms of radioactivity. With respect to radiation dose cobalt-60, which has a half-life of 5.27 years, is the dominant contributor at shutdown and remains a major contributor for about 60 years after which the dose rates stabilize at a level about four orders of magnitude less than those at shutdown. Typical dose rates from the bulk graphite are 10 mSv h^{-1} at shutdown, falling to 1 mSv h^{-1} after 20 years, 0.1 mSv h^{-1} after 40 years and 0.001 mSv^{-1} after 80 years. The reduction in dose rate is mainly a consequence of cobalt-60 decay. The UK Radioactive Waste Inventory [3] shows an overall average total of carbon-14 in the Magnox core graphite of about 3200 TBq.

Carbon-14

Carbon-14 is produced in gas-cooled reactors by neutron activation. The relevant reactions are:

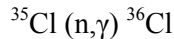
- (a) $^{13}\text{C} (n,\gamma) ^{14}\text{C}$
- (b) $^{14}\text{N} (n,p) ^{14}\text{C}$
- (c) $^{17}\text{O} (n,\alpha) ^{14}\text{C}$

Carbon-13 is a naturally occurring isotope (1.11%) of carbon. Nitrogen-14 is the predominant isotope of nitrogen (99.63%) and occurs as an impurity in graphite at ppm levels; however, the neutron activation cross-section is relatively large so this route is a significant source of carbon-14 in graphite. Carbon-14 is also produced in the carbon dioxide coolant and an additional source here is activation of the naturally occurring oxygen-17 isotope which constitutes 0.037% of naturally occurring oxygen.

A major issue in assessing the carbon-14 inventory of graphite is the level of nitrogen in the graphite. The first reported specification for graphite for the UK nuclear industry is in a report by Rose and Shaw [4] dating from 1956. This report listed desired physical and mechanical properties along with chemical composition. The graphite was analysed for 44 elements in order that their effect on the neutron capture cross-section could be assessed. From this a subset of 17 elements was specified. The report makes no reference to nitrogen impurities which are an important factor in determining the carbon-14 arisings in irradiated graphite. Neither is there any specific reference to activation products and subsequent radiation dose arising from the graphite. There are limits quoted for iron (20 ppm) and nickel (4 ppm) and it would be expected that nickel levels would be an indicator of cobalt levels. The chlorine level was set at 2 ppm. In the most recent UK Radioactive Waste Inventory [3], a nitrogen impurity level of 25 ppm has been assumed.

Chlorine-36

Chlorine-36 is formed from the activation of chlorine-35 (75.5% of chlorine) and has a long half-life of 300 000 years.



The chlorine arises from residual chlorine used to purify graphite. There has been a substantial number of measurements carried out to determine the chlorine levels including work commissioned by the UK NDA Radioactive Waste Management Directorate (RWMD ex-Nirex) which has been reported by Brown et al. [5]. However, it is known that chlorine-36 is transported around the circuit; hence, the original chlorine level may not accurately reflect the actual chlorine-36 level in the core graphite.

3.2. Tritium

Tritium is produced in nuclear reactors by neutron activation of ^2H , ^3He , ^6Li and ^{10}B and also by ternary fission. The primary source of tritium in Magnox reactor graphite is considered to be from lithium-6 which is present at 7.5% in natural lithium.

- (a) $^2\text{H} (n,\gamma) ^3\text{H}$
- (b) $^3\text{He} (n,p) ^3\text{H}$
- (c) $^6\text{Li} (n,\alpha) ^3\text{H}$
- (d) $^{10}\text{B} (n,2\alpha) ^3\text{H}$

4. Core design

The graphite cores were constructed from machined blocks and the core was assembled in situ. Moderator blocks are assembled to leave a small clearance between the blocks. The core is keyed together to produce a structure (see Fig. 3) which allows for some movement in the event of a seismic event. The moderator blocks have, of course, holes passing through them that form the fuel channels. The outer reflector blocks do not have channels and there are no clearances between the blocks. The Magnox core designs underwent progressive development and changes in the brick location and peripheral restraint arrangement. The basic designs are listed in Table 1. Early station cores were built from bricks and tiles with abutting tiles maintaining geometric stability. The earlier Magnox cores also contain zirconium pins for brick location; this approach was replaced by radial graphite keys in later designs. Core restraint arrangements vary. Early reactors and also the last reactor Wylfa have thermally compensated steel restraint hoops which surround the core at every brick level. In the case of Dungeness, Sizewell and Oldbury, the core expands as steel via the steel restraint cage. The outer ring of bricks is tied into the restraint cage by puller rods. Figure 4 shows the Oldbury reactor core under construction, with the interlocking brick and key arrangement and the side restraint system clearly visible.

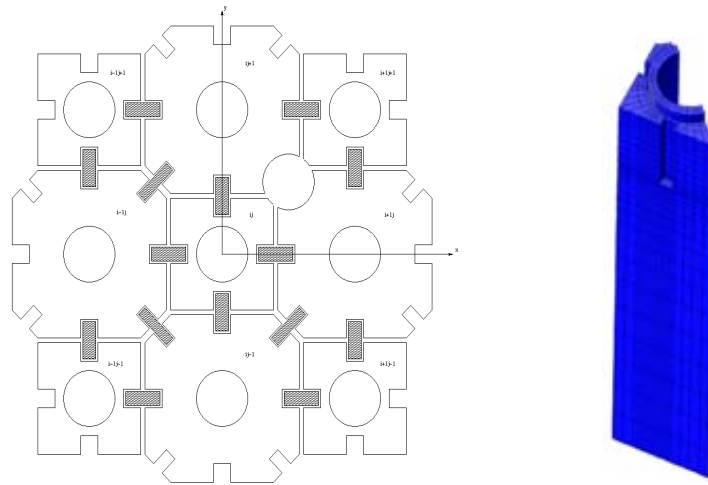


FIG. 3. Design of Magnox reactor graphite core.

Table 1. Magnox reactor graphite core constructions

Station	Graphite Core Peripheral Restraint	Thermal Movement of Peripheral Bricks	Graphite Brick Location	Charge Pans
Berkeley	Temperature Compensated Tie Bars	As graphite	Butting Tiles with Zirconium Pins	Supported on graphite
Bradwell	Temperature Compensated Tie Bars with outer cage	As graphite	Butting Tiles with Zirconium Pins	Supported on graphite
Hinkley Point A	Temperature Compensated Tie Bars with dowed reflector	As graphite	Butting Tiles with Zirconium Pins	Supported on graphite
Trawsfynydd	Temperature Compensated Tie Bars with outer cage	As graphite	Radially Keyed Tiles with cruciform keys	Supported on graphite
Dungeness A	Steel cage with puller rod attachment to peripheral bricks	As steel	Radial Keys	Supported on control rod guide tube
Sizewell A	Steel rings dowed to graphite and radially keyed to a restraint tank wall	As steel	Radial Keys	Suspended from standpipes as composite control/charge facility
Oldbury	Steel rings hung from boiler shield wall with puller rods attached to peripheral bricks	As steel	Radial Keys	Suspended from control rod guide tubes
Wylfa	Temperature Compensated Tie Bars	As graphite	Radial Keys	Suspended from standpipes as composite control/charge facility

View onto the Oldbury graphite core during construction, showing moderator bricks and side restraint system

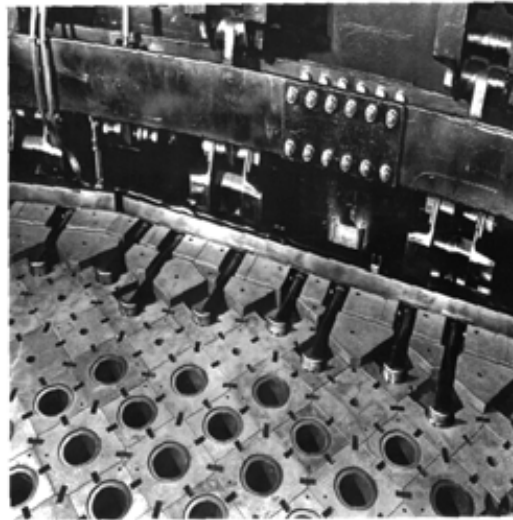


FIG. 4. Oldbury graphite core restraint system.

Typically, the graphite cores had the following main design and duty features:

- 24 sided polygons
- Typically 10 m high and 10–20 m diameter
- Channels ~100 mm diameter spaced by ~200 mm
- 1700–6200 fuel channels per reactor
- Gas pressure ranges from 100 psi to 400 psi
- Inlet gas temperatures 160–250°C
- Outlet gas temperature 345–370°C

The reactors were re-fuelled on load from above the pile cap via a charge machine with the exception of Hunterston A uniquely which was fuelled from underneath the core.

5. Dismantling

Removal of the graphite from the core will be a key issue in any dismantling work carried out to effect final site clearance. A report [6] on efficient methods for removal of the typically 30 000 separate graphite blocks was presented at the 1999 IAEA meeting on Nuclear Graphite Waste Management. Not surprisingly, this showed that the dismantling time was decreased if more blocks could be removed in a single lift. Various techniques for gripping graphite blocks for removal have been investigated (see [7]). These have included:

- Inside gripping
- Inside screw threading
- Inside grooving
- Rubber expanding
- External gripping

More rapid techniques may also need to be considered. It might be worth considering approaching mining and bulk handling companies to provide input on innovative methods of removal of the graphite from the core in effect looking at this exercise more as a mining exercise rather than a careful and time consuming reversal of construction. Rapid dismantling techniques might save time and radiation dose. Underwater dismantling of reactors to provide shielding has been discussed as an option. The effect of any such activity on graphite would need to be considered.

Proposals to investigate graphite cutting techniques have been reported by Holland et. al. [8] at the 1999 IAEA meeting. The aim of the project was to find the most suitable cutting technique for graphite blocks with a minimum waste production rate. The following techniques were proposed for evaluation.

- Thermal cutting
- Water jet cutting
- Mechanical cutting with a saw
- Plasma arc cutting
- Drilling

6. Disposal

The current UK RWMD position is that irradiated graphite is destined for the deep geological repository largely on account of the long lived carbon-14 and chlorine-36 content. It will be disposed of in 4 m length stainless steel RWMD approved boxes and encapsulated. The geological repository post-closure safety case relating to radionuclide release and transport assumes no benefit from the waste container. Consideration ought to be given to use of larger capacity multi-trip reusable transport containers. This would need to be accompanied by investigations of loading and unloading of such containers. The 55 000 t of Magnox graphite equates to about 100 000 m³ of packaged material and a significant overall disposal cost.

The RWMD position (e.g. see [9]) is based around the presence of long lived radionuclides in graphite. The RWMD (Nirex) Report N/122 on the Viability of a Phased Geological Repository develops the overall strategy and summarises safety and risk considerations for the repository [10]. The N/122 report talks in terms of a target radiological risk for the repository of less than 10⁻⁶ per year. The report accepts that natural background radiation gives a risk of 10⁻³–10⁻⁴ on the same basis.

Alternative techniques which might be considered for Magnox core graphite disposal are:

- Containerisation and encapsulation with geological disposal (Base Option).
- Volume reduce by incineration with or without abatement and/or isotope separation.
- Volume reduce by gasification including a steam reformation process — this may be a better option for removing chlorine-36 and tritium and provides a gaseous effluent reaction product (carbon monoxide) suitable for isotope separation.
- Carbon dioxide sequestration.
- Carbon-12/carbon-14 separation.
 - Incineration — carbon-14 separation by pressure swing adsorption of carbon monoxide.
 - Other separation techniques.
- Shallow land burial — however, there is no disposal site currently identified in the UK.
- A combination of volume reduction and shallow land burial: this involves partial treatment to remove chlorine-36, tritium and some carbon-14 followed by shallow land burial of the residual graphite.

7. Graphite in the natural environment

Graphite is a naturally occurring material with deposits in many countries including the UK; it used to be mined in the Lake District in the UK. This graphite has been formed a long time ago (like coal deposits) and there is no evidence to show that it has undergone isotopic exchange with carbon in the biosphere. This would be revealed by incorporation of carbon-14 into the graphite. This supports the view that naturally occurring graphite is very stable and has been around for many millions of years.

The naturally occurring material is a different crystalline form to the synthetic material and whether this was of significance in comparing its behaviour with reactor graphite would need to be considered.

Graphite is known to be a relatively stable material. It has no measurable solubility. It might be expected that bulk reactor graphite would be unlikely to undergo any appreciable exchange of carbon atoms with the surrounding biosphere.

Disposing of graphite in stainless steel containers may be wrong technically based on the relative position of these materials in the galvanic series (see Fig. 5). Graphite is a noble material like platinum. Stainless steel is more anodic than graphite, i.e. if coupled together then from an electrochemical potential and thermodynamic standpoint ($\Delta G = -nFE$) steel will tend to go from Fe to Fe^{2+} (i.e. corrode or rust), whilst graphite will remain as a graphite. Figure 5 is specifically for sea water and the position of some elements may change slightly in different environments but the relative positions of graphite and stainless steel remain the same. Containers fabricated from plastic, e.g. high density polyethylene, galvanised steel or cement may be more appropriate and adequate. Like platinum, graphite is used as an inert electrode in electrochemical and metal refining processes.

As another example of its stability, graphite is very difficult to combust requiring a forced oxidation process. Also when ground into graphite dust it does not represent an explosion hazard [11] unlike many other commonly occurring fine particulate materials such as coal dust and flour.

Other sources of organics present in the biosphere, e.g. trees, are also surprisingly stable — like sub-surface deposits of graphite. Bristlecone pines from the California/Nevada border which are ~5000 years old are used for calibrating the carbon-14 content of the atmosphere via tree-ring counting (science of dendrochronology). This relies on carbon-14 not exchanging from the rings. Interestingly, the carbon-14 concentration of the atmosphere has varied slightly (few %) over time, hence the requirement for calibrations of the concentration from determination of the carbon-14/carbon-12 ratio in tree rings of known age.

An important question regarding irradiated graphite disposal is whether the graphite will be stable with negligible degradation or isotopic exchange with the surrounding environment. The evidence with naturally occurring graphite suggests that it would be stable although obviously the consequences of release of any radioactivity in particular carbon-14 would need to be assessed. The following section looks at this issue.

8. Carbon-14 in the environment

The annual production rate of carbon-14 from cosmic rays is about 1000 TBq and there is of the order of 140 000 TBq in the atmosphere and 10 million TBq in the deep oceans. This helps to put the carbon-14 arisings from the nuclear industry in perspective.

There are more recent acute big variations in atmospheric carbon-14 concentrations as a result of atmospheric bomb tests (doubled the concentrations) and consumption of fossil fuels (now acting to slowly reduce C-14 concentrations in terms of specific activity, i.e. carbon-14 per gram of carbon).

Typical annual airborne radioactive discharges of carbon-14 from Magnox plant are shown in Fig. 6 using data presented in the BNFL Annual Report on Monitoring our Environment [12]. The total discharges of carbon-14 from the operating Magnox stations range from 1.1 TBq for Sizewell A to 3.1 TBq for Dungeness A. The total discharges from Magnox stations have fallen from 12 TBq to 8 TBq from 1999 to 2004. During this period, of course, a number of stations have closed. It is apparent from Fig. 6 that discharges from the decommissioned sites are very low, <0.1% of the level on generating sites.

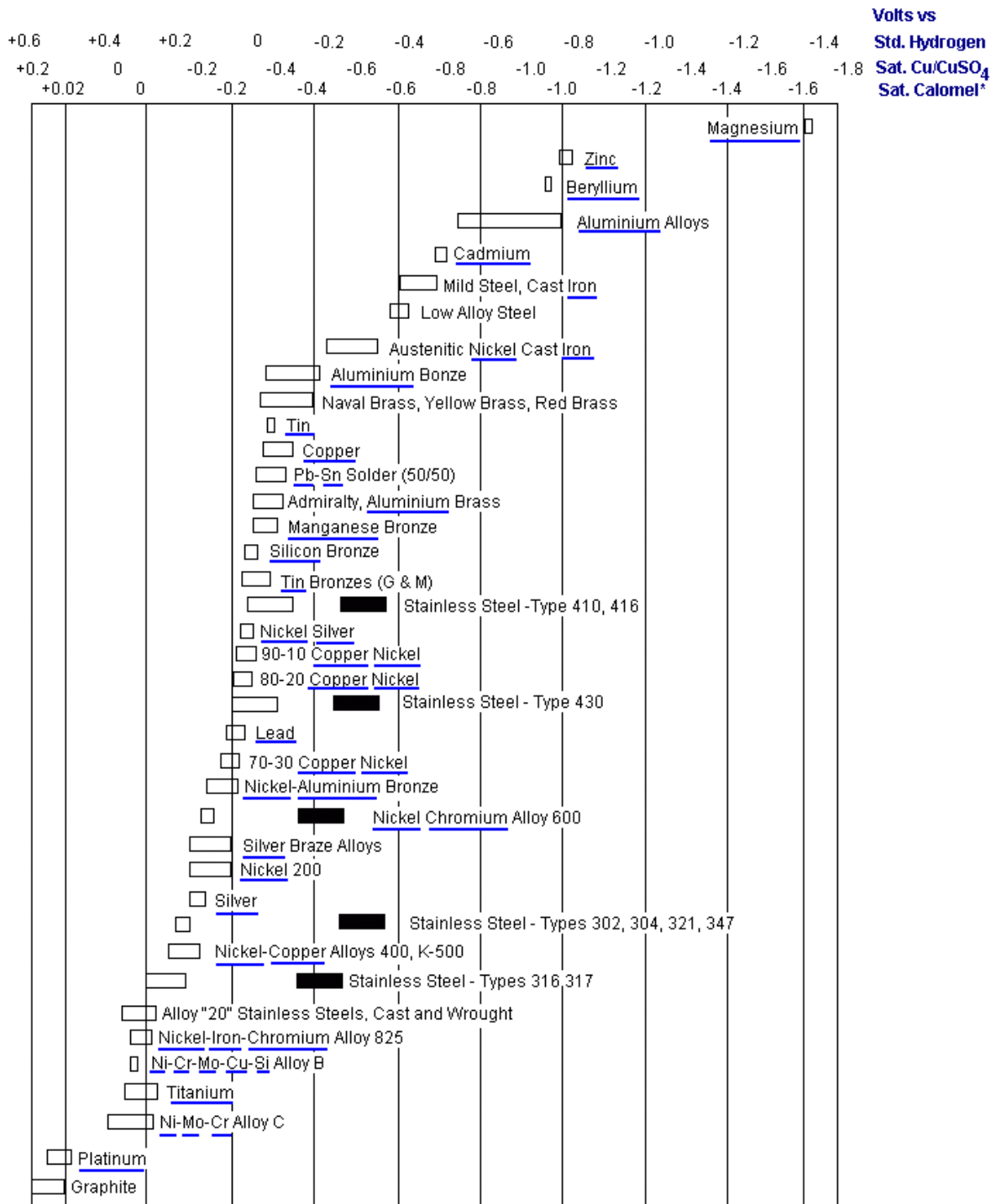


FIG. 5. Galvanic series in sea water.

A report by Briggs and Hart [13] looked at the collective dose from airborne and liquid discharges of carbon-14 and various disposal scenarios. Doses are compiled for the UK, the Rest of Europe and the Rest of the World with various populations assumed. For a global population of 10 billion (10^{10}), noting that it is at present about 6.5 billion and not due to reach 9 billion until 2050, the total dose over infinite time is about 100 man Sv per TBq of carbon-14 released to the environment directly or via graphite disposed of via shallow land burial with the models used. Expressed in terms of dose per Bq, carbon-14 thus gives rise to 100×10^{-12} man Sv = 1×10^{-10} man Sv per Bq of activity released to

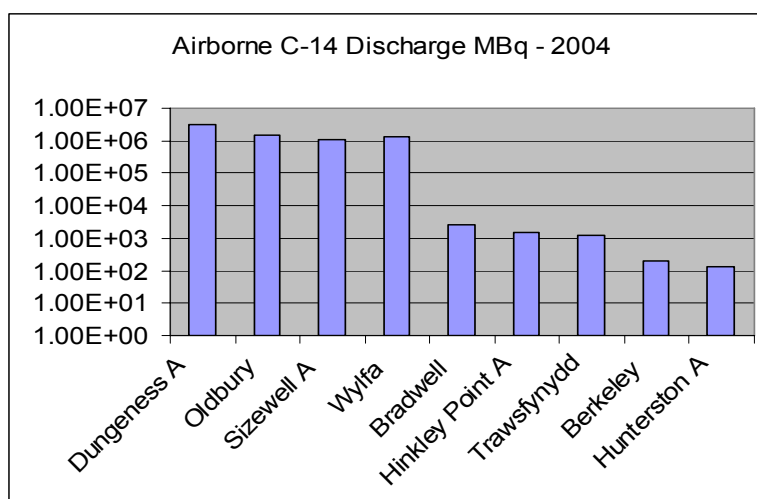


FIG. 6. C-14 airborne discharges.

the environment. For the purposes of infinite time this effectively covers about 50 000 years or ten half-lives for carbon-14.

Releases of naturally occurring carbon-14 occur by the burning of biomass, wood, etc. In marked contrast fossil fuel (i.e. coal, oil and gas) combustion to carbon dioxide will lower the specific activity of carbon-14 in the biosphere as the fossil fuels which typically were formed millions of years ago will be carbon-14 free. Hence, the effect of combustion of fossil fuels will be to dilute the carbon-14 in the atmosphere and immediate biosphere compared with the situation if no fossil fuels were combusted thus lowering the specific activity of carbon-14 (i.e. Bq per gram of carbon). This leads to lower concentrations of carbon-14 in plants and organisms than would otherwise be the case and hence lower radiation doses. In the case of a soft beta-emitter such as carbon-14, these are almost entirely internal doses arising from incorporation of carbon in body tissues.

It is interesting to note the potential effect of Carbon Capture and Storage (CCS) on carbon-14 collective doses as reported in Ref. [14]. CCS is increasingly being promoted as an answer to climate change and global warming by allowing the burning of fossil fuels without increasing the amount of carbon dioxide in the atmosphere. The adoption of CCS on a large scale will reverse the trend to lower the specific activity of carbon-14 and will lead to an overall increase in collective radiation doses. It might be argued of course that this is of minor consequence in the context of climate change and existing doses from naturally occurring radioactive materials. The adoption of nuclear power can, of course, make a significant impact on global warming by the reduction in fossil fuel usage, but any small increment it has on radiation dose attracts great attention. We need to have a level playing field in comparing the benefits and risks from adoption of various energy production schemes and in this context the effect of CCS on radiation dose ought to be examined.

Potential radiation doses from carbon-14 arising from the nuclear industry should be seen in the context of doses arising from naturally occurring carbon-14 and also other NORM (Naturally Occurring Radioactive Material) such as potassium-40 (0.012% naturally arising). NORM potassium-40 gives about 230 000 dpm (disintegrations per minute) to a 70 kg individual and potassium-40 is responsible for a radiation dose of around 300 μ Sv per annum (made up of 200 μ Sv from internal dose from potassium-40 within the body and 100 μ Sv from external potassium-40 gamma). Naturally occurring carbon-14 gives rise to similar dpm in the body.

9. Other radionuclides

There may be a potential issue with chlorine-36 in graphite because of its long half-life (300 000 years). However, the chlorine-36 is only ~10 TBq in total for Magnox graphite based on UK Radioactive Waste Inventory data. It is probable that chlorine-36 would almost certainly be transported from graphite as chloride and it is unlikely that this would give an appreciable dose to anyone given the likely isotopic dilution with natural chloride. The biological half-life of chloride is ten days which is similar to that for tritium and also carbon-14 although for the latter a range is often quoted from minutes to tens of days depending on the compound.

10. Key issues

The disposal of UK irradiated graphite in the proposed deep geological repository will take up ~30% of the volume and incur a significant cost. Alternative options may be cheaper and available sooner. There may be options for disposal of graphite in existing near surface facilities. In addition, there may be an option of incinerating the graphite and separating the carbon-14 component as a small volume for disposal. Alternative options could reduce the liability cost of graphite disposal and also facilitate Early Final Site Clearance (EFSC) where graphite core dismantling would be one of the first steps (Fig. 7). The cautious and conservative approach taken to date to the disposal of irradiated graphite, whilst appropriate with the information available at the time, should be re-examined.

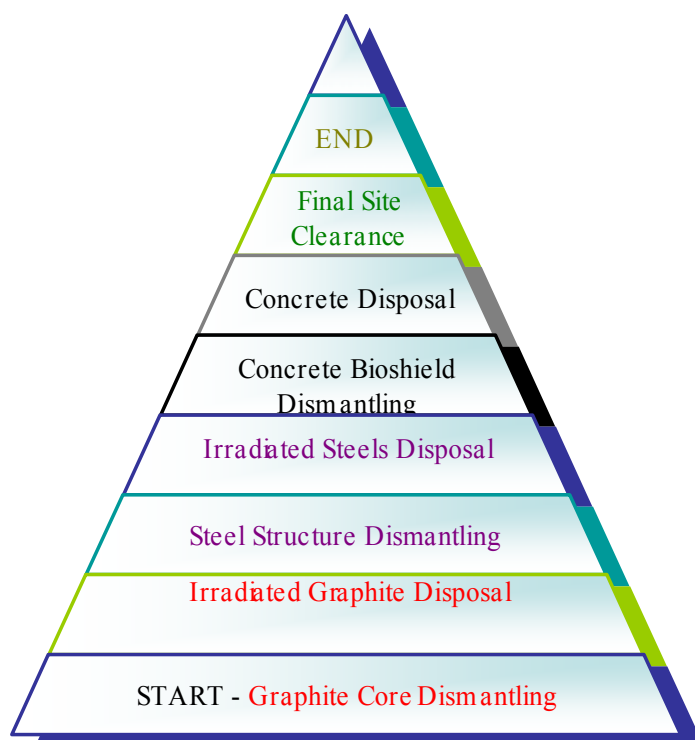


FIG. 7. Major steps in final site clearance.

However, more data and development of a safety case are required to support an alternative option (e.g. Fig. 8). There are uncertainties on the radionuclide inventory of the graphite for key radionuclides such as carbon-14 and tritium and there is little information available on the long term behaviour of irradiated graphite in the environment. In particular, there is little data available on the leaching characteristics.

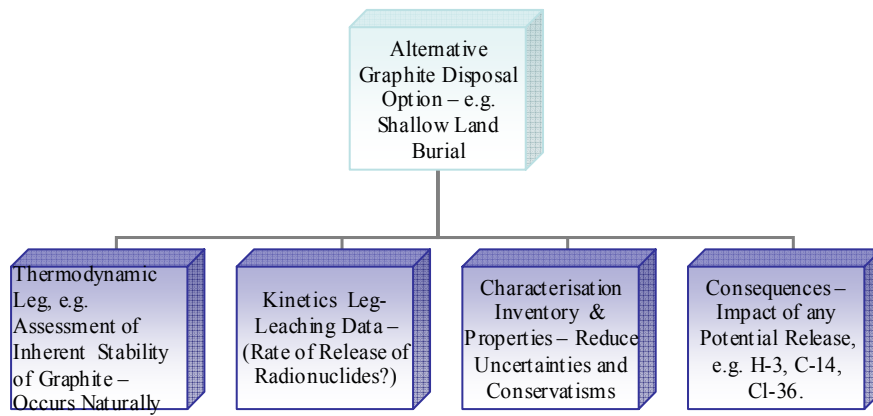


FIG. 8. Typical safety case legs to support an alternative graphite disposal option — Shallow Land Burial.

In summary, Magnox reactor graphite disposal is a major issue.

Key issues are:

- Radionuclide inventory and behaviour
- Graphite handling and core removal techniques
- Graphite disposal techniques
- Carbon-14/carbon-12 separation techniques
- Graphite leaching behaviour
- Collective and critical group dose issues for disposal scenarios

REFERENCES

- [1] NDA Business Plan, 2008/2011, March 2008.
- [2] NDA, Nuclear Decommissioning Agency Strategy — draft for consultation, 11 August 2005.
- [3] The 2007 UK Radioactive Waste Inventory — Main Report, Defra/RAS/08.002, NDA/RWMD/004 (2008).
- [4] ROSE, G., SHAW, R.A., The Provisional Specification of Grade A Quality Graphite, UKAEA Report, No. IGR-TM/C.068 (1956).
- [5] BROWN, F.J., PALMER, J.D., WOOD, P., Derivation of a Radionuclide Inventory for Irradiated Graphite-Chlorine-36 Inventory Determination, Paper Presented at IAEA Technical Committee Meeting on Nuclear Graphite Waste Management held in Manchester, 18–20 October 1999.
- [6] FUJII, S., SHIRAKAWA, M., MURAKAMI, T., Study on Efficient Methods for Removal and Treatment of Graphite Blocks in a Gas Cooled Reactor, Paper Presented at IAEA Technical Committee Meeting on Nuclear Graphite Waste Management held in Manchester, 18–20 October 1999.
- [7] ISHIKURA, T., FUJII, S., Graphite Handling and Waste Treatment for GCR Decommissioning, EPRI International Decommissioning and Radioactive Waste Workshop, 26–28 October 2004, Lyon, France.
- [8] HOLLAND, D., QUADE, U., BACH, F.W., WILK, P., A German Research Project About Applicable Graphite Cutting Techniques, Paper Presented at IAEA Technical Committee Meeting on Nuclear Graphite Waste Management held in Manchester, 18–20 October 1999.
- [9] GUPPY, R., Long-Term Management of Graphite Arising from the Nuclear Industry, *The Nuclear Engineer* **45** 4 (2004) 121–127.
- [10] NDA RWMD (Nirex), The Viability of a Phased Geological Repository Concept for the Long-Term Management of the UK's Radioactive Waste, Nirex Report, No. N/122, November 2005.
- [11] Graphite Dust Deflagration: A Review of International Data with Particular Reference to the Decommissioning of Graphite Moderated Reactors. EPRI, Palo Alto, CA:2007. 1014797.
- [12] BNFL, Monitoring our Environment, Discharges and Monitoring of the Environment in the UK, Annual Report 2004.
- [13] BRIGGS, A., HART, D., The Management of Carbon-14 and Iodine-129 Wastes — A Site Specific Survey of Current and Future Arisings, Possible Management Options and Potential Impact with Respect to the United Kingdom, DOE Report No. DOE/RW/89.031, June 1988.
- [14] PICK, M.E., Carbon Capture and Storage (CCS) — Collective Radiation Effects, Letter Published in *Chemistry World*, January 2008.

Graphite waste treatment and disposal

— A UK perspective on the current opportunities and issues

J. McKinney, S. Barlow

Radioactive Waste Management Directorate, UK Nuclear Decommissioning Authority,
Didcot, United Kingdom

Abstract. Within the United Kingdom there are large quantities of irradiated graphite present in Advanced Gas-Cooled (AGR), Magnox and test/prototype reactors. There are approximately 56 000 t of graphite on Magnox sites alone with a total UK inventory of some 81 000 t — equivalent to a raw volume of 65 000 m³. As reactors enter decommissioning phases, it is essential that there is a forward strategy in place that defines the end points for the graphite waste streams. The present baseline option is to treat all graphite as ILW and dispose in a geological repository. The purpose of this paper is to present possible treatment, storage and disposal options for Nuclear Decommissioning Authority owned graphite, in particular bulk reactor graphite, that have been identified for further evaluation.

1. Background

Within the United Kingdom (UK) there are large quantities of irradiated graphite present in Advanced Gas-Cooled (AGR), Magnox and test/prototype reactors. There are approximately 56 000 t of graphite on Magnox sites alone with a total UK inventory of some 81 000 t — equivalent to a raw volume of 65 000 m³.

As reactors enter decommissioning phases it is essential that there is a forward strategy in place that defines the end points for the graphite waste streams. The present baseline option is to treat all graphite as ILW and dispose in a geological repository. Irradiated graphite contains a number of active species including ³H, ¹⁴C, ³⁶Cl, ⁵⁵Fe, ⁶⁰Co and ⁶³Ni. Also, a proportion of the graphite waste will be contaminated with fission products and actinides as a consequence of fuel element failures. The long lived radionuclides ¹⁴C and ³⁶Cl will be particularly significant for the repository safety case. Furthermore, the short half-life radionuclide ³H (12.3 years) and irradiated steel components such as pins, seals and wires which can also be associated with graphite will be significant for packaging, transport and storage safety cases.

The majority of the graphite will arise as a result of reactor decommissioning at Nuclear Decommissioning Authority (NDA) and British Energy sites, although graphite wastes also arise on sites in the form of operational wastes. Graphite operational wastes are usually in the form of intact or fragmented reactor sleeves, struts, dowels or bolts and have been stored in a number of facilities, e.g. solid waste vaults or silos. Operational graphite wastes may also be associated with irradiated steel items. It should be noted that certain sites have specific graphite waste management concerns. For example, with Windscale pile graphite there are concerns over possible Wigner energy release during waste conditioning and storage. This particular issue is being dealt with at the site level, although local conditioning and packaging solutions must be considered as part of the overall national strategy.

It should also be noted that Low Level Waste (LLW) graphite arising under the current baseline will in all probability need to be treated as Intermediate Level Waste (ILW) as the inventory of long lived radionuclides ¹⁴C and ³⁶Cl would be such as to exceed authorization limits for disposal at the LLW repository near Drigg in Cumbria. Key data on the characteristics of UK graphite are summarized in Tables 1–3.

Table 1. Volume and mass of graphite reported in the 2004 UK radioactive waste inventory

Graphite characteristic	LLW	ILW	Total
<i>Mass</i>			
core graphite ^a (t)	32 000	49 000	81 000
other graphite ^b (t)	32 000	29 000	61 000
<i>As-raw waste volume</i>			
core graphite (m ³)	26 000	39 000	65 000
other graphite (m ³)	25 000	25 000	50 000
<i>Packaged volum^c</i>			
core graphite (m ³)	36 000	91 000	127 000
other graphite (m ³)	28 000	38 000	66 000
All wastes total volume ^d (4) — as raw waste (m ³)	2 055 000	217 000	
All wastes total volume — packaged (m ³)	2 500 000	349 000	

^a Core graphite is waste that contains solely graphite and arises from final stage decommissioning.

^b Other graphite is waste that contains a mixture of materials including graphite.

^c Packaged volume is the volume when conditioned and packaged.

The 2004 Inventory assumes as its reference that these wastes will be packaged for geological disposal.

^d Total volume is the volume of all wastes as reported in the 2004 Inventory.

Table 2. Key radionuclide data for graphite waste

Inventory ^a (TBq)	Core graphite	Other graphite
chlorine-36	2.31E+01	5.52E-01
carbon-14 (2004 Inventory)	1.27E+03	7.65E+02
carbon-14 (revised estimate) ^b (2)	6.07E+03	2.33E+02
cobalt-60	2.97E-01	1.36E+06
Tritium	3.82E+01	2.47E+05

^a All activities are undecayed activities reported in the 2004 Inventory for stocks and future arisings, with the exception of C-14 (revised estimate).

^b Carbon-14 (revised estimate) is the current best estimate from Nirex.

Table 3. Decay of short lived activity in graphite

Short lived inventory in graphite	2004	2050	2100
cobalt-60 (TBq)	2.83E+05	6.68E+02	9.30E-01
tritium (TBq)	1.24E+03	9.28E+01	5.54E+00

* Activities are for graphite wastes recorded as 'in stock' as of 1 April 2004.

Data presented in Tables 1, 2 and 3 are taken from the 2004 UK Radioactive Waste Inventory which is updated on a three-yearly cycle. The last published update [1] reported data on waste in store on 1st April 2004, together with data for waste predicted to arise in the future.

It should be noted that the science underpinning the estimate of ^{36}Cl was examined in detail by a research programme commissioned by Nirex in 1993, and reported in a suite of reports that were published in 1997 [2]. These reports are available on a CDROM *Reporting of the Chlorine-36 Story* available from the NDA.

It should also be noted that Table 2 provides two entries against the inventory for ^{14}C . The reported radionuclide activity of ^{14}C has varied significantly throughout the updates of the inventory due to changes in data gathering processes and the attributed levels of uncertainty. The inventory of ^{14}C in graphite is primarily determined by the concentration of nitrogen in the graphite during manufacture. Various workers have postulated values in the range of 10–25 ppm. It is now thought that a concentration of 25 ppm should be assumed in ^{14}C inventory estimates for the graphite types utilised in UK. The revised estimate of $6.07\text{E}+3$ TBq in core graphite takes into account further work undertaken by Nirex subsequent to the issue of the 2004 Inventory and is derived on the assumption of 25 ppm nitrogen.

Given the significant issues being raised in connection with graphite management, a workshop on Reactor Decommissioning Wastes was held by NDA on the 2nd and 3rd May 2006. The workshop was well attended from industry and regulator representatives, including EA, SEPA, NII, EdF, Paul Scherrer Institute, British Energy, UKAEA, BNG Magnox, Nirex, Nexia and Bradtec. The main objectives of the meeting were as follows:

- (i) To develop a common industry-wide understanding of the issues surrounding reactor decommissioning wastes;
- (ii) To have a good understanding of the impact of accelerated reactor decommissioning on waste management and disposal;
- (iii) To seek the initial views of regulators for a range of treatment, storage and disposal options;
- (iv) To agree on technical issues that require further underpinning;
- (v) To agree on major work demands and opportunities for the industry.

The prime, but not exclusive, focus of the workshop was on graphite wastes. The workshop was successful in gaining an industry-wide view of the graphite issue and identified a broad range of ideas that could be considered further. Magnox, with Hyder Consulting and Bradtec, is now assessing each of the possible treatment, reuse and disposal options identified.

2. Strategic options

A number of high level strategic options have been identified and are proposed to cover all treatment, reuse and disposal options considered at the Reactor Decommissioning Wastes workshop. These strategic options are being considered as part of the forward programme:

- Option 1: To treat all graphite waste as ILW and ensure the national repository caters for the large volumes of material. **This is the baseline option.**
- Option 2: To condition graphite wastes to remove the long lived radioisotopes and dispose of the residual graphite at LLWR at Drigg or alternative LLWR.
- Option 3: To condition LLW and/or ILW graphite wastes to remove most of the contamination, for free release or reuse of the graphite where possible.
- Option 4: To dispose of graphite wastes in a separate repository (or repositories), including a shallow disposal option.
- Option 5: To use interim storage of ILW graphite wastes and waste conditioning for either LLW disposal or free release.

In the next few years, the NDA would like to declare a preferred graphite waste treatment and disposal strategy, as any of the above alternative options will have a direct impact on its approach to designing and implementing a repository.

Option 1

Within this option all reactor graphite, both ILW and LLW, is conditioned and packaged for disposal to a national geological repository. This would require packaging and disposal of some 65 000 m³ of core graphite in the raw waste form, which following packaging might be expected to increase in volume to some 127 000 m³. These are significant volumes and due to the sophisticated nature of the geological disposal packaging system, the cost of geological disposal for these wastes may be significant. Other graphite only waste streams could be considered if easily segregated and relatively free from contamination.

Published assessments of the performance of a geological repository for the predicted arisings of ILW, including ILW final stage decommissioning graphite [3], show that key radionuclides are ³⁶Cl and ¹⁴C. ³⁶Cl is a particular problem due to its long half-life and mobility within the repository system. Modelling predicts that the risk from ³⁶Cl will peak at about 40 000 years post-closure. ¹⁴C is a potential problem due to its predominance within graphite and its potential ability to return to the biosphere by the gas-pathway. If ¹⁴C labelled gases are in the form of CO₂, there is confidence that these will be trapped in the near field through carbonation reaction; however, if present in the form of methane, these small molecules will potentially be mobile and cause post-closure risk targets for the gas-pathway to be exceeded. Work to investigate this further and to determine whether ¹⁴C would remain in the gas phase or be absorbed into groundwater is in progress and is reported in Ref. [4].

It should be noted that any acceleration of decommissioning leading to earlier packaging and disposal will lead to an increase in the percentage of graphite that is deemed ILW, since ⁶⁰Co and ³H will have decayed to a lesser extent. An increasing inventory of ⁶⁰Co has dose implications requiring additional considerations, especially during processing, packaging and transportation. This may impact on operator doses and dictate further shielding requirements and may require use of IAEA Type B transport containers (i.e. packaging in a 3m³ Box), rather than the larger 4 m Box (which would be qualified to the IP-2 standard and restriction of contents to LSA/SCO materials).

Options 2 and 3

If a LLWR route was deemed possible through an appropriate waste treatment and conditioning process, then a very approximate disposal cost comparison could be made. Alternative LLW repositories may be available in the future and further cost savings may be possible. At Drigg LLWR, the safety case stipulates authorized discharge limits for isotopes which are present in irradiated graphite and include ¹⁴C and ³⁶Cl. Without further pretreatment, it is very likely that graphite LLW will breach these authorized discharge limits. It may be possible to condition the graphite wastes which are at the bottom-end of ILW and LLW, so as to allow the final disposal of these wastes to either a LLW repository or free release. Possible treatment options will be discussed in the next section. Heat or chemical treatment of graphite wastes may lead to a large waste volume reduction although secondary wastes will need careful consideration. The simple cost equation is that the cost of disposing all graphite as ILW will have to be demonstrably greater than the cost of any treatment process plus the cost of dealing with secondary wastes.

For options 2 and 3, a number of conditioning methods that could be explored include:

- partial oxidation
- electrochemical pulverization and contaminant dissolution
- complete chemical dissolution using strong acidic mixtures, chemical leaching of contaminants, simple washing techniques
- combination of electrochemical and chemical treatment
- complete oxidation, e.g. gasification
- physical size reduction, e.g. crushing, cutting
- reuse options

For any graphite treatment process the resultant waste streams need to be fully understood with the relevant underpinning safety, environmental and cost studies in place. For example, any high temperature graphite oxidation process may lead to a graphite product, off-gas active effluent and higher activity ash waste (Fig. 1). Complete gasification of the graphite followed by sequestration could also be considered. Each of these waste streams should be examined in detail before any final decision is made on the proposition that high temperature graphite processing is a realistic alternative to encapsulation and geological disposal. Furthermore, BPEO studies would help the NDA and its Site Licensee Companies to understand that secondary waste treatment may be necessary for the process to gain stakeholder acceptance.

Option 4

As noted earlier, core reactor graphite will contribute some 127 000 m³ packaged volume to the geological repository. Graphite does contain long lived activity in the form of ¹⁴C and ³⁶Cl, but otherwise exhibits characteristics associated with LLW and short lived ILW (in this respect, the inventory associated with short lived ³H and ⁶⁰Co is relevant). Given appropriate packaging and repository design, there may be another solution which is to dispose of graphite wastes within a separate dedicated facility.

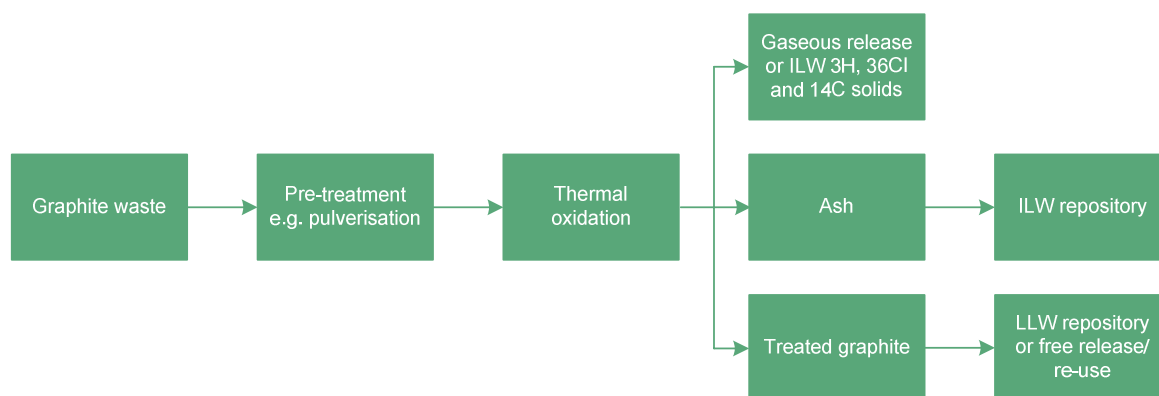


FIG. 1. Options 2 and 3 — to condition graphite waste by thermal oxidation to remove the long lived radioisotopes and dispose of the residual graphite at LLWR near Drigg or alternative LLWR.

Option 4 considers the possibility of a separate near surface ILW graphite repository with the possibility of accepting special designed graphite waste packages. The presence of long lived activity in the form of ¹⁴C and ³⁶Cl requires a safety case that provides a long return time to the biosphere. It is thought that this can be achieved by provision of a high performance waste package with long life and low permeability, together with a repository site providing low hydraulic gradient and permeability. Such an approach is being explored elsewhere (e.g. France).

Such an approach might also be of benefit to the geological repository. By removing a high volume waste stream, the volume required for excavation may be reduced or alternatively space may be provided for additional wastes. The possibility of co-processing graphite with other similar wastes or infilling waste packages with other appropriate decommissioning wastes, e.g. crushed concrete, could be considered.

Option 5

Interim storage may be used to allow for the decay of short half-life species and could undergo further conditioning ready for final disposal, thus minimizing dose uptake to workers (e.g. ³H is a major active component). The current baseline position of Safestore, i.e. the graphite reactors are left in a care and maintenance regime for an extensive period of time, could be considered as an interim storage option. Interim storage of any non-encapsulated graphite should take into account accelerated corrosion due to galvanic coupling.

3. Forward plan

Five potential strategic and disposal options have been proposed and can be broken down into three distinct areas:

- Improved baseline position with respect to ILW disposal of graphite: to consider alternative disposal regimes and improved waste management practices
- To investigate graphite treatment methods to allow safe disposal in a LLW repository
- To investigate graphite treatment methods to allow for the reuse of the graphite product within the nuclear industry.

Taking into consideration these strategic position statements, the NDA is developing a forward plan which addresses the following:

Overview of the graphite issue

Develop understanding of quantities, characterization, radionuclide inventory and the international situation, e.g. building on current NDA sponsored work. Challenges of disposal and the associated post-closure safety case. UK situation in the world context. Introduce the list of all credible management options.

Technological treatment solutions

Review of current and emergent technologies with full listing and description. Pros and cons with an assessment of potential benefit. Status of current technical maturity and associated risk. Consideration to be given to full life cycle of any proposed solution. Conclusions of such a study, including a gap analysis of the main issues highlighted.

Following on from the May 2006 workshop, work has been commissioned by Magnox Electric to review technological treatment solutions.

Technology implementation

It is expected that more than one solution will be applicable to graphite waste streams. It is envisaged that technology implementation will be achieved by the development of graphite treatment and disposal 'toolbox'. The toolbox will help to guide the industry to the correct choice of technology (or technologies) depending on the origin, condition, contamination and volume of the irradiated graphite waste stream. Pictorially, the toolbox could be a 3-D diagram of graphite type/waste stream *versus* treatment/disposal method *versus* applicability.

Underground disposal

Consideration needs to be given to repository concept assumptions and environmental, safety and cost-benefits of deep disposal weighed against those for surface disposal. Errors and uncertainties in radionuclide inventory need to be reduced, particularly those associated with ^{14}C . Existing programmes to enhance the robustness of post-closure safety cases need to be enacted. Consideration to be given to graphite disposal waste forms, including possible opportunities to use graphite as a 'filler' for ILW packages.

Cost (macroeconomic), safety and environmental assessment of options for managing graphite

Specific coverage on these issues to ensure that NDA can develop views on options being proposed.

Proposed Research and Development programme

Including international collaborations, underpinning scientific studies and continued support to the development of a world-class UK capability.

Forward strategic planning and scenario development

Taking account of the above, interim recommendations for UK strategy, suitable for discussion with stakeholders.

4. Recommendations

The programme on the potential treatment and disposal options for irradiated graphite is in progress at Magnox Electric. Work to enhance understanding of C-14 generation and migration during repository post-closure is also being pursued by NDA [4]. However, in support of these development programmes, NDA is recommending that three further areas of work should be pursued in line with the issues raised in the Forward Plan:

- (i) A limited generic Research and Development (R&D) programme to help scientifically underpin any choice between options, which also keeps abreast of current worldwide developments
- (ii) A specific graphite disposal options programme
- (iii) Independent peer review that evaluates the options being proposed

Close consideration should be given to any developments within the following programmes of work; (a) site specific studies investigating methods of graphite treatment, e.g. Windscale piles, Hunterston sleeves, (b) current and future LLW waste treatment and disposal, and (c) site end states.

Research and Development programme

Magnox Electric will be responsible for carrying out all necessary R&D to support its bulk reactor graphite waste treatment programmes. In addition, a limited NDA coordinated R&D programme should provide focus on graphite waste behaviour and available treatment technologies from a worldwide perspective. Further scientific underpinning of potential options may be achieved by a variety of means including:

- International developments — NDA needs to achieve and maintain a worldwide view of R&D initiatives and developments. If appropriate, NDA or its contractors may want to lead certain work packages or enter into collaborative programmes.
- Scope bounded academic research projects that may be funded by NDA contractors.
- NDA direct funded initiatives for generic research and development (e.g. seedcorn funded work, doctorate research schemes, etc.).
- Reviewing relevant historic programmes of work.

Graphite disposal programme

Within this programme of work it is envisaged that a number of options should be investigated using the relevant expertise in the UK. This work would be expected to be led by the newly expanded NDA, involving academic institutions, consultants and overseas agencies. The options to be considered may be broken down into the following areas:

- Separate graphite repository
- Variations of current UK repository concept

Peer review

To ensure continued credibility within any development programmes it is essential that proposed irradiated graphite treatment and disposal solutions are able to withstand detailed scrutiny and challenge. This can be achieved through peer review initiatives such as independent forums, independent input into optioneering workshops and the appropriate use of external consultants. Peer review groups involving international organisations is encouraged, which is already the case in the Magnox programme. It is essential that peer review is programmed into any forward development programme.

The programme being managed by Magnox Electric is expected to recommend a number of graphite waste management options that are worthy of further investigation. At this point, it is envisaged that a peer review group will evaluate the recommended options and propose to the NDA and Magnox a preferred approach to option down selection. A new programme of work will take into consideration the Magnox recommendations, the peer review comments and work carried out in generic R&D and graphite disposal programmes. The timing and execution of further work studies will be dependent on the decision timetable for a repository.

It is expected that Magnox will directly lead the next stage of work with support from NDA (Radioactive Waste Management Directorate), other Site Licensee Companies, Nexia and other key consultants from the UK and abroad. Any national initiatives to establish their feasibility, e.g. graphite disposal strategies, will be led at an early stage by the NDA in conjunction with key stakeholders such as Government Departments, the Regulators, waste producers and planning authorities.

Finally, it is proposed that a UK Graphite Working Group is established to help implement the above recommendations and take into consideration the proposed way forward. This Graphite Working Group may form part of the peer review process.

REFERENCES

- [1] Nirex, The 2004 UK Radioactive Waste Inventory, Nirex Report N/090.
- [2] Nirex, The Nirex Research Programme to Improve Data on Chlorine-36 in Radioactive Wastes (1998).
- [3] Nirex, The viability of a phased geological repository concept for the management of the UK's radioactive waste, Nirex Report N/122.
- [4] NORRIS, S., et al, Graphite Wastes: Disposal Issues (This Conference).

Current status and future objectives for graphite and radium-bearing waste disposal studies in France

O. Ozanam

ANDRA, Chatenay-Malabry Cedex, France

Abstract. The French planning act of June 28, 2006 states that disposal options for graphite and radium-bearing waste should be developed. Graphite waste has been generated in France mainly by nuclear UNGG reactors; these reactors have been stopped since 15–40 years. The waste is considered to be low level and long lived waste. The disposal design options under study are all envisioned in a near surface repository: shallow land burial and emplacement cells with access drifts from the surface until 100 m deep. The main objectives for the next years are development of disposal options, siting, and better understanding of the Chlorine-36 behaviour in the graphite waste.

1. Introduction

In the planning act N°2006-739 of June 28, 2006 related to sustainable management of radioactive materials and waste, the French parliament stated that “a research and investigation programme shall be established with a view to developing disposal options for graphite and radium-bearing waste in order for a corresponding disposal facility to be commissioned in 2013”. Taking into account the necessary periods of instruction by the regulators and for administrative operations, the time schedule to conduct remaining studies is very tight. In addition, the site selection process has not yet identified available and suitable sites.

This paper focuses on the graphite waste management and presents the main characteristics of the graphite waste to be disposed of in France, the various disposal design options under study for these waste and the main objectives for the next years.

2. Waste inventory

The waste inventory is generated by six nuclear UNGG reactors and five experimental nuclear gas reactors (Fig. 1). The UNGG reactors have been stopped since 15–40 years. The total mass of irradiated graphite waste is around 22 400 t. The most part is composed of graphite from moderators' blocks and reflectors (18 500 t) and from sleeves (3600 t).

The radioactive graphite content of the sleeves and moderators blocks is mainly tritium (26%), Co-60 (37%), Ni-63 (20%), C-14 (17%), Cl-36 (0.2%), from an 2001 evaluation. According to this radiological content, these wastes are considered as low level and long lived waste.

The reactors should be decommissioned under water. This operation will provide additional waste, i.e. ion-exchange resins to decontaminate water. The characteristics of these resins are not presently well known. Studies are necessary to determine if these resins could be disposed of in the disposal facility designed for the graphite waste.

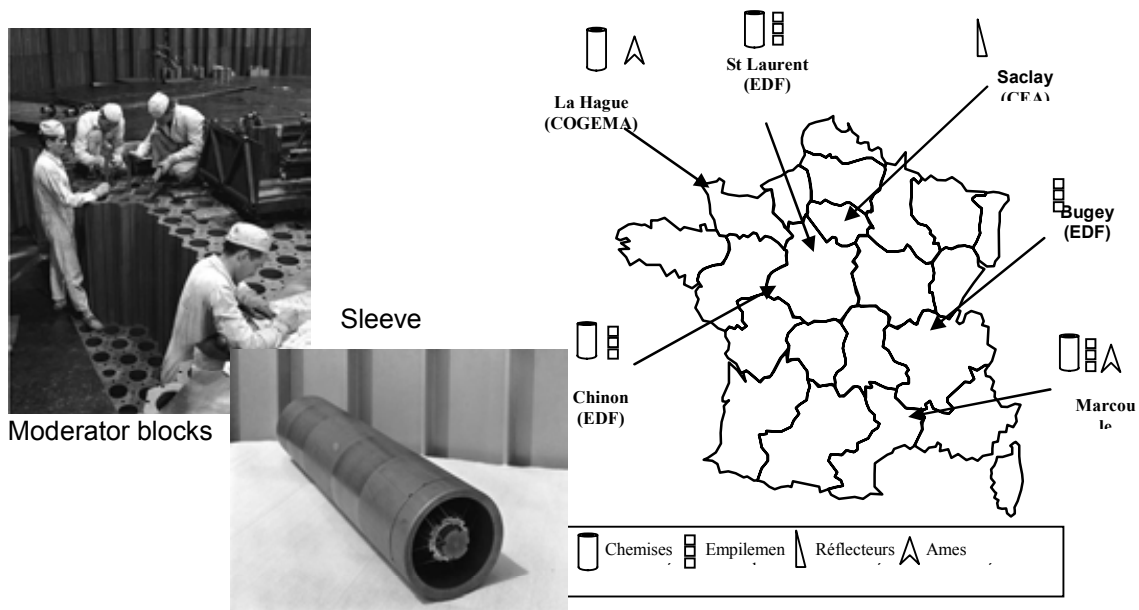


FIG. 1. Graphite waste storage location.

3. Waste package

During the decommissioning operation the graphite waste will be placed and blocked in concrete waste packages, as illustrated in Fig. 2. The studied package could contain 1–3 t of graphite for a global unit volume of 5–10 m³. With packages of 10 m³, the total volume of packages to be disposed of varies approximately from 60 000 to 80 000 m³, according to the size and form of the graphite elements.

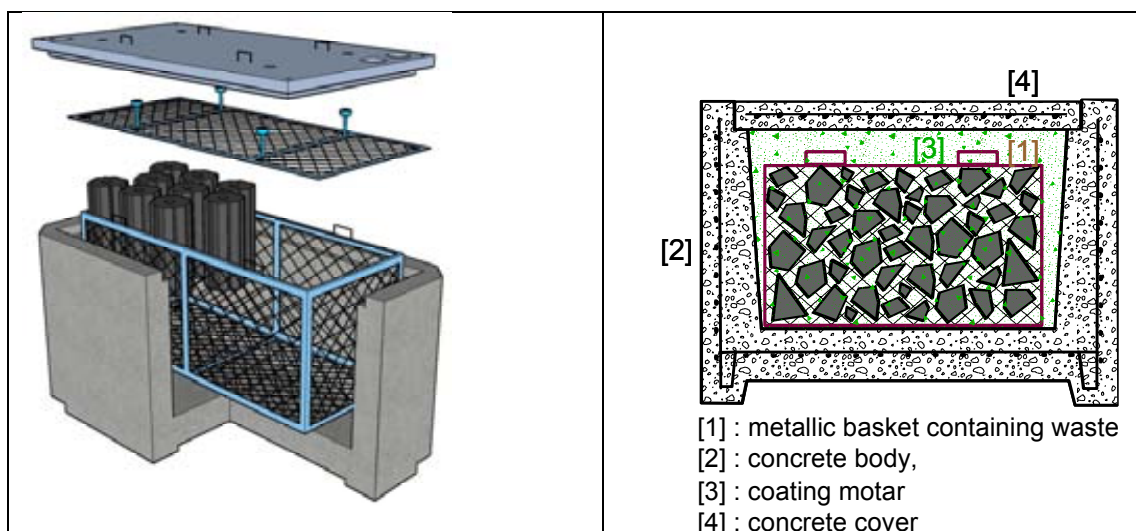


FIG. 2. Example of studied graphite waste package.

4. Disposal design options

Disposal in a near surface repository is envisioned. Two main options are considered for the graphite waste packages:

- One option is a shallow land burial, in which waste packages are emplaced in concrete cells and closure includes backfilling the area above those cells;

- The other option includes emplacement cells to be constructed at near surface level with access drifts from the side of a hill, to maintain a natural cover above.

The first option has been studied at the stage of the preliminary design. The disposal cells are placed between -15 and -24 m under ground level as illustrated in Fig. 3. This option implies high performances imposed to the waste package and disposal cell during a long time to limit Cl-36 impact. However, some variations of this solution are also under study in order to have technical solutions for various disposal depths, i.e. by using diaphragm wall.

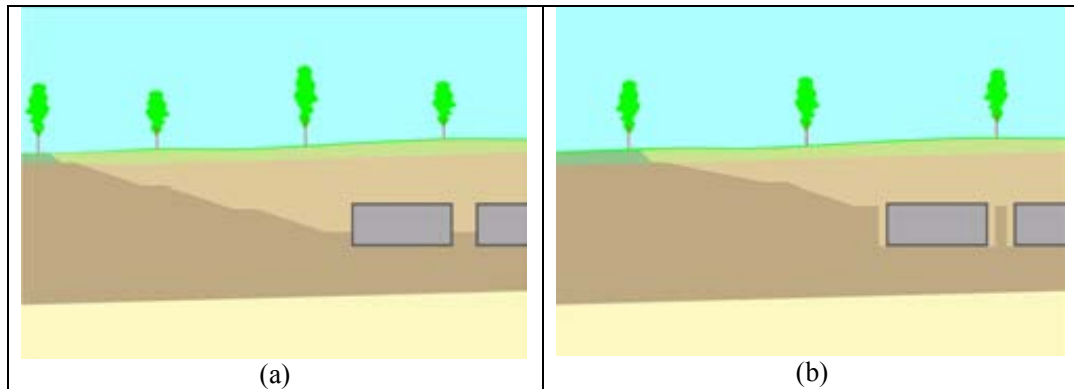


*FIG. 3. Shallow land burial disposal option
(a) for depth from -15 to -30 m, (b) for greater depth (with diaphragm wall).*

The second option is under study. It allows disposing the waste packages at a greater depth between around 50 and 100 m.

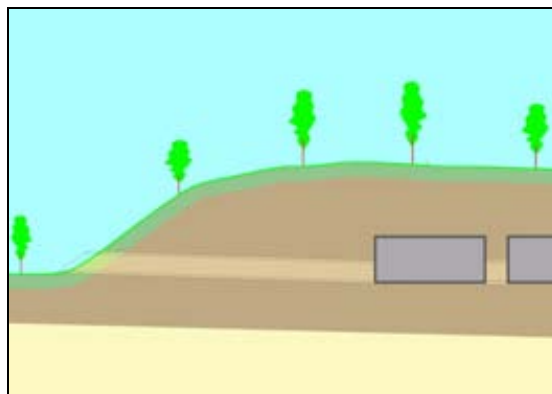


FIG. 4. Near surface disposal option with natural cover.

These various options offer a greater flexibility for the site selection process and for the choice of the disposal cell depth, which might need to be adapted to the site properties.

5. Main objectives for the next years

Transfer assessments of radionuclide release fluxes show that the main radionuclide responsible for disposal impact is Chloride-36, which is difficult to retain or delay. Other radionuclides such as Carbon-14 are retained and delayed mainly by the concrete of the package and emplacement cells. The scope of research work concerning a better understanding of the Cl-36 behaviour in the graphite waste is currently defined and scheduled for the next years.

The other main objectives are development and assessment of various disposal options, siting and preparation of geological survey.

Aspects of graphite disposal and the relationship to risk: A socio-technical problem

G.B. Neighbour, M.A. McGuire

Department of Engineering, University of Hull, United Kingdom

Abstract. This paper sets out to explore the different aspects of irradiated graphite disposal in relation to general nuclear waste policies. A brief review of the development of nuclear waste policy in the United Kingdom is first presented within a socio-political context and then the paper seeks to explain that in reality the “problem” lies within a socio-technical context. In particular, using various observations and a reflective approach, the paper shows that much of the problem lies with the subjective risk being a dominant factor and this is very much related to classical design theory. The analysis establishes that, despite significant investment and effort into studies for potential solutions, social-technical issues provide barriers to progress, and distorts the methodology to establish the most suitable disposal strategy. Furthermore, comments are made how design theory relates to various disposal options and formulation of safety cases and offers suggestions to create more effective solutions in future by minimizing subjective risk and, indeed, objective risk.

1. Introduction

There is a general consensus that the perceived inability to deal with the disposal of nuclear waste has caused harm to potential new build of nuclear reactor systems in the western economies despite other pressures such as global warming. Here, the authors present an argument centred on irradiated nuclear graphite, a major waste stream in the decommissioning of nuclear reactors, but parallel arguments can equally be presented for all types of nuclear waste, which illustrates that the circumstances are complex and the proposed solutions for waste disposal are artificially constrained. Certainly, it is evident that the many national programmes have been working towards disposal of nuclear waste for many years, e.g. see [1]: indeed, almost as long as the nuclear programmes have existed! In most cases, land-based permanent deep repositories have tended to be the preferred intended solution (the base case), although most solutions have been shown to be technically acceptable and comply with safety limits ([2], [3]). In some cases, this direction is the consequence of a combination of scientific study and of environmental and political influences directed against the release of any radioactive material into the immediate (i.e. measurable) environment. However, despite this, observation reveals that these strategies have serious logical flaws. For example, in the United Kingdom (UK), no such deep repository exists and there are no approved plans for the construction of such a repository. Indeed, taking the UK as an example, successive Governments have first signed up to a moratorium on sea dumping, established an agency (NIREX UK) to facilitate the design and construction of a deep waste repository (which had an original planned opening in 2000), set up public enquiries for a number of potential sites, accepted the recommendation to place the site adjacent to the existing Sellafield nuclear complex in West Cumbria and then, in March 1997, endorsed the refusal of the local planning authorities to allow construction even of a rock structure laboratory on the chosen site, let alone a repository. After a few years stagnation, the UK Government set up CoRWM¹ which, at great expense, reconsidered all (15 generic) options (ignoring new build) and consulted widely with the public only to conclude that a deep repository was the correct solution (giving

¹ The Committee on Radioactive Waste Management (CoRWM) was set up by the Government as an independent body in November 2003 to recommend a strategy for long term management of the UK’s higher activity, solid, radioactive waste.

15 recommendations [4]). The recommendations were accepted by Government in October 2006 including the open and transparent partnerships with potential host communities for disposal facilities (i.e., principle of volunteerism). Simultaneously, the UK restructured the nuclear industry with the creation of the Nuclear Decommissioning Agency (NDA)² (which subsumed NIREX) responsible for liabilities worth £50 billion. Consequently, the UK has no national disposal facilities for intermediate or high level wastes, and the problem that the life of existing surface stores and packaging is unlikely to exceed 100 years remains. It is also interesting to note here that the approach taken by UK Government often follows a “decide-announce-defend” paradigm that tends to antagonize the general public. It is also worthy to compare the situation here with the general principle of ‘polluter pays’, but the current structure introduces discontinuity in terms of where the control lies and whether the polluter has the ability to reduce costs. This raises important issues in context of the design process discussed later.

In a previous paper [5], the lead author reviewed the global sources of irradiated graphite and all the options available for nuclear graphite disposal and stated that “the UK with no long term storage facility, no other politically acceptable options, a need to recommence the selection process several steps back down the chain of technical investigation and public consultation, a delay of at least 10–15 years in the provision of a disposal facility, [would result in] an accumulating mountain of radioactive waste in supervised surface storage”. This is indeed what appears to have happened over the last decade and the analysis here helps to provide an understanding for this outcome.

2. Current situation

Irradiated graphite is a significant proportion of legacy wastes and also forms part of waste streams of future reactor designs, e.g. PBMR, with ~0.25 Mte of irradiated graphite material existing worldwide. Until recently, the disposal route for radioactive graphite has generally been assumed to be the same as other intermediate level waste items; that is disposal at a deep repository. However, it should also be noted that the condition of irradiated graphites are variable in terms of microstructure (–property relationships), physical condition, activation and contamination [6]. Furthermore, it is generally accepted that the default position is a combination of “safe store” policies (resulting from safety concerns relating to handling/disposal) and absence of suitable disposal facilities (but it is assumed they will eventually exist), nevertheless there is also pressure to “accelerate” decommissioning! A decade ago, the expected time of stage 3 decommissioning was 135 years³; however, some estimates put this closer to 50 years today based on experience such as that gained at Windscale prototype AGR which is at an advanced stage of decommissioning. It is also becoming increasingly clear that nuclear regulatory authorities are becoming uneasy about long delays, especially in the UK, on the basis that personnel with experience and detailed knowledge of the particular reactor designs will not be available when the dismantling task is finally undertaken. This is in accord with public opinion which regards the “safe storage” period as leaving today’s problems for future generations to resolve. There is a need to minimize the impact of such wastes, but that does not necessarily mean waste minimization. For example, commonly, there is an assumption that all materials are waste and not a ‘resource’. It is therefore legitimate to ask whether such aspects have been considered within the ‘design space’ for determining a solution for this ‘problem situation’. This leads to suggest three key questions.

- How much progress been made in the last decade?
- Do we understand the problem?
- Do we have a strategy to deal with the problem?

² The Nuclear Decommissioning Authority (NDA) came into being on 1 April 2005 and now has responsibility for overseeing decommissioning work on all of the UK’s civil public sector nuclear sites (at present 20). In 2005, there were 470 000 cubic metres of radioactive waste with no long term management strategy. The organization essentially “project manages”.

³ The original hypothesis for 135 years was to allow many isotopes to decay such that the task will therefore be much simpler in respect of the remote techniques needed and much improved in terms of operator doses.

An observation that can be made is to suggest that a further consequence of driving towards one particular disposal goal has been the commitment of very large investment resources aimed at developing and refining sub-processes such as waste immobilization, specific storage container designs and handling procedures. In consequence, there is an understandable reluctance on the part of the nuclear operators and industry to take a wider view of the options, which is seen as an unacceptable step backwards and economically unsustainable. However, there are some indications that public opinion may effect a change in philosophy towards including supervised surface storage or shallow burial, which would give some reassurance that the condition of the material remains monitored and would also make available the possibility of future transfers to more acceptable permanent disposal solutions (e.g. [2]–[5]).

3. Risk and socioeconomic factors

Ideally, evaluation of graphite disposal should be based on objective reasoning and fact. Previous studies have concluded that a number of alternative options are all technically feasible and have sensible “objective” risks/“dose limitations” attached (e.g. [1], even after an assumed dismantling after 10 years). However, the ‘precautionary principle’, coupled with subjective assessments, tends to create a trend to minimize radioactive release (e.g. OSPAR⁴ convention) with the consequence to retain material in interim storage [7]. Analysis indicates that this arrives as a need to satisfy public concerns over disposal of nuclear wastes; the public appear not to tolerate any risk, which induces political pressure to apply over-stringent controls [8]. The situation is exasperated when, in communicating with the general public, different activities are compared according to estimated risks normalized to a common unit, e.g. deaths/year/exposure to a unit of radioactive dose (using a linear model). Over recent years, even when dialogue with the general public is essential, concepts such as BATNEEC⁵, BPEO⁶, ALARA⁷ and ALARP⁸ have reinforced the duty on operators to minimize the radiological exposure to the human population and have, in fact, placed pressure on the nuclear industry to find and use the best technical judgements, plant and expertise available at a high financial cost [9]. The irony is that, at least in radioactive waste disposal, this may not be what the general public wants. Wynne [8], in the context of levels of radioactive discharges from the UK fuel reprocessing site at Sellafield, reported that, in the evaluation of risk estimates and costs of the available technologies to control the discharges, the implicit value of one human life as employed in the calculations was ~US \$38 million (at 1990 levels), which is an irrationally high level of investment for little social benefit, e.g. it is comparable to the cost of a new hospital. It is clear that the demands of the public in regard to nuclear-related industries are extremely high. Therefore, the inference can be drawn that the desire to achieve the ultimate minimum risk, from using a single measure of performance such as deaths/year/exposure to a unit of radioactive dose, will not satisfy the general public. To convince the general public of an acceptable solution to graphite disposal, some change of social attitudes is required: i.e., it is necessary to establish a tolerable risk under certain socially acceptable and trusted conditions. For example, as Wynne comments:

“...in order for mining to exist at all as an institution, miners have to be able to trust that if ever they are trapped alive, a rescue will be attempted.”

Thus, it has become increasingly necessary to involve the public perception of science and scientists in any equation relating to the choice of a controversial process or activity whether this public perception

⁴ The 1992 “Convention for the Protection of the Marine Environment of the North-East Atlantic”.

⁵ Best Available Techniques Not Entailing Excessive Cost.

⁶ Best Practical Environmental Option — the option which, in the context of releases from a prescribed process, provides the most benefit and/or least damage to the environment as a whole, at acceptable cost, in the long term as well as in the short term.

⁷ As Low As Reasonably Achievable.

⁸ As Low As Reasonably Practicable.

is justified or not. For example, this is evidenced by the activities of CoRWM which have been shown not to alter the perceived technical wisdom.

Williams [10] provides a rationally argued discussion of relative risks in the nuclear industry, drawing useful comparisons with the risks of other types of industrial and community activity, including the risk of death “from the UK nuclear industry” which includes the disposal of waste (1 in 40 000 000), that from all natural causes at age 40 (1 in 850) and that from smoking (1 in 200). The public do not perceive extremely hazardous activities as in any way “risky” if they are familiar — like driving their cars on crowded roads. In the UK in 2005, according to the Office of National Statistics, there were 3 201 deaths and 271 000 injuries due to road traffic accidents [11]. The problem with public perception of nuclear matters is, in part, their unfamiliarity, and so politicians have reacted more to the emotional arguments rather than attempting serious debate on such issues, although environmental pressures have changed the landscape. There is clearly an increasing tendency in Government to apply to the nuclear industry controls which are far more stringent than those applied to ostensibly non-nuclear industries. The public perception and mistrust of many options has a strong political importance which has frustrated the decision making process. Public education has generally failed to reduce the level of “subjective” risk felt by the general public because an approach based on minimum risk is often taken. Greater education is not the answer: many instances have simply failed in the past [see, for example, [12]].

Subjective risk or perceived risk can, by analogy to objective risk, be expressed as equal to the Threat or Hazard Outrage. Essentially, the industry has failed to understand the subjective risk felt by the general public and changed its approach accordingly. If we consider what subjective risk that affects public perception is, then we can include the following attributes:

- Natural vs. industrial
- Familiar vs. exotic
- Not memorable vs. memorable (immediate or delayed)
- Chronic vs. catastrophic (dispersion vs. single event)
- Knowable vs. unknowable
- Tolerable/intolerable (Not dreaded vs. dreaded)
- Individually controlled vs. controlled by others
- Fair vs. unfair (direct/indirect/cumulative/equitable social distribution)
- Morally irrelevant vs. morally relevant
- Trustworthy sources vs. untrustworthy sources
- Responsive process vs. unresponsive (beneficial/harmful)
- Reversibility or irreversibility
- Whether anonymous or known victims were involved
- Whether there was uncertainty and disagreement about the risks (pessimisms)

How these attributes relate to each other as an n^{th} dimensional function for the total measure of subjective risk for a range of industries is a current exercise being conducted by the University of Hull [13]. It is clear that single measures of risk ignore many of these attributes and also the sociological aspects experienced by the public. This emphasizes “the need to involve the public to a greater extent”, as suggested by the CoRWM recommendations. The final decision in the disposal of nuclear wastes, and in particular irradiated graphite, most likely will have to consider “public concern” and indeed integrate such attributes into the formal risk–cost decision making process.

4. The design process — Integration and iteration

In developing a solution for nuclear graphite disposal, is the engineer’s paradigm “right first time, every time” followed? To achieve this paradigm, a structured design methodology must be adopted such as that outlined by Pugh [14] or Pahl and Beitz [15]. An illustration of Pugh’s design process amended by Wallis [16] to include environmental concerns is presented in Fig. 1. An interesting observation is the involvement of the “customer” throughout the process. In any design process, and finding a solution to graphite disposal is de facto a design process, it is important to establish who is

the customer and indeed the end user. This simple question does not lead to a simple answer because of the large number of stakeholders involved in the process in the case considered here. From one perspective, the customer may be seen as UK Government (after all they appear to pay) or at least society as the beneficiary. However, how does this rest with the principle of the polluter pays? Is it clear who the polluter actually is? From another perspective, the customer may be seen as the 'operator', but this ultimately leads to one or the other being a displaced customer (i.e., the user who has been separated from the person responsible for the purchase, although the needs of both have to be satisfied in the transaction, e.g. the analogy being children's toys).

Equally, from a design process, it is important to use a large 'design space'; this enhances finding the right solution. A design space is a mental construct of an intellectual space that envelops or incorporates all of the potential solutions to a design problem. Put simply, the larger number of ideas and concepts generated, the greater the probability that the best solution will be found. To give a simple example, imagine a product that has 6 functional parts and each part has 5 options to fulfil the functional requirement. This should lead to, theoretically, 5^6 or 15 625 concepts. It is very common to find 'optioneering' studies that contain only a handful of options or concepts, and thus represents a very small 'design space'. Within a large design space there will be a large number of potential designs and/or the number of design variables is large, as is the number of values they can assume. In order to use the design space, techniques can be used to create divergent thinking and thus enable engineers to "think outside of the box" to generate design alternatives (see Fig. 3). On the other hand, at appropriate times, convergent thinking, to narrow the design space, can be used to focus on the "best" alternatives so as to converge to a solution within known boundaries or limits. This process is illustrated in Fig. 2 with three main phases representing conceptual, embodiment and detail design. It is important to observe the narrow sections at the beginning and end representing the 'problem definition' and converged 'final solution'.

In summary, the thesis in this paper is that the design process with identifying a disposal solution has become dysfunctional in several respects: the subjective risk skewing the process; the complex structure of the nuclear industry and conflicting goals of the stakeholders; and a lack of a principled approach to design. The dysfunctional design process is illustrated in Fig. 2 where 'optioneering' studies effectively jump the conceptual design phase, driven by perceived political acceptability and business case or objectives, and thus is unlikely to achieve the best solution. The tools and techniques, outlined in Fig. 3, appear not to be used in creating divergent thinking in the early stage of design, but rather current practice appears to be dominated by the 'later stage' tools. This ultimately leads to 'incremental' rather than 'disruptive' technologies in handling irradiated graphite waste.

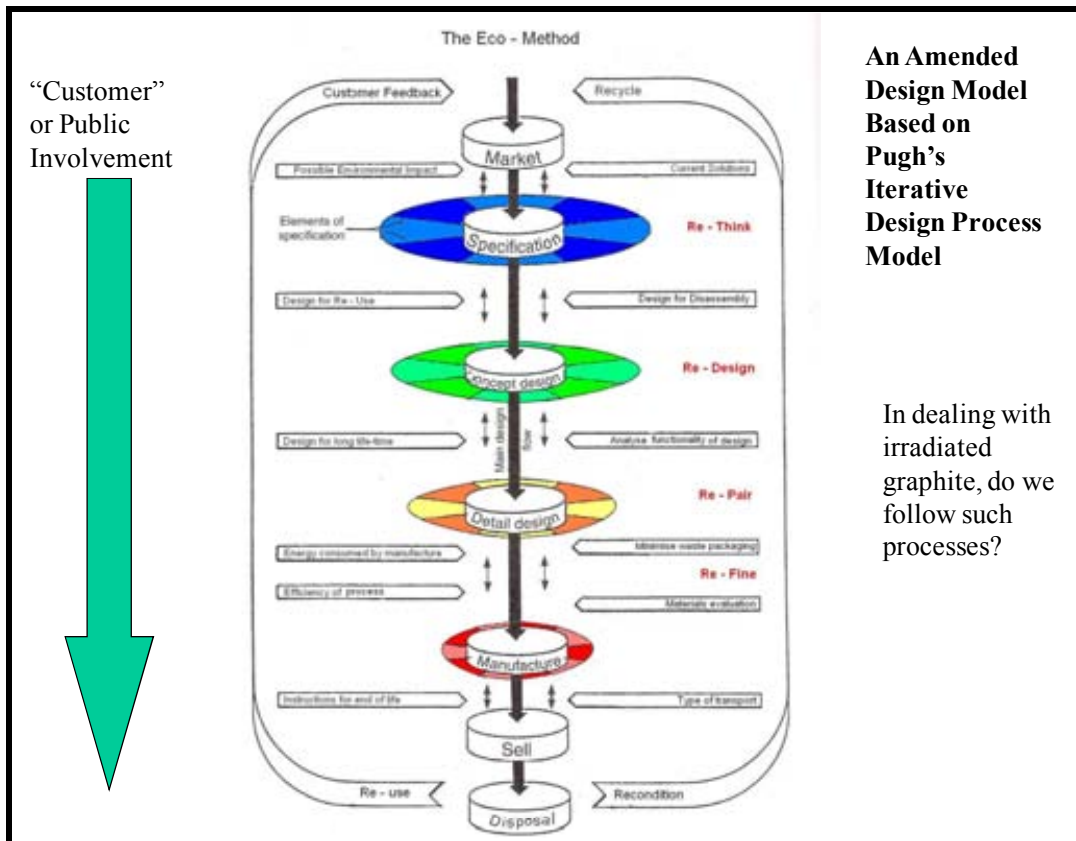


FIG. 1. An illustration of Pugh's design methodology with the inclusions of environmental concepts.

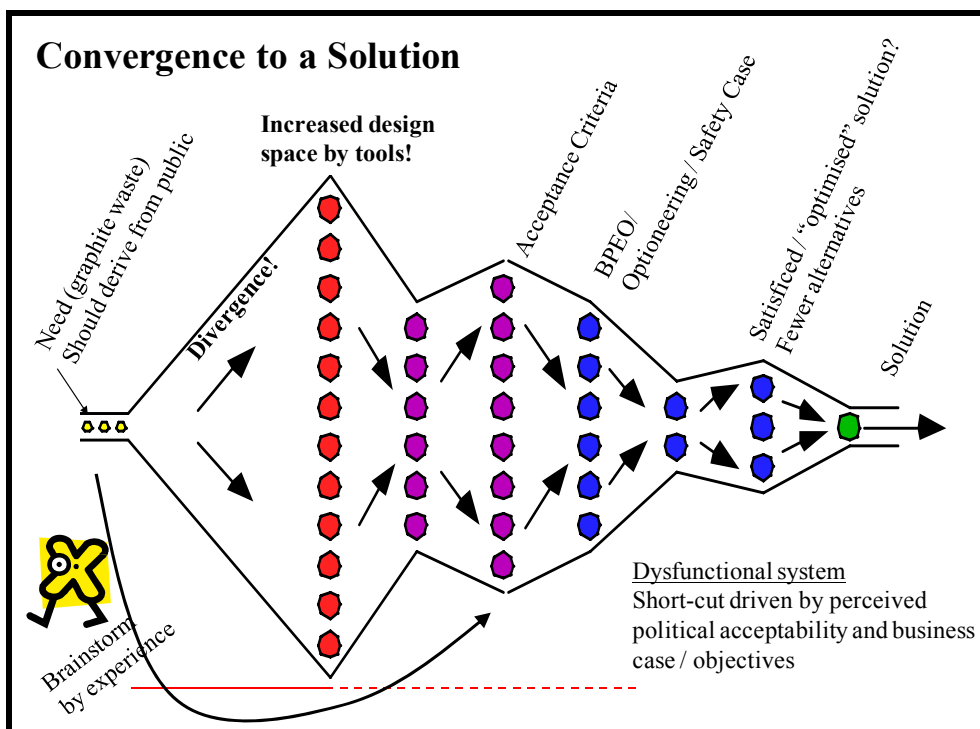


FIG. 2. An illustration of the design process involving divergent and convergent thinking.

Design Concepts & Tools Checklist (Not Exhaustive)

- **Early Stage (excluding sub-processes)**
 - Mission statement, systems thinking (holism, mess to difficulty, emergence, rich picture, inference maps, multiple-cause maps, other diagrammatic methods, hard and soft-systems modelling, needs, metrics, **BDM, PDS, QFD**, (negative) brainstorming, benchmarking, conceptual design, design approaches such “**form follows function**” and **axiomatic**, synectics (analogies), **morphological charts**, **product creativity templates** (attribute dependency, replacement, displacement, component control), objectives trees, interviews, focus groups, observation, functional & user **decomposition**, product (modular or integral) architecture, BOM.

- **Later Stage**
 - MADA, DfE (µ-concepts), DFMA, (various) prototyping, FMEA, ETA, HAZOP, **Eco-Compass** & other Environmental impact tools, BATNEEC, BPM, BPEO, EIA, LCA, Material Selection Indices, Hazards & Risk Calculations (QRA & F-N “Farmer” curves) with alternative dose-response models, Tolerability of Risk (TOR), Reliability Analysis, PSA

FIG. 3. Concepts and tools checklist for the early and later stages of the design process.

In the design theory proposed by Suh [17], an argument was put forward to express design as a science (as a paradigm) with two fundamental axioms⁹. Suh remarks:

“Although the design of products and organisations must often be done in a multidimensional world, managers and engineers are often taught optimization techniques for a one-dimensional world. They do not know how to think in several dimensions because they have not been given the tools and techniques that can deal with the problems of the complex world.”

Suh’s paradigm¹⁰ is illustrated in Fig. 4 in which design may be formally defined as the creation of synthesized solutions in the form of products, processes or systems that satisfy perceived needs through the mapping between the functional requirements (FRs) in the functional domain and the design parameters (DPs) of the physical domain, through the proper selection of DPs that satisfy FRs. This mapping process is non-unique; therefore, more than one design may ensue from the generation of the DPs that satisfy the FRs; in other words, the actual outcome also depends on a designer’s individual creative process. Therefore, there can be an infinite number of plausible design solutions and mapping techniques. The design axioms provide the principles that the mapping technique must satisfy to produce a good design, and offer a basis for comparing and selecting designs. In Fig. 4, Axiom 1 states that, during the design process, as FRs in the functional domain are mapped with DPs in the physical domain, the mapping must be such that a perturbation in a particular DP must affect only its referent FR. Axiom 2 states that, among all designs that satisfy the Independence Axiom (Axiom 1), the one with minimum information content is the (relative) best design. That is Axiom 1 promotes an optimal design, in that it always maintains the independence of FRs, so that the best design is a functionally uncoupled design that has the minimum information content.

⁹ Generally accepted proposition or principle, sanctioned by experience.

¹⁰ Suh’s approach is similar to the medieval philosopher William of Occam who wrote: “No more things should be presumed to exist than are absolutely necessary to explain the phenomena”, also known as Occam’s razor, or more simply the minimum number of entities to reach your stated goal!

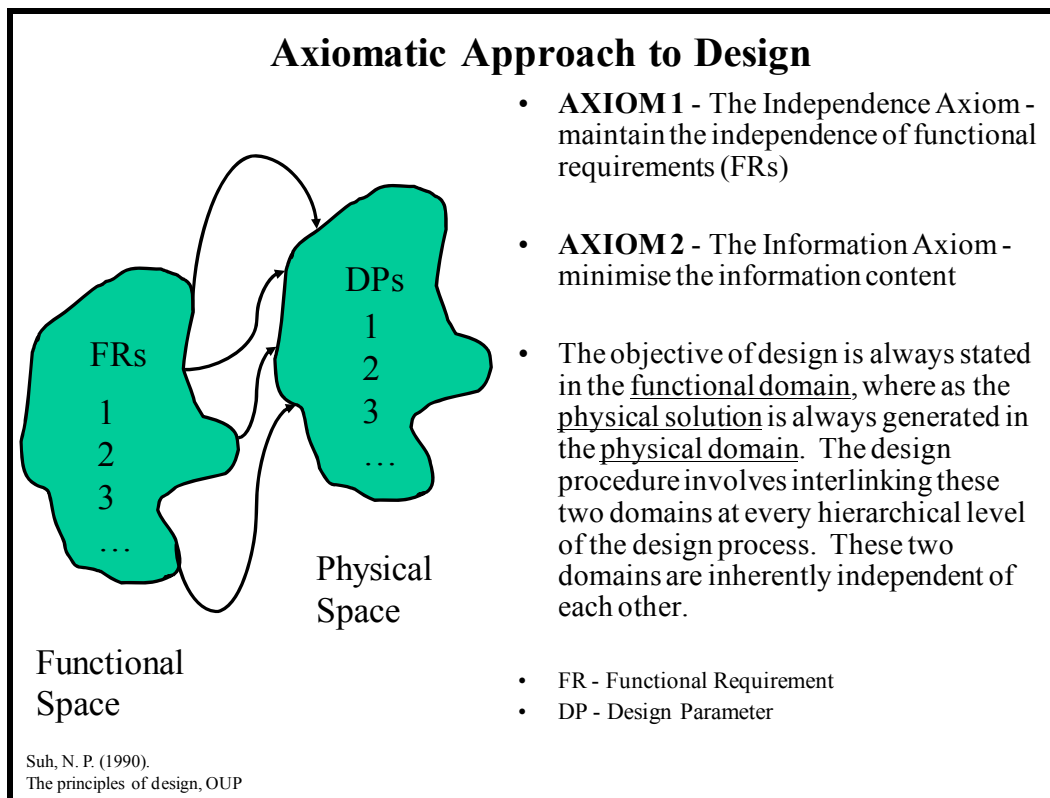


FIG. 4. Suh's axiomatic approach to design.

In applying the axiomatic approach to irradiated graphite disposal, the FRs of the designed solution can be reduced to:

- Protect human health and the environment (ALARP)
- Ensure a sustainable development (future generations) and thus seek a high position on the hierarchy of waste (see Fig. 5)
- Secure unmanned containment of radioactive species (or reuse/recycle)

These FRs can be related to multi-legged safety cases, possible post-use site investigation, waste acceptance criteria to be derived, etc. Certainly, confidence can be gained by adopting FRs, but it is also important to recognize that approaches such as waste minimization, which are often seen as advantageous, can be in conflict. These FRs are very different from the perceived design (acceptance) criteria or attributes, which do not necessarily map to FRs, often seen in the literature in design selection or BPEO, such as:

- Public support/opposition/perception/localization (NIMBY)
- Radiological implications/need for supervision
- Stability and certainty/robustness of solution (“handing on the problem to future generations” and avoiding failure, e.g. leaching and migration)
- Timeliness and speed of solution
- Cost and complexity
- Volume of secondary wastes
- Immediate and delayed risk
- Suitability of containment/reversibility
- Release (dilute and disperse/contain and control)
- Political aspects
- Emerging technologies

It is also interesting to note that these perceived criteria are different when compared with 34 generic packaging attributes (for all products) and indeed attributes should be weighted using the Binary Dominance Method. These attributes can be grouped into critical, desired, add value and superfluous attributes [18]. The question thus becomes: are the current processes, undertaken in pursuit of a solution for irradiated graphite disposal, consistent with design theory? Certain aspects of the current process can be noted. Firstly, in comparison with the ‘waste hierarchy’, there is a tendency to ignore the preferred options higher in the chain, as shown in Fig. 5. In essence, there is a paradox between the preferred option, which is effectively “landfill”, over other methods as shown in the waste hierarchy. Meehan [19] reports that the current process involves:

- Open and transparent options assessment processes involving wide range of stakeholders and their engagement and consideration of policy issues, including local government planning policies;
- Consideration of all disposal options (national, regional, local and on-site), assessed against range of criteria spanning safety, environment and cost;
- Licensee making recommendations to the NDA, taking into account stakeholder views and preferences on site end uses.

Furthermore, Harris [20] describes the ‘letter of compliance’ process, as illustrated in Fig. 6, which contravenes established design theory in that the design concepts and specification stages are interchanged. Further, the most common reason why designs fail is often down to inadequate market and customer research (needs analysis), inadequate design specification, politics not products, “throw it over the wall” approach, too many changes downstream where the development costs are highest, and inability to manufacture the product because manufacturing constraints were not considered. Some of these aspects are evident in the process outlined in Fig. 6. This supports the thesis that the design process has become dysfunctional.

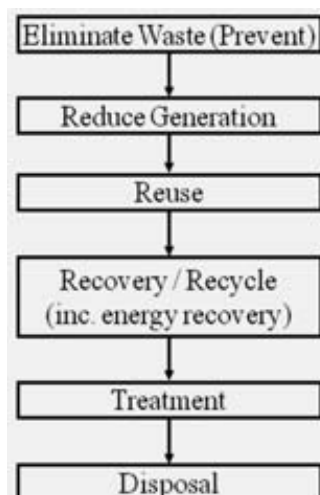


FIG. 5. The waste hierarchy.

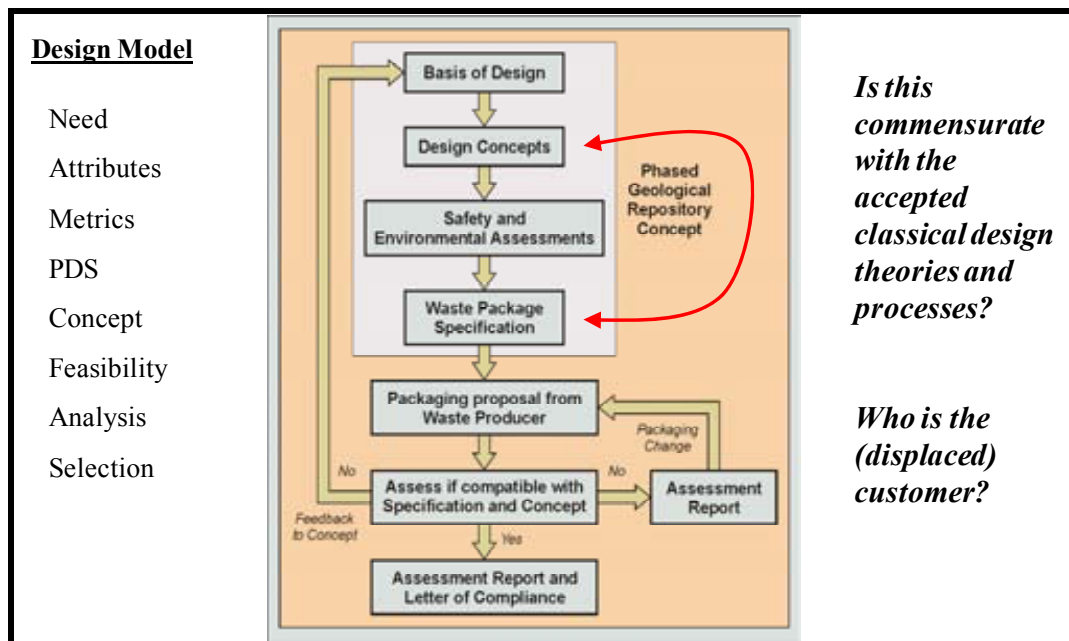


FIG. 6. Letter of compliance process (amended from [20]).

5. The safety case and the relationship to the design process

Traditionally, a safety case is a structured set of arguments in pursuit of a declared objective, at a given stage of development of plant, demonstrating long term integrity with minimum risk to people. This would also be the case for any deep repository or other solution. In order to minimize objective risk, the safety case should incorporate the following features:

- Multi-legged approach (with defence in depth, diversity and redundancy)
- Prevention, protection and mitigation
- Traceability, robustness, reproducibility of data
- Treatment and understanding of the uncertainties in (input) parameters
- Underlying knowledge and confidence building (e.g. intelligent customer)

Ideally, such arguments should not be presented “after the fact”, but they should be a direct result of the initial design case and FRs as suggested by Suh. In essence, the safety case should not be an after-thought, but it should be an integral, but lesser, part of the entire design process, in this case taking account the social issues and subjective risk. Under current practice, the sole requirement would be to demonstrate the chosen option satisfied the safety assessment principles (SAPS [21]), with public acceptance often placed last. In spirit, the approach is objective driven and does not focus upon the FRs suggested by Suh.

It should be noted that the SAPs (2006) do not consider in any substantive manner the design process and what it should be, despite ‘design’ being a very frequently used word in the document. Thus, in summary, there is a need to focus upon the FRs as outlined by design theory (latent principle). Otherwise, the unintended consequence is the overengineering of any proposed solution which may not be the most appropriate.

6. Observations and summary

The experience to date shows that the current progress has been slow, resulting by default in the necessity for long term supervised storage. This has involved much higher radiological and financial (and committed) costs with accumulating radioactive waste in supervised storage. Simultaneously, regulators have become uneasy about long delays (with the declining pool of personnel with

experience and detailed knowledge) and public opinion uneasy in leaving today's problem for future generations. This has led to CoRWM's recommendations with emphasis on the socio-technical solution of a deep repository. Most proposed solutions appear to focus on detailed technical issues based upon a "satisficing" approach¹¹ with the need to minimize the objective risk, but this is actually minor in comparison to the public's want of social exchange, demonstrable control, responsiveness and ability to reverse/change the disposal options. For example, the OECD [22] appears to place great emphasis on the "safety case" as driving the development process for deep repositories. This is also the case in [23] and [24]. These documents give "acceptance criteria" to encourage, in reality, a "satisficing" rather than a true BPM approach.

So what is going wrong with the process? Designers (and safety case authors) are often given criteria/parameters to which to brainstorm ideas for 'optioneering'. Often the acceptable option is driven by perceived safety case arguments rather than extending the design space. Thus, the absence of a design process extending the design space (or at least there is little evidence of this in the literature) is noted according to classical design theory. Some key design principles, concepts, tools and techniques are simply being missed. This may reflect reluctance by industry to take a wider view of the options as this may be seen as an unacceptable step backwards and economically unsustainable. There may also be a sense of waiting for technology to become available to provide other options such as incineration, reuse or recycling/reprocessing. However, such options will only become available in response to an identified market for the service: a 'Catch 22'.

In future, there is a need to encourage the use of a structured, integrated and fully-developed design process to promote effective solutions and "due diligence" for the hierarchy of wastes, etc. using 'early design' tools, in addition to those already used, to increase the 'design space' and to find a large number of potential options. Socioeconomic and political pressures are actually socio-technical issues as embodied by the concept of subjective risk and the need for social exchange. From a design perspective, this reflects a 'displaced customer pull or needs' approach and any solution must reflect this. Linking design theory to safety case management provides a stronger basis to reduce subjective risk and leads to better, longer term, accepted solutions (and probably less cost). Any safety case needs to be explicitly linked to FRs. Perhaps, in short, this can be written as risk of failure to achieve the design intent is a function of the design FRs, or more formally (subjective and objective) risk = f (design(FRs)).

REFERENCES

- [1] WHITE, I.F., et al., Assessment of Management Modes for Graphite from Reactor Decommissioning, European Commission Report EUR 9232 (1985).
- [2] H.M. Department of the Environment, Assessment of Best Practical Environmental Options for Management of Low- and Intermediate-Level Solid Radioactive Wastes, HMSO (1986).
- [3] OECD NUCLEAR ENERGY AGENCY, Post-Closure Safety Case for Geological Repositories: Nature and Purpose, Publication No. 3679, OECD/NEA, Paris (2004).
- [4] Committee on Radioactive Waste Management, Managing our Radioactive Waste Safely — CoRWM's Recommendation to Government, CoRWM 700 (2006).
- [5] WICKHAM, A.J., NEIGHBOUR, G.B., DUBOURG, M., The Uncertain Future for Nuclear Graphite Disposal: Crisis or Opportunity? Proc. of Nuclear Graphite Waste Management: Technical Committee meeting held in Manchester, United Kingdom 18–20 October 1999, IAEA-NGWM/CD 01-00120, IAEA, Vienna (2001).
- [6] NEIGHBOUR, G.B. (Ed.), Management of Ageing in Graphite Reactor Cores, ISBN-10: 0854043454; ISBN-13: 978-0854043453, RSC Publishing, Royal Society of Chemistry, Cambridge (2007).

¹¹ In decision making, 'satisficing' explains the tendency to select the first option that meets a given need or improves upon the existing solution and appears to address most needs rather than generate the "optimal" solution, i.e. incremental.

- [7] OECD NUCLEAR ENERGY AGENCY, The Roles of Storage in the Management of Long-Lived Radioactive Waste: Practices and Potentialities in OECD Countries, No. 6042, OECD/NEA, Paris (2006).
- [8] WYNNE, B., Methodology and Institutions: Value as Seen from the Risk Field, Published in Valuing Nature: Economics, Ethics and The Environment (FOSTER, J., Ed.), Raitledge London (1997) 135–152.
- [9] KEMP, R.V., BENNETT, D.G., WHITE, M.J., Recent Trends and Developments in Dialogue on Radioactive Waste Management: Experience from the UK, Environment International 32 (2006) 1021–1032.
- [10] WILLIAMS, D.R., What is Safe? The Risks of Living in a Nuclear Age, The Royal Society of Chemistry (1998).
- [11] National Statistics website, www.statistics.gov.uk/csi/nugget.asp?id=1208
- [12] BALL, D.J., Environmental Risk Assessment and the Intrusion of Bias, Environment International 28 (2002) 529–544.
- [13] PRICE, R., NEIGHBOUR, G.B., Private Communication (2007).
- [14] PUGH, S., Total Design: Integrated Methods for Successful Product Engineering, Addison-Wesley (1995).
- [15] PAHL, G., BEITZ, W., Engineering Design: a Systematic Approach (2nd Ed), Springer-Verlag (1996).
- [16] WALLIS, A., Incorporating Environmental Concepts into Design Methodology, Final Year Project Report, Department of Engineering, University of Hull (2005).
- [17] SUH, N.P., The Principles of Design, Oxford University Press (1990).
- [18] NEIGHBOUR, G.B., Private Communication (2007).
- [19] MEEHAN, A., What will we do with the Low Level Radioactive Wastes from Reactor Decommissioning? BNG Reactor Sites, RWIN Presentation (10 October 2006).
- [20] HARRIS, A., Application of Immobilisation Technologies in the Context of Letter of Compliance Process (amended), NDA/NIREX, RWIN Presentation (10 October 2006).
- [21] HSE, Safety Assessment Principles for Nuclear Facilities (2006).
- [22] OECD NUCLEAR ENERGY AGENCY, Confidence in the Long-Term Safety of Deep Geological Repositories: its Development and Communication, OECD/NEA, Paris (1999).
- [23] HSE, Nuclear Power Station Generic Design Assessment — Guidance to Requesting Parties (2007).
- [24] INTERNATIONAL ATOMIC ENERGY AGENCY, Geological Disposal of Radioactive Waste, IAEA Safety Standards Series, WS-R-4, IAEA, Vienna (2006).

Radiation damage in graphite — A new model

M.I. Heggie, I. Suarez-Martinez, G. Savini, G.L. Haffenden, J.M. Campanera

Chemistry Department, University of Sussex, Brighton, United Kingdom

Abstract. The standard model for interpretation of radiation damage of graphite invokes self-interstitials and vacancies and their aggregation to explain observed dimensional changes. Vacancies aggregate into lines which heal and contract the basal planes, interstitials aggregate into interlayer disks which expand the dimension perpendicular to the layers. Small clusters of interstitials (C_n , $n = 4 \pm 2$) appear which expand the interlayer distance, d_{002} , but for an unknown reason can disappear and not evolve into disks. First principles calculations show that these aggregations are improbable at low temperatures (below 250°C) and that the observed annealing at these temperatures would be impossible. Our calculations show the inadequacies and motivate a new, robust and atomistically based model. At low temperatures, point defects are immobile, but form sturdy links between planes which cause buckling. Since the planes are effectively ‘flexible but inextensible’, the crystal expands perpendicular and contracts parallel to the basal planes. At higher temperatures, radiation damage causes collisions with planes, which then fold. At all stages, point defects do form, but their aggregation effects are minority effects at all but the highest temperatures. This new model has major implications for the interpretation of Wigner energy.

The first atomic piles used graphite moderators, as have, subsequently, many civilian and military reactors. This made radiation damage in graphite an intense field of study in the third quarter of the last century. Damage was introduced by particulate radiation, most often by neutrons, and physical property changes were recorded. Example properties are electrical and thermal resistance, coefficient of thermal expansion and dimensional changes. Recent work on the formation of carbon onions, diamond and nanotubes under radiation or mechanical damage has reinvigorated this field ([1], [2]).

Standard defect characterization tools for semiconductors (spectroscopy and electron spin resonance) have strong limitations in graphite, so the link between atomic structure and macroscopic measurements has always been speculative. Weak beam transmission electron microscopy (TEM) picks out dislocations and hence can provide evidence in support of the standard model, since interstitial disks are faulted prismatic dislocation loops [3, [4]. However in recent times, high resolution TEM (HRTEM), which images graphite planes side on, applied to radiation damage in graphite and carbon fibres only shows evidence for bending and breaking of planes ([5], [6]), and little evidence for the appearance of new ones.

The standard model invokes interstitials and vacancies and their aggregation (with their own kind, largely avoiding annihilation with each other). Vacancy concentrations can be measured by etching — using oxygen at elevated temperatures each single vacancy can generate an etch pit visible by microscopy after decoration with gold. They are found to be an order of magnitude smaller than the estimated number of displacements per atom (d.p.a.) [7]. Interstitials which aggregate into prismatic loops can change crystal dimension, X_c , perpendicular to planes. The positive $\Delta X_c/X_c$ (also known as e_{zz}) is accompanied by smaller and negative $\Delta X_a/X_a$ (e_{xx}), parallel to the planes. The amount of change from loops is always reported as less than a half [4], and most often a tenth, of the measured change. In seeking to explain dimensional change as arising from redistribution of material, the standard model is confronted with a ‘dark matter’ problem, similar in nature to the cosmological one.

Let us focus on the experimental evidence for dimensional change and stored energy. Figure 1a is a schematic of dimensional changes in HOPG at different temperatures from Kelly and Brocklehurst.

Line shapes are linear to parabolic and do not saturate with dose above 250°C and sigmoidal below, i.e. dimensional change saturates.

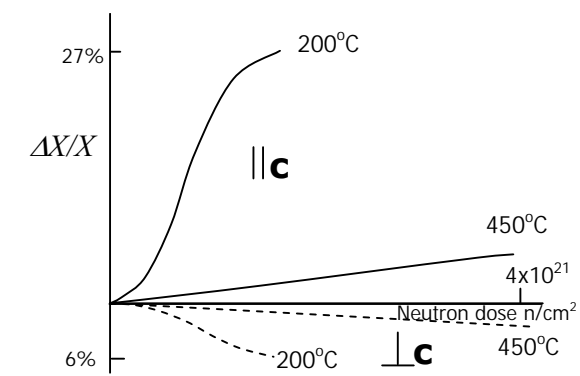


FIG. 1a: Schematic of fractional changes in dimensions ($\Delta X/X$) parallel to c (solid lines, $X=X_c$) and perpendicular to c (broken line, $X=X_a$) in HOPG with neutron dose ([2], [3]).

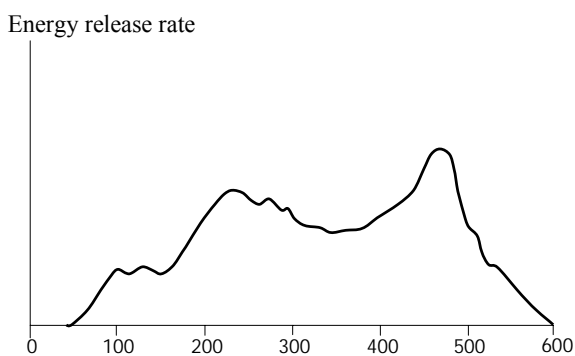


FIG. 1b. Annealing of radiation damage performed at 20 K [8] (original data from T. Iwata).

Radiation damage stores energy and historically this was thought to be largely in the form of point defect formation energies. Greater energy is stored at lower temperatures and for cryogenic irradiations this energy starts being released (annealed) on warming to liquid nitrogen temperature (77K) (Fig. 1b). Original speculations were that interstitials moved at these low temperatures and clustered into dimers, trimers etc. releasing energy during the clustering. This required that the interstitial migration energy be very small (e.g. the summary in [9] cites ‘measurements’ as low as 0.027 eV).

First principles modelling affords a new insight on the atomistic processes and density functional theory (DFT) within the local density approximation (LDA) has proven itself to be quantitative and predictive for carbon systems [10]. Our findings are these:

- (1) The migration energy of the interstitial is not low and, at 1.2 eV, is entirely consistent with the activation energy for formation of interstitial loops [3][4]. This is also confirmed by others [11].
- (2) point defect clusters do not give rise to greatly enlarged interlayer spacings. These large spacings did arise in early simplistic models of the interstitial and allowed small angle cold neutron scattering measurements [12] to be interpreted inappropriately as due to a homogeneous distribution of C_n clusters, $n = 4 \pm 2$. There are volume changes but these are small and they cannot account for large differential dimensional changes seen at, for instance, 200°C (Fig. 1a).

What has become clear in recent work [10] is that point defects give rise to strong interlayer bonds — this applies to the self-interstitial which has the spiro structure and to the interplanar divacancy. Another of these interlayer defects is the intimate Frenkel pair, which was shown to self-destruct and release ca. 10 eV of energy at 200°C under standard experimental conditions for the analysis of stored energy [13]. There is usually a dominant peak recorded at 200°C in these experiments (see Fig. 1b) at 473 K) and recent remarkable high resolution TEM work has confirmed that there are visible interlayer defects which anneal at this temperature in double walled nanotubes [14].

The effect of these links can be to link together plane segments of different length, and the result is buckling. It is much easier to compress the longer plane by buckling than the shorter one by stretching — in fact the shorter plane practically preserves its length. Figure 2a depicts a superlattice to demonstrate this effect. The supercell orientations are $\langle 2\bar{1}\bar{1}0 \rangle$, $\langle 01\bar{1}0 \rangle$ and $\langle 0001 \rangle$, containing two graphene layers (original height, $|c| = 0.67\text{nm}$, width, $10|a| = 2.46\text{ nm}$ and depth, $\sqrt{3}|a| = 0.426\text{ nm}$). One plane is shortened by a lattice vector giving a width of $9|a|$ and the shortening is accommodated by

buckling. Optimization of superlattice vectors and atom positions reveals that: 1) the buckling wavelength became the largest possible (the cell width), 2) dimensional changes of $\Delta X_a/X_a = -5\%$ and $\Delta X_c/X_c = 63\%$ were obtained after simultaneous geometry and superlattice vector optimization (compared with undistorted graphite of width equal to the mean of the two layer widths). Next we discuss the nature and origin of such a structure.

Recall that an edge dislocation can be regarded as an extra half-plane of material (of width equal to the Burgers vector, \mathbf{b} , whose termination is conventionally marked with the symbol \mathbf{T}). The half-plane can be any crystal plane and must not be confused with the graphene planes of graphite. In a perfect basal edge dislocation it is either a $(1\bar{1}00)$ or $(2\bar{1}\bar{1}0)$ plane, both of which are perpendicular to the graphene planes (partial dislocations are also possible). Within the supercell, the longer plane can be regarded as a dipole of basal edge dislocations separated along \mathbf{c} (i.e. their climb direction). Where the extra half-planes overlap is a column of extra material.

Our artificial supercell of Fig. 2a requires an infinite array of these climb dipoles (or equivalently a dipole of horizontal grain boundaries). It is then clearly capable of reproducing the HOPG data, with adjustments for wavelength. This structure within the supercell is a perfect basal edge dislocation dipole separated in the climb direction and it was obtained computationally by atom removal, which implies the difficult process of aggregation of vacancies. However, Fig. 2b shows how a similar structure can be obtained more physically by dislocation glide combined with interlayer pinning at a point defect. The cell of Fig. 2a was inverted and the layers connected (short to long and vice versa) to the original cell to yield a doubling of the supercell width. Spiro-interstitials were introduced as pinning points at the short–long junctions. The amount of dimensional change ($\Delta X_a/X_a = -4\%$, $\Delta X_c/X_c = 48\%$) obtained after superlattice vector and geometry optimization is clearly still compatible with that achieved in experiment below 250°C . The amount of energy stored is 16.5 eV per unit cell. Approximately 2×5.7 eV should come from the two undistorted interstitials and the rest, 5.1 eV, from buckling and internal stresses — i.e. nearly one third of the energy stored in this cell is in the buckling.

The amount of shear (and hence, buckling, dimensional change and stored strain energy) that can be withstood by the pinning points is a maximum at 0K and decreases through thermal activation to zero around 250°C . It is patently compatible with the characteristic low temperature line of Fig. 2a and firmly establishes the principle. This configuration can be obtained by two basal edge dislocations gliding together on neighbouring planes and being held together by interlayer pinning at point defects.

At 200°C , the interstitial becomes mobile and the intimate Frenkel pair begins to annihilate, removing the pinning and buckling. In measurements of Wigner energy [15], about 90% of stored energy is released by 300°C presumably from this combination of intimate Frenkel pair annihilation and buckling removal, combined with some ‘standard model’ processes. The standard model applied to stored energy contains the unhelpful idea that there is a spectrum of trap release energies for interstitials that gives rise to the progressive release of stored energy during annealing as in Fig. 1b. In the model here, it is clear that the lower temperatures of irradiation decrease the depinning rate and enhance the accumulation of internal stresses from buckling. Progressive annealing occurs as the unbuckling reduces the stresses on the pinning points and which thus require increasing thermal activation in order to release. At 200°C the internal stresses are near zero and unpinning must be entirely by thermal activation (1.2–1.4 eV).

For any irradiation temperature between 0°K and 200°C it is found that annealing under usual conditions commences ca. 50°C above the irradiation temperature [16] — this is the point at which thermally activated unpinning (barrier 1.2 eV) is increased by a factor of a thousand over the rate during irradiation at, say, room temperature. Note that 1.2 eV has long been used to characterize the thermal annealing concomitant with irradiation in Materials Test Reactor data [15].

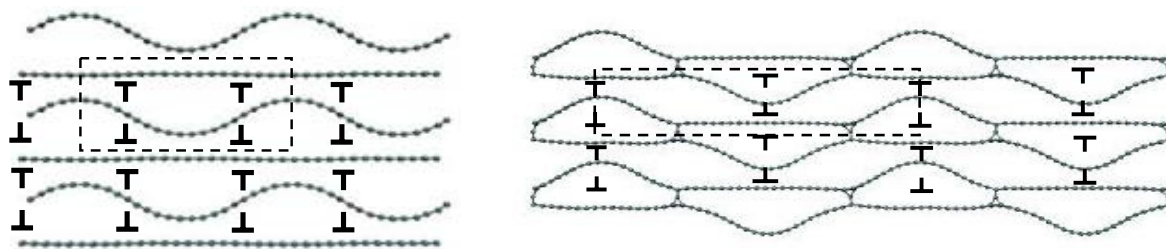


FIG. 2a. Superlattice of climb dipoles of basal edge dislocations. FIG. 2b. Buckled graphite held by interlayer pinning points (in this case, spiro-interstitials).

(Dislocations represented by the T symbol and the supercell is depicted by broken lines.)

Finally we note one curious, previously unexplained anomaly. Irradiation causes electrical resistance parallel to the planes to increase and perpendicular to decrease. It would not be unnatural to associate these changes with the cross-linking defects [10]. Cross-linking bonds to host atoms convert atoms to sp^3 hybridisation and disrupt the in-plane π system, scattering charge carriers within planes. At the same time they link planes electrically, increasing c axis conductivity. Annealing generally reverses these changes — we argue through progressive elimination of cross-linking defects. However, in the first stages of annealing, an increase in basal resistivity and a decrease in c -axis resistivity is observed just as though the irradiation were being continued [18]. There is no current explanation for this, but Fig. 3 offers a compelling illustration of how the process of unbuckling will create new cross-links in the first stages of annealing and give rise to this anomaly. Interstitials created in buckled regions with large interlayer separations cannot cross-link — they remain associated with one plane, i.e. as adatoms. A small temperature rise enables the buckling to reduce by the slip of planes past pinning points. In so doing, the interplanar distance decreases and allows new cross-links to form — thus the annealing gives the appearance of increasing (rather than reducing) radiation damage.

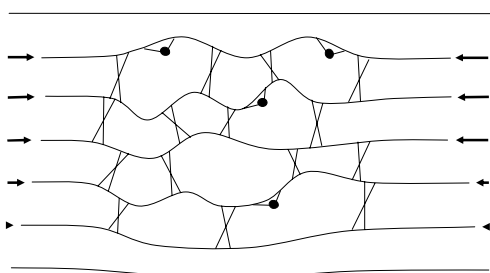


FIG. 3a. Schematic post cryo-irradiation. Buckling caused by spiro-interstitials (represented by crosses). Severe buckling leaves adatoms unable to cross-link (black circles). Arrows indicate basal contraction forces.

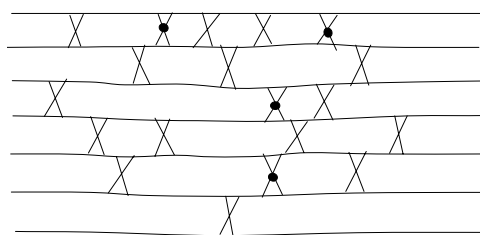


FIG. 3b. After short anneal. 'New' interstitials, i.e. cross-linking, defects appear (crosses with black circles).

Now we turn to high temperature irradiation. Here, the standard model appears plausible and its microscopic processes probably do occur at a reasonable rate. It has been reconciled quantitatively with electron microscope observations of dislocation loops [3] at high temperatures (above 900°C). These models invoke an effective interstitial migration energy of 1.2 eV, in complete agreement with our findings (although this migration energy appeared baffling at the time, because it was thought to be improbably high).

However, there are substantial problems with the standard model. Loops and lines must be nucleated and grow, yet there is no evidence for nucleation discontinuities in dimensional change [4]. TEM images of loops reveal that the density of loops can be an order of magnitude lower than that necessary for the recorded dimensional change [4]. The near volume conserving nature of Fig. 1a down to moderate temperatures (450°C) would require either that the migration of I and V were not rate-

limiting or that their rates were equal. Annealing this damage would be very difficult (requiring release of V and/or I from large clusters), making it irreversible at moderate temperatures.

In addition, there is currently no theory for irradiation creep — the remarkable property of graphite under irradiation that it can yield to low applied stresses even at temperatures as modest as 300°C [19].

A model that does not have these problems, invokes similar concepts to the low T model and offers a link with irradiation creep is based on basal edge dislocations which are not trapped by interlayer pinning points, but instead mutually trap each other. Figure 4 illustrates the process for two sets of four basal edge dislocations which are forced by neutron collisions to pile up and glide past each other on nearby planes. The result is a ‘ruck and tuck’ defect (shown schematically in 4a), which has two alternate descriptions in dislocation theory. In addition to being considered as a pile up of climb dipoles (Fig. 4b, where the dislocations are $\mathbf{b} = \frac{1}{3} a \langle 11\bar{2}0 \rangle$, $\mathbf{l} = \langle 1\bar{1}00 \rangle$), it can also be an unfaulted climb dipole (Fig. 4c, where the dislocations are $\mathbf{b} = c \langle 0001 \rangle$, $\mathbf{l} = \langle 1\bar{1}00 \rangle$).

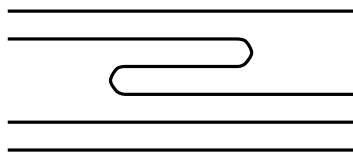


FIG. 4a.
Ruck and tuck defect
(schematic). The relaxation of
the planes is not shown.

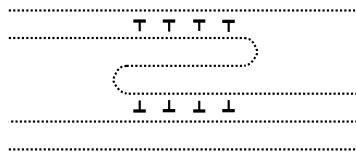


FIG. 4b.
Pile up of basal
edge climb dipoles.
T symbols are dislocations,
graphene planes are dotted.

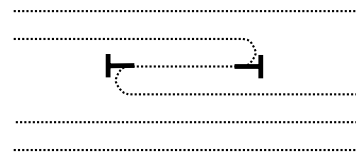


FIG. 4c.
Unfaulted climb dipole of
prismatic dislocations.
T symbols are dislocations,
graphene planes are dotted.

Thus, formation of a prismatic climb dipole, which is close in nature to the loops of the standard model and is normally regarded as requiring climb via point defect migration, can be achieved by basal glide alone. This is a very important point: in a layered material, the glide of basal edge dislocations can perform mass transport.

The ruck and tuck formation process can be much more easily reversible than diffusive mechanisms. At very high damage temperatures (> 800°C), 60–80% of the dimensional change is unannealable [20], indicating a substantial role for the standard model. At lower temperatures, it is almost completely annealable in pyrolytic carbons, compatible with dominance of the new model.

We note that the single dislocation dipole, especially if it has a multiple Burgers vector, could restructure into the ‘ruck and tuck’ defect of Fig. 4a, but it can also be created by the collision of two or more oppositely signed basal edge dislocations gliding towards each other on nearby planes.

This defect could also arise by a progressive pile-up of basal dislocations. Pile-up is normally resisted by the Peach Köhler force between dislocations of like-sign, but in graphite this force is strongly diminished by allowing perpendicular expansion. Figure 5 illustrates how passage of a single basal dislocation can grow the prismatic dipole. It does so by ‘depositing’ a segment of its extra half-plane at the ruck and tuck defect. Two edge dislocations of opposite sign moving in opposite directions on neighbouring glide planes can nucleate one of these defects. Pairs gliding on more distant planes will give multilayer folds (for brevity not considered here).

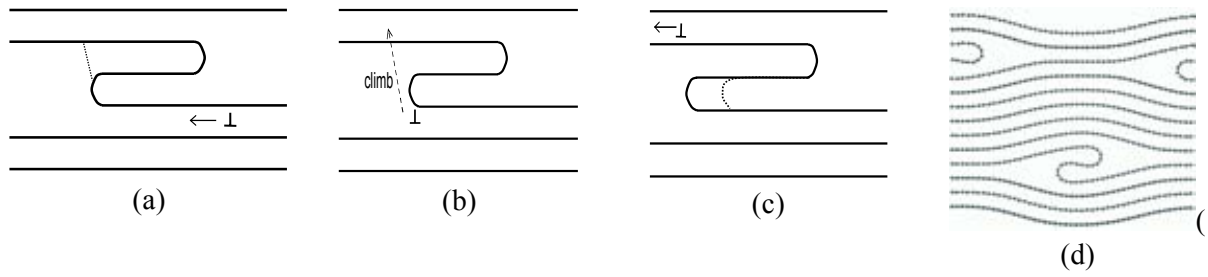


FIG. 5 (a–c): A basal edge dislocation sweeping right to left (a), climbs a plane (b) and extends the ruck and tuck defect (c). Note that compression along c will suppress this climbing effect, tension along c will enhance it. The dotted line in 5(a) indicates where the ruck and tuck defect might pinch off to form a nanotube after thermal treatment. Figure 5(d): Orthorhombic superlattice of ruck and tuck defects along the boat direction. There are 80 C added in two sets of 40 C in a unit cell which initially has 1104C.

Figure 5(d) is an example ruck and tuck defect optimized by the Universal Force Field [21] implemented in Cerius²® which has been found to give principal elastic constants close to those of DFT/LDA calculations. There are 80 added atoms, and the overall formation volume is $10\,394\text{ \AA}^3$ while the dimensional change from a comparable perfect graphite cell is $\Delta X_a/X_a = -9\%$, $\Delta X_c/X_c = 18\%$. The amount of energy stored and formation volume are 0.46 eV and 1.16 atomic volumes per added atom, but recall that such atoms arise from basal dislocation motion, not from Frenkel pairs.

Putting the two models of graphite planes for different temperatures together (Figs 2a, 5d), one can see that they are related — they are different geometries of the same topological defect (a prismatic dislocation dipole or Frank loop if in closed form) that are stable or metastable depending on the imposed dimensions. The ruck and tuck defects require a long mean free path to form, which is hindered by the pinning points at low temperatures. We note that at high fluences the Wigner peak at 200°C disappears and the stored energy becomes stable to much higher temperatures. It is possible that overlapping radiation volumes allow unpinning, increase the mean free path of basal dislocations and allow formation of ruck and tuck defects which are stable to higher temperatures.

Clearly, the link between radiation damage and mechanical treatment of graphite becomes obvious and many of the defects suggested here are visible in TEM of ball-milled graphite [22]. This link was made earlier, but in reverse, trying to draw ideas from the standard model of radiation damage and apply them to ball milling [23]. Furthermore, it is interesting to speculate that the ruck and tuck defect could in some circumstances pinch off during annealing (Fig. 5a) to produce a nanotube, affording a direct mechanistic explanation for the mechanochemical production of nanotubes [1].

Finally, we consider the forces which create and move basal dislocations. Each collision with a graphite atom of the ca. 1 MeV neutrons typical of ^{235}U fission transfers on average ca. 50 keV to the primary knock-on atom or P.K.A. [24]. Unlike the neutron, the P.K.A. interacts strongly with the lattice and produces a dense, localised ($\approx 10^5\text{ \AA}^3$) cascade of damage within 10^{-14} s , while the neutron flies away from the locality.

In the standard model the momentum and energy transfer goes into thermal excitation and Frenkel pair production (estimated two thirds distant and one third intimate pairs [8]). There is no description of momentum conservation. Momentum transfer is into lattice vibrations. Amplitudes will be high and vibrations that involve interlayer shear will be important. Formally, these vibrations, which involves phonons at low amplitudes, can alternatively be represented as the creation and movement of basal dislocations (in glide pairs) at high amplitudes. They then bear the same relationship to acoustic shear waves in the crystal as solitary waves do to surface waves on water. Figure 6 illustrates two scenarios (dominant momentum transfer perpendicular to the planes and parallel to the planes) instants after a single collision event. Transfer parallel (Fig. 6a) is substantial for two reasons — (i) it is aligned with the motion of the outgoing phonon/dislocation and (ii) it is not limited by displacement of the PKA, which could limit momentum transfer.



FIG. 6a. Momentum transfer parallel to graphene planes, emitting climb dipoles of edge dislocations

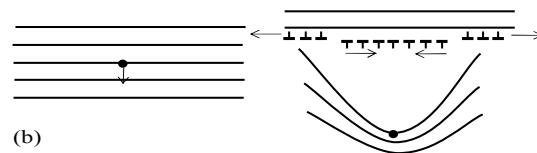


FIG. 6b. Momentum transfer perpendicular to planes, emitting basal edge dislocations from the impact.

It is the neutron collision which controls the overall deposition of momentum into a locality, but subsequent cascade collisions can mean that the momentum is imparted to several layers (and not just one as depicted in the Figures). This corresponds to climb dipoles gliding on glide planes separated by several interlayer distances.

The expanding dislocations so created can travel long distances because the Peierls stress is essentially zero [25] and thus phonon damping can be neglected. The occurrence and growth of basal dislocations during irradiation has been reported several times [26] but it appears they are regarded as such a common place that they have not been pursued in relation to dimensional change.

It appears likely that there can be some ruck and tuck formation coming from single neutron collisions (as for example the expanding climb dipoles of Fig. 6a) which must be first order in neutron collisions and give an initial linear dimensional change. But as collision density increases, expanding dislocation loops from different collisions interact and cause dimensional change which is then second order in neutron collisions and hence gives quadratic dimensional change.

In conclusion, through a combination of first principles and other calculations and analysis of literature and the standard model, we have presented a strong case for a re-interpretation of radiation and mechanical damage in graphite (and layered materials in general) in terms of basal dislocations, which are either pinned or mutually trapped. These effects should be common to other important layered materials, such as clays, ceramic semiconductors, MgB_2 and h-BN.

METHODS

The AIMPRO code [27] is used with a pdpp basis (four Gaussians per atom, each combined with an expansion up to $l = 1$ in spherical harmonics (an $l = 2$ function is added to one of the exponents)) and HGH pseudopotentials [28]. Special k points given by Monkhorst-Pack algorithm [29].

ACKNOWLEDGEMENTS

We gratefully acknowledge support from British Energy Generation Ltd and discussions with M. Bradford and A. Steer. The views expressed in this paper are those of the authors and do not necessarily represent the views of British Energy Generation Ltd.

REFERENCES

- [1] CHEN, Y., et al., The nucleation and growth of carbon nanotubes in a mechano-thermal process, *Carbon* 42 (2004) 1543–1548.
- [2] BANHART, F. Irradiation effects in carbon nanostructures, *Reports of Progress in Physics* 62 (1999) 1181–1221.
- [3] BROWN, L.M., KELLY, A., MAYER, R.M., The influence of boron on the clustering of radiation damage in graphite, II. Nucleation of interstitial loops, *Philosophical Magazine* 19 (1969) 721–741.

- [4] REYNOLDS, W.N., THROWER, P.A., The nucleation of radiation damage in graphite. *Philosophical Magazine* **12** (1965) 573–593.
- [5] MUTO, S., TANABE, T., Damage process in electron-irradiated graphite by transmission electron microscopy, I. High-resolution observation of highly graphitized carbon fibre, *Philosophical Magazine A* **76** (1997) 679–690.
- [6] ASTHANA, A., et al., Investigations on the structural disordering of neutron-irradiated highly oriented pyrolytic graphite *Journal of Applied Crystallography* **38** (2005) 361–367.
- [7] HINMAN, G.W., HAUBOLD, A., J.O., G., LAYTON, J.K., Vacancies and interstitial clusters in irradiated graphite, *Carbon* **8** (1970) 341–351.
- [8] KELLY, B.T., *The Physics of Graphite* (Applied Science, London, 1981).
- [9] THROWER, P.A., MAYER, R.M., Point defects and self-diffusion in graphite. *Physica Status Solidi (a)* **47** (1978) 11–37.
- [10] TELLING, R.H., EWELS, C.P., EL-BARBARY, A.A., HEGGIE, M.I., Wigner defects bridge the graphite gap, *Nature-Materials* **2** (2003) 333–337.
- [11] LI, L., REICH, S., ROBERTSON, J., Defect energies of graphite: Density-functional calculations. *Physical Review B* **72** (2005) 184109.
- [12] MARTIN, D.G., HENSON, W., Scattering of long wavelength neutrons by defects in neutron irradiated graphite, *Philosophical Magazine* **9** (1964) 659–672.
- [13] EWELS, C.P., et al., Metastable Frenkel pair defect in graphite: source of Wigner energy. *Physical Review Letters* **91** (2003) 025505.
- [14] URITA, K., et al., In situ observation of thermal relaxation of interstitial-vacancy pair defects in a graphite gap, *Physical Review Letters* **94** (2005) 155502-4.
- [15] LEXA, D., KROPF, A.J., Thermal, structural, and radiological properties of irradiated graphite from the ASTRA research reactor — Implications for disposal, *J. Nucl. Mater.* **348** (2006) 122–132.
- [16] PRIMAK, W., Fast-neutron damaging in nuclear reactors: its kinetics and the carbon atom displacement rate, *Physical Review* **103** (1956) 1681–1692.
- [17] BELL, J.C., et al., Stored Energy in the graphite of power-producing reactors, *Philosophical Transactions of the Royal Society* **254** (1962) 361–395.
- [18] IWATA, T., NIHIRA, T., MATSUO, H., Irradiation and annealing effects on the c-axis electrical resistivity of graphite, *J. Physical Society of Japan* **36** (1974) 123.
- [19] ENGLE, G.B., EATHERLY, W.P., Irradiation behaviour of graphite at high temperature, *High Temperatures — High Pressures* **4** (1972) 119–158.
- [20] PRICE, R.J., BOKROS, J.C., Annealing of neutron-irradiated pyrocarbons, *Carbon* **9** (1971) 555–572.
- [21] RAPPE, A., et al., a full periodic-table force-field for molecular mechanics and molecular dynamics simulations. *Journal of the American Chemical Society* **114** (1992) 10024–10035.
- [22] HUANG, J.Y., HRTEM and EELS studies of defects structure and amorphous-like graphite induced by ball-milling, *Acta Metallurgica* **47** (1999) 1801–1808.
- [23] LACHTER, J.L., BRAGG, R.H., Interstitials in graphite and disordered carbons, *Physical Review B* **33** (1986) 8903–8905.
- [24] KINCHIN, G.H., PEASE, R.S., *Reports of Progress in Physics* **18** (1955) 1–51.
- [25] TELLING, R.H., HEGGIE, M.I., Stacking fault and dislocation glide on the basal plane of graphite. *Philosophical Magazine Letters* **83** (2003) 411–422.
- [26] THROWER, P.A., The study of defects in graphite by transmission electron microscopy, *The Chemistry and Physics of Carbon* (Walker, P.L., Jr., Ed.) **5** (1969).
- [27] BRIDDON, P.R., JONES, R., LDA calculations using a basis of Gaussian orbitals, *Physica Status Solidi B-Basic Research* **217** (2000) 131–171.
- [28] HARTWIGSEN, C., GOEDECKER, S., HUTTER, J., Relativistic separable dual-space Gaussian pseudopotentials from H to Rn. *Physical Review B* **58**, 3641–3662 (1998).
- [29] MONKHORST, H., PACK, J., Special points for Brillouin-zone integrations, *Physical Review B* **13** (1976) 5188–5192.

Thermodynamic modelling of an irradiated reactor graphite thermochemical treatment process

S.A. Dmitriev^a, O.K. Karlina^a, V.L. Klimov^a, G.Yu. Pavlova^a, M.I. Ojovan^b

^aState Unitary Enterprise SIA “Radon”, Moscow, Russian Federation

^bEngineering Materials Department, University of Sheffield, United Kingdom

Abstract. Operation of uranium-graphite reactors resulted in production of significant amounts of irradiated graphite waste in form of dust, powder, chips and lumps. This waste resulted both from technological operations and incidents and contains inclusions of metallic and ceramic nuclear fuel and other reactor components. This waste contains activation products such as ¹⁰Be, ¹⁴C, ³⁶Cl, ⁴¹Ca and ⁵⁹Ni, actinides in fuel particles such as ^{234,236,238}U, ²³⁷Np, ^{239,240,242}Pu, ²⁴³Am and ^{242,243,244}Cm, decay products such as ^{134,135,137}Cs, ⁹⁰Sr, ¹⁵¹Sm and ^{154,155}Eu. Disperse radioactive wastes intended for long term storage and disposal in Russia must be solidified accordingly to Russian regulatory requirements. To solidify disperse irradiated graphite waste we suggested to use self-propagating high temperature synthesis (SHS) based on exothermic chemical reaction: $3C(\text{graphite}) + 4Al + 3TiO_2 = 3TiC + 2Al_2O_3$. The product of this reaction is a sintered corundum-titanium carbide ceramics retaining waste radionuclides including chemically bounded biologically hazardous radionuclide ¹⁴C. The potential emission of ¹⁴C during the SHS reaction can be assessed using thermodynamical modelling of irradiated reactor graphite thermochemical treatment process. Thermodynamic analysis of the system C–Al–TiO₂ gives data on optimal composition and permitted deviations of component fractions. We found component proportions when inadmissible compounds are formed in the final ceramic product such as hydrolytically unstable oxycarbides and aluminium carbides. Based on well-consistent data from thermodynamic modelling and experimental results it was found that REE (Y, La, Ce, Nd, Sm, Eu, Gd) in the system C–Al–TiO₂ form in the final ceramic product chemically durable aluminates with the structure of perovskite, β-alumina and garnet.

1. Introduction.

There were built and put into operation 13 industrial uranium-graphite reactors during 1948–1965 in the former USSR [1]. A part of these reactors were only intended to production of weapon plutonium, others in addition to plutonium production generated heat and electrical power for industrial and civil purposes (Table 1). The reactors shut down need decommissioning.

Table 1. Uranium-graphite reactors in Russia

Facility (location)	Name	Coolant circuit	Start operating	Shut down
PO «Mayak» (Ozersk)	A	Running	1948	1987
	AI (IP)	Same	1951	1987
	AB-1	Same	1949	1989
	AB-2	Same	1951	1990
	AB-3	Same	1952	1990
Ore mining and processing enterprise (Zheleznogorsk)	OK-120	Same	1958	1992
	OK-135	Same	1962	1993
	OK-206	Closed	1961	–
Siberian Chemical Combine (Seversk)	I-1	Running	1955	1990
	EI-2	Closed	1958	1990
	OK-140	Same	1961	1992
	OK-204	Same	1964	–
	OK-205	Same	1965	–

Operation of uranium-graphite reactors resulted in production of significant amounts of irradiated graphite waste in form of dust, powder, chips and lumps. This waste resulted both from technological operations and incidents and contains inclusions of metallic and ceramic nuclear fuel and other reactor components. This waste contains activation products such as ^{10}Be , ^{14}C , ^{36}Cl , ^{41}Ca and ^{59}Ni , actinides in fuel particles such as $^{234,236,238}\text{U}$, ^{237}Np , $^{239,240,242}\text{Pu}$, ^{243}Am and $^{242,243,244}\text{Cm}$, decay products such as $^{134,135,137}\text{Cs}$, ^{90}Sr , ^{151}Sm and $^{154,155}\text{Eu}$. Similar waste can be produced when cleaning-decontaminating surfaces of graphite blocks heavily contaminated by radionuclides.

Among radionuclides present in irradiated graphite the long lived radionuclide ^{14}C with half-life of 5730 years is particularly hazardous to biosphere. ^{14}C is readily incorporated into organic matter molecular structure of leaving species including humans (Fig. 1), moreover it enters into RNA and DNA molecules [2, 3]. This work is primarily devoted to isolation of ^{14}C from environment during the treatment of irradiated reactor graphite.

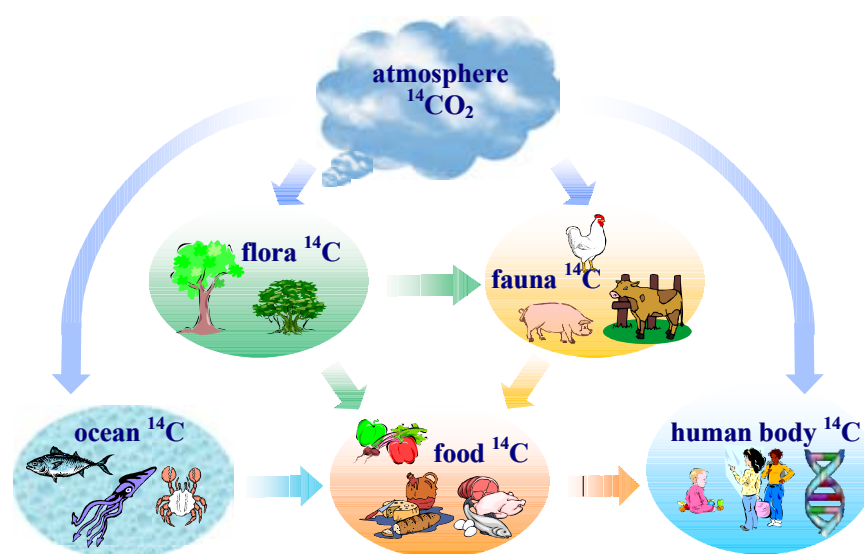
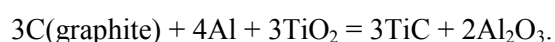


FIG. 1. Schematic of ^{14}C ingress into human body.

2. Thermochemical treatment method: Thermodynamical analysis

Incineration of irradiated graphite would be a final solution of graphite waste [4], however this option is not feasible as the genetic consequences of $^{14}\text{CO}_2$ emissions are currently weakly understood. Absorption of CO_2 including $^{14}\text{CO}_2$ produced on graphite incineration using aqueous solutions or molten salts [5–10] make the technological process too complex and results in generation of new waste streams which require further processing. A feasible processing technology is particularly important for irradiated graphite fine powders contaminated with nuclear fuel fragments and fission products. Disperse radioactive wastes intended for long term storage and disposal in Russia must be immobilized (consolidated) accordingly to Russian regulatory requirements which were developed accounting for International Atomic Energy Agency (IAEA) recommendations [1].

To solidify disperse irradiated graphite waste we suggested to use self-propagating high temperature synthesis (SHS) based on exothermic chemical reaction:



The product of this reaction is a sintered corundum-titanium carbide ceramics retaining waste radionuclides including chemically bounded biologically hazardous radionuclide ^{14}C [12–15]. As a result, graphite, including carbon ^{14}C , is chemically bounded into stable titanium carbide. High temperature is developed due to reaction of titania metallothermic reduction and carbide formation. As

a consequence, partial evaporation and dissociation of the reaction products and deviation from the stoichiometric equilibrium inevitably occur.

A detailed thermodynamic simulation performed for the abovementioned reaction and C–Al–TiO₂ system is aimed at determination of reaction temperature and phase composition of the reaction products [16–21]. The technology aspects are not discussed in detail.

Thermodynamic simulation is, in essence, a numerical experiment and, at present, is widely used for prediction and analysis of characteristics of high temperature processes and reactions in multicomponent systems. The software TERRA [22] involving the IVTANTHERMO database [23–27] on thermodynamic properties of chemical substances was used for thermodynamic simulation in this paper.

As usual, in the all thermodynamic calculations the gaseous phase was treated as the ideal gas and a formation of the following species was considered: O, O₂, C, C₂, C₃, CO, CO₂, C₂O, C₂O₃, Al, Al₂, AlO, AlO₂, Al₂O, Al₂O₂, Al₂O₃, AlC, AlC₂, Al₂C₂, Ti, TiO, and TiO₂. The C, Al, Al₂O₃, Al₂OC, Al₄O₄C, Al₄C₃, Ti, TiO, TiO₂, Ti₂O₃, Ti₃O₅, Ti₄O₇, and TiC species were taken into account as condensed phase constituents. Not found in the available databases, thermodynamic functions of Al₂OC and Al₄O₄C have been calculated especially [28]. Thermodynamic functions of TiC were taken from the NIST-JANAF tables [29]. The calculation results are shown in Figs 2 and 3 as ternary diagrams.

According to calculations, maximum equilibrium temperature in the C–Al–TiO₂ system is 2327 K, which corresponds to melting temperature of Al₂O₃.

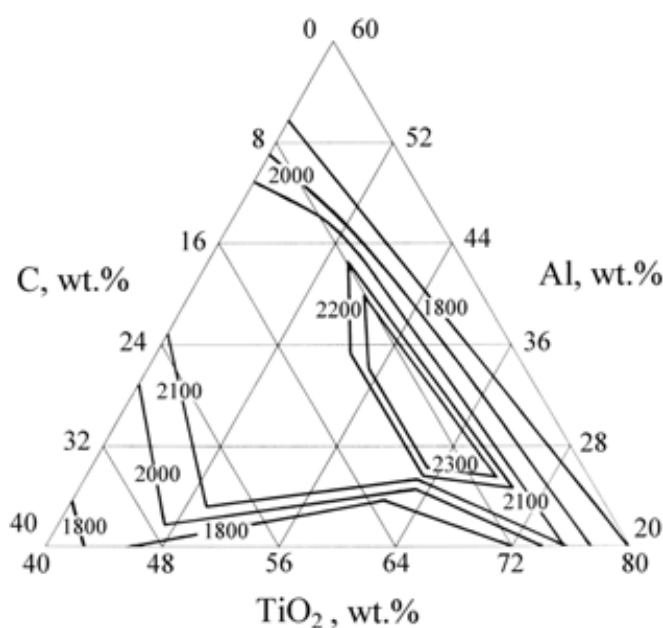


FIG. 2. Calculated equilibrium isotherms (temperature in K) in the C–Al–TiO₂ reacting mixtures at pressure of 0.1 MPa.

Equilibrium phase compositions in the reacting C–Al–TiO₂ mixtures are shown in Figure 3. As can be seen, the domain of mixture formulations, providing a formation of the stable chemical compounds such as TiC, Al₂O₃ and Ti_xO_y, is rather wide (areas 9–12 on the diagram), but only stoichiometric area 9 contains Al₂O₃ and TiC with no titanium oxides. At high content of carbon in the starting batch, the aluminium oxycarbides, Al₂OC and Al₄O₄C, are formed along with the aluminium carbide, Al₄C₃.

The mixture formulations corresponding to diagram areas 1–8 are unsuitable for thermochemical treatment of graphite due to the presence of elemental C, Al, Ti, aluminium carbide and oxycarbides.

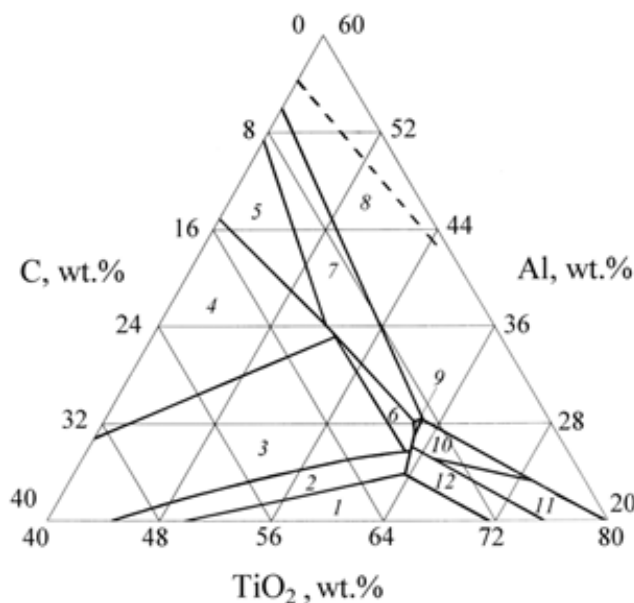


FIG. 3. Calculated equilibrium phase composition of condensed reaction products in the reacting C–Al–TiO₂ mixtures at pressure of 0.1 MPa.

Phase areas: 1 – Al₂O₃, TiC, Ti₂O₃, C; 2 – Al₂O₃, TiC, C; 3 – Al₂O₃, TiC, Al₄O₄C, C; 4 – Al₄O₄C, Al₂OC, TiC, C; 5 – Al₄O₄C, Al₂OC, TiC, Al; 6 – Al₂O₃, Al₄O₄C, TiC; 7 – Al₂O₃, TiC, Al₄O₄C, Al; 8 – Al₂O₃, TiC, TiO, Al; 9 (stoichiometry) – Al₂O₃, TiC; 10 – Al₂O₃, TiC, TiO; 11 – Al₂O₃, TiC, TiO, Ti₂O₃; 12 – Al₂O₃, TiC, Ti₂O₃.

The aluminium carbide, Al₄C₃, and aluminium oxycarbides, Al₂OC and Al₄O₄C, hydrolyze easily in the end reaction products.

Table 2 shows the equilibrium composition of the condensed phases in the reacting mixtures in the system C–Al–TiO₂. Composition of the combustion products are shown for individual areas of the phase diagram of Fig. 3. From these data one can conclude that the gaseous phase is present in the combustion products of C–Al–TiO₂ system. The main gaseous products are resulting from the thermal dissociation of aluminium oxide e.g. Al, Al₂, Al₂O as well as oxidation of graphite e.g. CO and CO₂. Alumina thermal dissociation products do not condense nearby the reaction zone when they pass through pores of ceramic matrix formed by SHS. The main carrier of carbon in the gaseous phase is CO. The content of CO₂ in the gas phase formed is several orders of magnitude lower compared CO one. The yield of CO sharply increases when the content of graphite in the initial mixture deviates from stoichiometrical, which is ~9 mass%. When the content of graphite is kept constant (~9 mass%) and the content of Al in the batch changes within 28–36 mass% and that one of titanium dioxide within 63–55 mass% the temperature of reactions remains about 2 327 K (Fig. 2). The concentration of CO in the reaction products in this case remains as low as ~10⁻⁵–~10⁻⁶ mass%. This amount corresponds to a carry-over of carbon in form of both CO and CO₂ as high as ~10⁻⁵–~10⁻⁶ mass% relatively to the carbon content in the initial batch. Taking the content of ¹⁴C in the irradiated reactor graphite as high as ~10⁻³ mass% [30], we can assess the emission of ¹⁴C during the SHS of carbide-corundum ceramics as high as ~10⁻⁹ g per 1 kg of irradiated graphite.

Table 2. Equilibrium temperature and composition of the products of combustion of mixtures at individual points of the phase diagram in Fig. 3 [21]

Area of the phase diagram												
Component	1	2	3	4	5	6	7	8	9	10	11	12
Component content in the initial mixture C/Al/TiO ₂ , mass%												
15/20/65	16/24/60	14/31/55	14/36/50	12/40/48	9/36/55	6/32/62	9/36/62,9	8/26/66	6/23/71	11/23/66		
Equilibrium temperature, K												
1648	2010	2171	2297	2354	2319	2327	2154	2328	2326	2177	1903	
Component volume content in the gas phase, %												
CO	0,9998	0,9999	0,9892	0,8465	0,5133	0,8716	0,1511	0,0015	0,0065	0,9967	0,9997	0,9998
CO ₂	0,00020	0,00002	0,00001	0,00001	-	0,00001	-	-	-	0,00013	0,00017	0,00019
Al	-	-	-	0,0356	0,0912	0,0237	0,1136	0,1629	0,1329	0,0012	-	-
Al ₂	-	-	-	0,00010	0,00055	0,00004	0,00063	0,00051	0,00074	-	-	-
Al ₂ O	-	0,00003	0,00777	0,11750	0,39435	0,10459	0,73458	0,83488	0,85953	0,00184	0,00004	-
Al ₂ C ₂	-	-	0,000002	0,000238	0,000358	0,000014	0,000011	-	-	-	-	-
Gas phase yield from the final product (without Al, Al ₂ O, Al ₂ C ₂) relatively to the initial batch mass, mass%												
5,3	4,7	3,2	1,2	0,2	2,8	~10 ⁻⁵	~10 ⁻⁸	~10 ⁻⁶	0,7	0,7	0,06	5,7
Carbon carry over with gaseous phase (CO + CO ₂) relatively to the initial graphite content, mass%												
15,3	12,6	9,9	3,7	0,71	11,1	1,4·10 ⁻⁴	1,6·10 ⁻⁷	3,2·10 ⁻⁶	3,5	3,5	0,42	22,2
Mass fractions of components in the condensed phase												
C	0,0585	0,0521	0,0164	0,0132	-	-	-	-	-	-	-	-
Al	-	-	-	0,0424	-	-	0,0904	0,0906	0,0021	-	-	-
Al ₂ O ₃	0,3992	0,4758	0,1199	-	-	0,4269	0,3851	0,4335	0,5251	0,4945	0,4348	0,4608
Al ₂ OC	-	-	-	0,0980	0,1034	-	-	-	-	-	-	-
Al ₄ O ₄ C	-	-	0,4372	0,5075	0,4921	0,0979	0,1121	-	-	-	-	-
TiO	-	-	-	-	-	-	-	0,1766	0,0189	0,1180	0,1155	-
Ti ₂ O ₃	0,1644	-	-	-	-	-	-	-	-	-	0,1515	0,0865
TiC	0,3779	0,4721	0,4265	0,3812	0,3621	0,4753	0,4124	0,2993	0,4539	0,3876	0,2982	0,4527

3. Experimental

The SHS experiments were planned so that the most difficult stages of previous technologies [12, 13], such as preliminary pressing of initial batch and hot pressing of reaction products were avoided. Besides, experiments and thermodynamic modelling were not limited to stoichiometrical compositions, but were done for a larger area of the system C–Al–TiO₂. This stage of research was done using non-radioactive graphite.

The initial components to prepare simulant mixtures were taken as fine-dispersated powders. The aluminium and titanium dioxide were taken as available industrial products, the graphite was obtained by crushing graphite blocks from uranium-graphite reactors. Mixture components were thoroughly mixed, the mixture obtained was poured into alundum crucibles with the volume of 0.2–1 L. Combustion reaction in the case of SHS in air atmosphere was ignited by the use of a small amount of titanium powder on the surface. When the SHS was carried out in an inert atmosphere (argon) we have used the termite mixture. After the ignition a front of combustion was formed which brightly glowed so that the downward motion of reaction front was seen through the crucible walls. Several stages of SHS process are shown in Fig. 4. The final SHS product is a hard porous ceramic material.

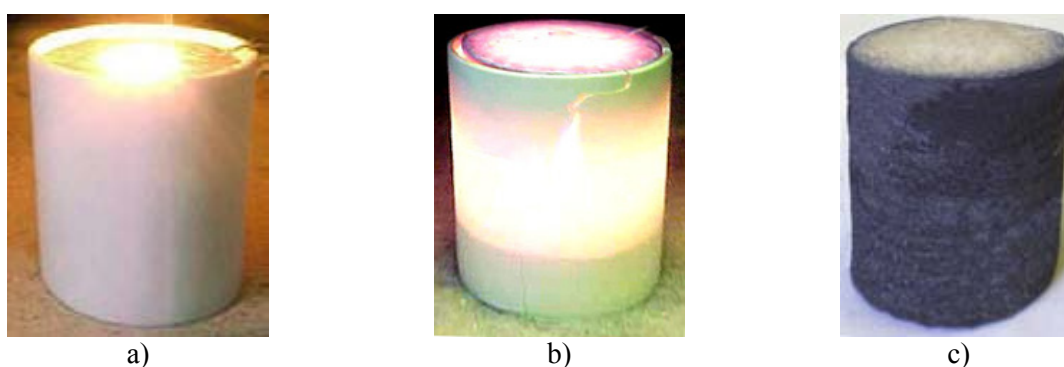


*FIG. 4. View of reactor graphite waste processing using SHS.
a — reaction initiation; b — reaction propagation; c — end product.*

The results of laboratory tests were compared with data from thermodynamic modelling for the final product phase composition. Ceramics produced with compositions corresponding to phase areas 2, 3, 6, 9 and 10 on phase diagram (see Fig. 3 and Table 2) were analysed on X ray diffractometer DRON-4 with radiation CuK_α (Fig. 5). Basically accounting to sensitivity of XRD we found a satisfactory compliance of calculated and experimental data on final product phase composition (Table 3).

To analyse the composition of gaseous phase resulting from combustion in the system C–Al–TiO₂ the content of graphite was taken above the stoichiometrical in order to be able to obtain necessary gas volumes for analyses. Combustion and sampling were carried out using a dedicated gasometrical unit made of stainless steel. The operational volume of this unit where SHS occurred was preliminary cleaned out by blowing and filling with argon. The results of gas chromatography analysis were as follows in vol. %: CO 1.6–3.7, CH₄ 0.47–0.92, O₂ 1–3.2, H₂ 3.6–6.7, N₂ + Ar the remaining. Unexpected presence in the gaseous phase of methane and hydrogen is due to interaction of graphite with moisture from initial components, as well as due to remnant oxygen and nitrogen in the operating chamber volume. In the conditions of our experiment the carry-over of carbon via gaseous phase during thermochemical treatment was ~0.04 mass%, which corresponds to the carry-over of ¹⁴C as high as ~4·10⁻⁶ g per kg of graphite. The difference from calculated value of ¹⁴C carry-over is due to deviation from stoichiometry in these experiments.

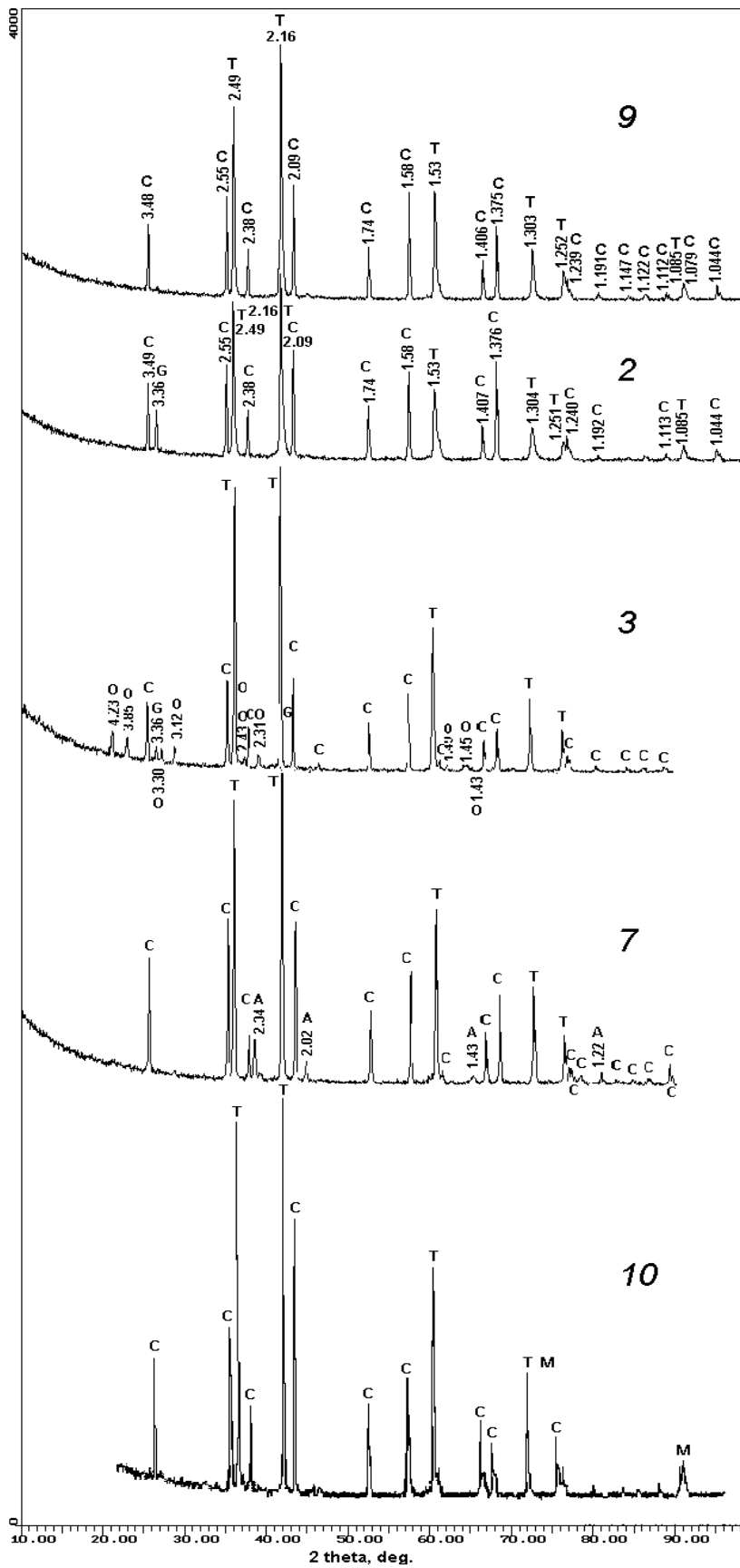


FIG. 5. X-Ray phase analysis of samples of carbide–corundum material (the number on each diffractogram corresponds to a phase region in Fig. 2): A — aluminum; C — corundum; G — graphite; O — aluminum oxycarbide; T — titanium carbide; M — titanium oxide.

Table 3. Comparison of computed and experimental final product compositions in the system C–Al–TiO₂

Phase area on phase diagram (Fig. 3)	Final product composition	
	Calculated	XRD data (Fig. 5)
2	Al ₂ O ₃ , TiC, C	Al ₂ O ₃ , TiC, C
3	Al ₂ O ₃ , TiC, Al ₄ O ₄ C, C	Al ₂ O ₃ , TiC, Al ₄ O ₄ C, C,
7	Al ₂ O ₃ , TiC, Al ₄ O ₄ C, Al	Al ₂ O ₃ , TiC, Al*
9	Al ₂ O ₃ , TiC	Al ₂ O ₃ , TiC
10	Al ₂ O ₃ , TiC, TiO	Al ₂ O ₃ , TiC, TiO

* Al₄O₄C content was below device detection limit.

Thus the thermodynamic modelling and experimental tests have shown that high temperature processing of reactor graphite by immobilizing the carbon in form of titanium carbide in a carbide–corundum ceramics is feasible within a limited area of components ratio which is close to stoichiometrical. During thermochemical processing there is a small carry over of carbon in form of CO, CO₂ and CH₄, which can cause a carry over of $\sim 10^{-9}$ – $\sim 10^{-8}$ g of ¹⁴C from 1 kg of irradiated graphite.

4. Future work

The development of the irradiated reactor graphite SHS processing technology is carried out at SUE SIA «Radon» in following areas:

- Thermodynamic modelling and experimental study of REE behaviour in the system C–Al–TiO₂ during thermochemical treatment;
- Thermodynamic modelling and experimental study of behaviour of activation products during thermochemical treatment;
- Study of hydrolytic durability of carbide–corundum matrix of final product;
- Study of feasibility to immobilize fragments of reactor elements in form of fragments of fuel elements, lumps of graphite blocks etc.;
- Experiments with real irradiated reactor graphite, measurement of ¹⁴C and other radionuclides carry-over during thermochemical treatment.

Some of preliminary results on these areas were recently published [31–35].

REFERENCES

- [1] KULIKOV, I.D., et al., Atomic Energy **87** 2 (1999) 118–129.
- [2] RUBLEVSKY, V.P., GOLENETSKY, S.P., KIRDIN, T.S., Radioactive carbon in biosphere, Atomizdat, Moscow (1979).
- [3] VASILENKO, I.YA., OSIPOV, V.A., RUBLEVSKY, V.P., Nature **12** (1992) 59–65 (in Russian).
- [4] FROLOV, V.V., et al., Atomic Energy **97** 5 (2004) 370–374.
- [5] WIECZOREK, H., OSER, B., Verfahren zur Beseitigung von mit Schadstoffen beaufschlagten Kohlenstoffpartikeln mit Hilfe von Oxidation, European Patent 0 145 799 B1., Priority 13.12. 1983.
- [6] NATANZON, Ya.V., et al., Patent of USSR 1718277 A1., Priority date 31.05.1989.
- [7] FLOID, G.M., GEPPE, K.P., MATUSEVCH, R.U., ROBILYARD, C.R., Patent of Russia 2141076 C1., Priority date 05.04.1994.
- [8] CERQUEIRA, N., et al., Incineration of radioactive waste graphite sludge in a transferred ARC plasma furnace, Proc. Intern. Conf. on Incineration & Thermal Treatment Technologies, May 10–14, 1999, Orlando, Florida (on CD-ROM, PI–6.pdf).
- [9] BRADBURY, D., MASON, J.B., Process for the treatment of radioactive graphite, International Patent WO 01/27935 A2, Priority 14.10.1999.

- [10] KUROYAMA, S., Method of processing the graphite used in nuclear reactors, Patent GB 2 359 923 A., Priority 03.03.2000.
- [11] Safety rules in managing radioactive wastes from nuclear power stations NP-002-04. — Moscow: Federal service on ecological, technological and atomic survey (2004).
- [12] MERZHANOV, A.G., et al., Patent of Russia 2065220 C1., Priority date 18.03.1994.
- [13] KONOVALOV, E.E., et al., Atomic Energy 84 No. 3 (1998) 239–242.
- [14] KLIMOV, V.L., et al., Patent of Russia 2192057 C1., Priority date 28.06.2001.
- [15] DMITRIEV, S.A., et al., Patent of Russia 2242814 C1., Priority date 01.04.2003.
- [16] OJOVAN, M.I., KARLINA, O.K., KLIMOV, V.L., PAVLOVA, G.YU., Graphite processing with carbon retention in a waste form, Materials Research Society Symposium Proc., Warrendale, Pennsylvania: Materials Research Society **608** (2000) 565–570.
- [17] DMITRIEV, S.A., et al., XIV Russian Meeting on Experimental Mineralogy, 2–4 October 2001, Abstracts, Chernogolovka: Institute of Experimental Mineralogy RAS, Chernogolovka (2001), p. 289.
- [18] KLIMOV, V.L., et al., 14th Int. Conf. on chemical thermodynamics, 1–5 July 2002, S. Petersburg, Abstracts, NII Chimii SPbGU, S. Petersburg (2002), p. 340.
- [19] OJOVAN, M.I., et al., Investigation of reactor graphite processing with the carbon-14 retention, Proc. Materials Research Society Symp., Materials Research Society, Warrendale, Pennsylvania **757** (2003) 615–620.
- [20] KARLINA, O.K., et al., Thermodynamic analysis and experimental investigation of phase equilibria in the thermochemical processing of irradiated graphite in the C–Al–TiO₂ system, Atomic Energy **94** 6(2003) 405–410.
- [21] KARLINA, O.K., et al., Atomic Energy **101** 5 (2006) 372–379.
- [22] TRUSOV, B.G., The software TERRA to model phase and chemical equilibrium at high temperatures, Proc. III Int. Symp. on Combustion and Plasmochemistry, 24–26 Aug. 2005, Almaty, Kazakhstan, Kazakh University, Almaty (2005) 52–57.
- [23] GURVICH, L.V., The reference books and data banks on the thermodynamic properties of substances at high temperatures, Rev. Int. Hautes Tempér, Réfract., Fr., **27** (1991) 167–179.
- [24] BELOV, G.V., IORISH, V.S., YUNGMAN, V.S., IVTANTHERMO for Windows, database on thermodynamic properties and related software, CALPHAD **23** 2 (1999) 173–180.
- [25] Thermodynamic Properties of Individual Substances, Fourth Edition, Vol. 1, Part One, Part Two. (GURVICH, L.V., VEITS, I.V., ALCOCK, C.B., Eds), Hemisphere Publishing Corporation, New York, Washington, Philadelphia, London (1989).
- [26] Thermodynamic Properties of Individual Substances, Fourth Edition Vol. 2, Part One, Part Two (GURVICH, L.V. VEITS, I.V., ALCOCK, C.B., Eds), Hemisphere Publishing Corporation, New York, Washington, Philadelphia, London (1991).
- [27] Thermodynamic Properties of Individual Substances, Fourth Edition, Vol. 3, Part One, Part Two (GURVICH, L.V. VEITS, I.V., ALCOCK, C.B., Eds), Begell House Inc., New York (1996).
- [28] KLIMOV, V.L., BERGMAN, G.A., KARLINA, O.K., Thermodynamic properties of aluminum monooxycarbide Al₂OC, J. Phys. Chem. **80** 11 (2006) 1816–1818 (in Russian).
- [29] NIST–JANAF Thermochemical Tables, Fourth Edition (CHASE, M.W., Jr. Ed.), J. Phys. Chem. Ref. Data (1998) Monograph No. 9, p. 1952.
- [30] BUSHUEV, A.V., et al., Atomic Energy **92** 6 (2002) 514–522.
- [31] DMITRIEV, S.A., et al., Proc. SUE SIA on Radon, Scientific works in 2002, Issue 10 (SOBOLEV, I.A., DMITRIEV, S.A, KARLINA, O.K., Eds), Radon Press, Moscow (2003) 18–25.
- [32] DMITRIEV, S.A., et. al., Proc. SUE SIA on Radon, Scientific works in 2003, Issue 11 (DMITRIEV, S.A, BARINOV, A.S, KARLINA, O.K., Eds), Radon Press, Moscow (2005) 15–16.
- [33] DMITRIEV, S.A., et. al., *ibid.* p. 45–52.
- [34] DMITRIEV, S.A., et al., Proc. SUE SIA on Radon, Scientific works in 2004, Issue 12 (DMITRIEV, S.A, BARINOV, A.S, KARLINA, O.K., Eds), IBDG, Moscow (2006) 11–15.
- [35] DMITRIEV, S.A., et al., *ibid.*, p.15–21.

Current status of the radiological characterization of the irradiated graphite from the RBMK-1500 reactor in Lithuania

R. Plukiene^a, D. Ancius^a, A. Plukis^a, R. Plukiene^a, D. Rikikas^b, A. Smaizys^c,
P. Poskas^c, E. Narkunas^{c*}

^aInstitute of Physics, Vilnius, Lithuania

^bCEA Saclay, Gif-sur-Yvette, France

^cLithuanian Energy Institute, Kaunas, Lithuania

Abstract. Ignalina Nuclear Power Plant (INPP) operates two RBMK-1500 water cooled graphite-moderated channel-type power reactors. The total mass of graphite in the cores of both units at INPP is about 3600 t. Knowledge of the radiological characteristics and radioactive inventory of irradiated graphite are essential in planning of the decommissioning processes and in the choice of graphite treatment or storage methods. The dependence of graphite activity levels on irradiation time, neutron flux values, concentration of impurities are addressed in this paper. Principal contributors to the total activity as well as other radionuclides important from the radiological point of view are identified and the uncertainties of calculations due to different nuclear data libraries and the uncertainty given by the impurity level in graphite are analysed.

1. Introduction

The Ignalina NPP is a two unit power plant located in the north-eastern part of Lithuania, near the borders of Latvia and Belarus. Each of the Ignalina NPP units contains graphite moderated, boiling water cooled RBMK-1500 reactor. Design electrical and thermal power of the RBMK-1500 reactor is 1500 MW and 4800 MW, respectively.

The core of the Ignalina NPP Units 1 and 2 contains about 3600 t of graphite. The graphite stack consists of individual graphite blocks and can be described as a cylinder, made up of 2488 graphite columns, constructed from different types of graphite blocks. The blocks are rectangular parallelepipeds, with a base of 0.25 m × 0.25 m, and heights of 0.2, 0.3 and 0.6 m. The blocks possess a 0.114 m diameter bore opening through the vertical axis, and this provides a total of 2044 channels which are used for placing fuel assemblies, control rods and other equipment into the core.

The neutron spectrum in the reactor is thermalized by the graphite stack. Due to intensive neutron irradiation (neutron flux density is up to 10^{14} n/(cm²·s)) graphite becomes activated. Activation of impurities in the graphite is one of the main sources of reactor graphite radioactivity.

Mainly, two Lithuanian institutions — Institute of Physics and Lithuanian Energy Institute — are involved in experimental and numerical investigations of the graphite used in RBMK-1500 reactor. The purpose of this paper is to present the achievements on radiological characterizations of the irradiated graphite at Ignalina NPP.

* Author to whom any correspondence should be addressed.

2. Conservative approach to activation modelling of the reactor active core

The neutron activation modelling was performed for two cases (“Case A” and “Case B”).

The intention of “Case A” modelling was to achieve preliminary results of conservative computer modelled neutron activation analysis in RBMK-1500 reactor active core graphite blocks and to highlight the effects of the irradiation time, neutron flux value and impurity content and concentrations on activity levels of different radionuclides.

The aim of “Case B” modelling was to update the “Case A” model for numerical evaluation of graphite activation, taking into account reactor operation history (close to the reality) and impurity content with maximal concentrations, specific only to Ignalina NPP reactor graphite, in order to decrease the conservatism.

2.1. Calculation method and assumptions

General activity estimation scheme used in this modelling state is presented in Fig. 1.

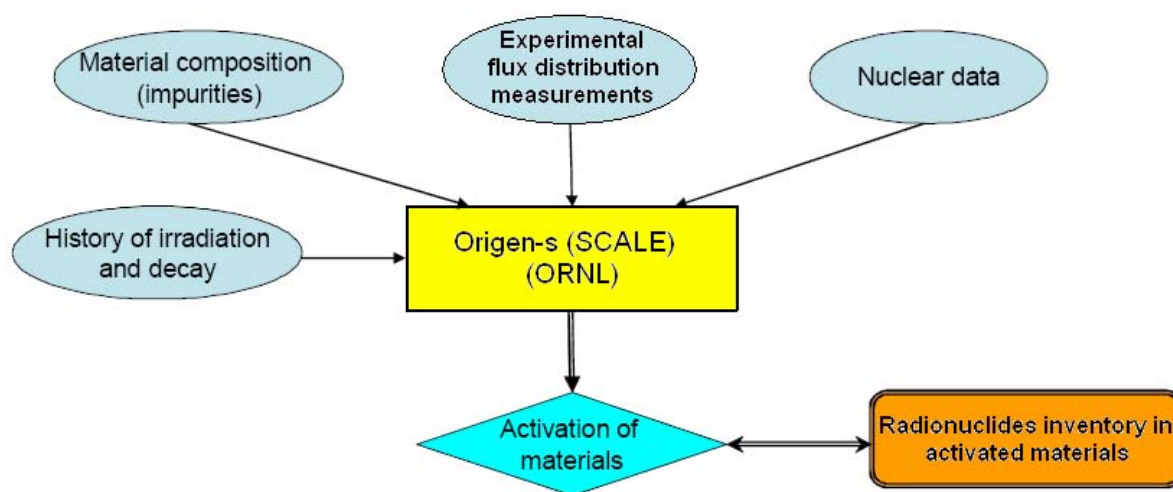


FIG. 1. General activity estimation scheme.

ORIGEN-S computer code (SCALE computer codes system) was used for the activation modelling. The code considers radioactive disintegration and neutron absorption (capture and fission) and enables to identify isotopic content, activities and concentrations of neutron activated elements.

“Case A”

List of impurities in RBMK type reactors graphite, their maximal and minimal concentrations of each element that were used in the “Case A” calculations were taken from [1] and [2]. To have conservative case the maximal concentrations of all impurities were used in the calculations. For comparison purposes the minimal concentration values of impurities were used also. It was assumed that isotopic content and percentage of a certain impurity in the non-irradiated graphite is the same as naturally occurring isotopic content.

The activity calculations were made only for active core graphite blocks. Radionuclides emerging in activated graphite and their specific activity levels were evaluated at the time just after the irradiation (i.e. at the time of final reactor shutdown), and for several decay periods after the irradiation, i.e. after the final reactor shutdown. In this case, it was conservatively assumed that neutron flux density is $3 \cdot 10^{13}$ n/(cm²·s) and it is constant during irradiation period and that graphite irradiation time is 20 years.

The following effects on induced radioactivity in graphite blocks were evaluated also:

- Dependence of induced activity on neutron flux, when irradiation time is constant;
- Dependence of induced activity on irradiation time, when neutron flux is constant;
- Dependence of induced activity on impurities concentration (activity levels were calculated for minimal and maximal impurities concentrations).

The radionuclides inventory and activities of irradiated graphite were calculated for the moment just after the final reactor shutdown (no cooling period) when evaluating radioactivity dependence on all above mentioned parameters. When evaluating radioactivity dependence on impurities concentrations, calculations were also performed for several cooling time periods after final shutdown.

Neutron flux density values that were used in calculations were based on the experimental neutron flux measurements at Ignalina NPP Unit 1 reactor active core [3]. Obtained flux values at nominal reactor power ($P_{th} = \sim 4200$ MW) were the following:

- Thermal neutrons: $(2.8-3.4) \cdot 10^{13}$ n/(cm²·s)
- Neutrons with energy above 7.25 MeV: $(2.5-3.8) \cdot 10^{11}$ n/(cm²·s)
- Neutrons with energy above 8.15 MeV: $(1.2-1.8) \cdot 10^{11}$ n/(cm²·s)

“Case B”

General activity estimation scheme used in “Case B” modelling is the same, as for “Case A” modelling (Fig.1).

The activity estimation in this case was similar to the analysis presented above (“Case A”), with two basic exception — initial impurity content, concentrations and reactor operation history.

Impurity content for this case was based on the impurities specific only to INPP reactors graphite [2][4], while initial content of impurities in above “Case A” was based on very conservative assumption — there were used all impurities with the maximum concentration, which were determined in graphite for any NPP with RBMK type reactors.

Also a close to reality reactor operating history of Ignalina NPP Unit 1 reactor was used in this case. It was assumed that reactor operates for 21 years (21 cycles) at different regimes, but during each separate cycle (one cycle corresponds to one reactor operation year) reactor operation regime (neutron flux) is constant. Ignalina NPP Unit 1 reactor operation history (average annual thermal powers during 1984–2004 years) is presented Fig. 2 [5].

The neutron fluxes for each separate 21 cycles were recalculated according to reactor thermal power during that cycle and neutron flux measurements results at nominal reactor power, presented in above “Case A”.

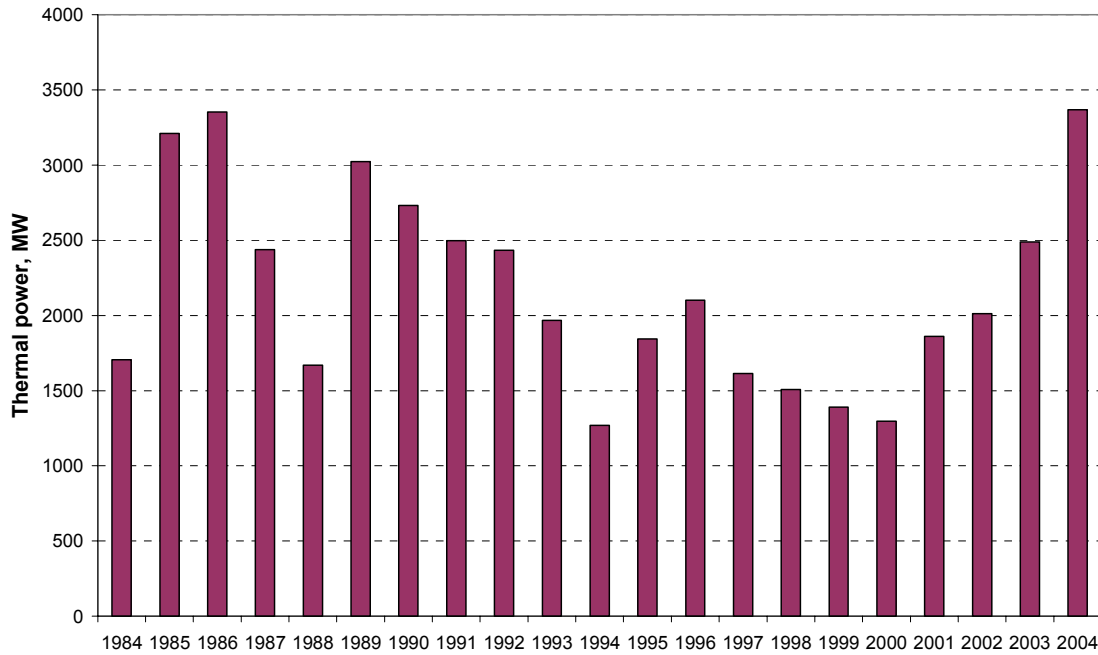


FIG. 2. Average annual thermal powers of Ignalina NPP Unit 1 reactor [5].

Taking into account all above mentioned assumptions and conditions, the activation modelling of INPP Unit 1 reactor RBMK-1500 active core graphite blocks was performed. Radionuclides emerging in activated materials and their specific activity levels were evaluated at the time just after the irradiation and for 150 years cooling period.

2.2. Results

“Case A”

Only main results of above mentioned modelling “Case A” are presented here. Detailed description of modelling methodology, assumptions and achieved results may be found in Refs [6] and [7].

Activity dependence on neutron flux for the most important nuclides is presented in Fig. 3.

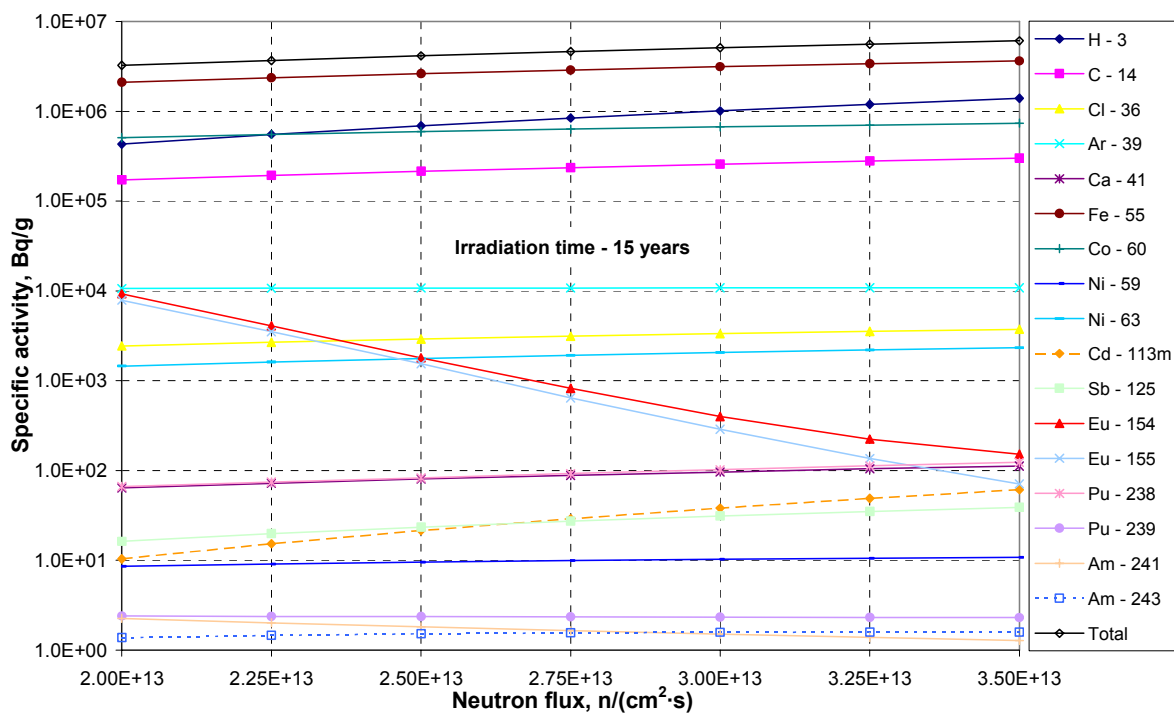


FIG. 3. Induced activity dependence on neutron flux for the main nuclides.

It can be seen that total activity of activated impurities increases when neutron flux is increasing. However, activities of several nuclides (^{154}Eu , ^{155}Eu , ^{239}Pu and ^{241}Am) decrease when flux is increasing. In this calculation, case maximal level of total activity is less than $6.10 \cdot 10^6$ Bq/g.

Activity dependence on irradiation time for the most important nuclides is presented in Fig. 4.

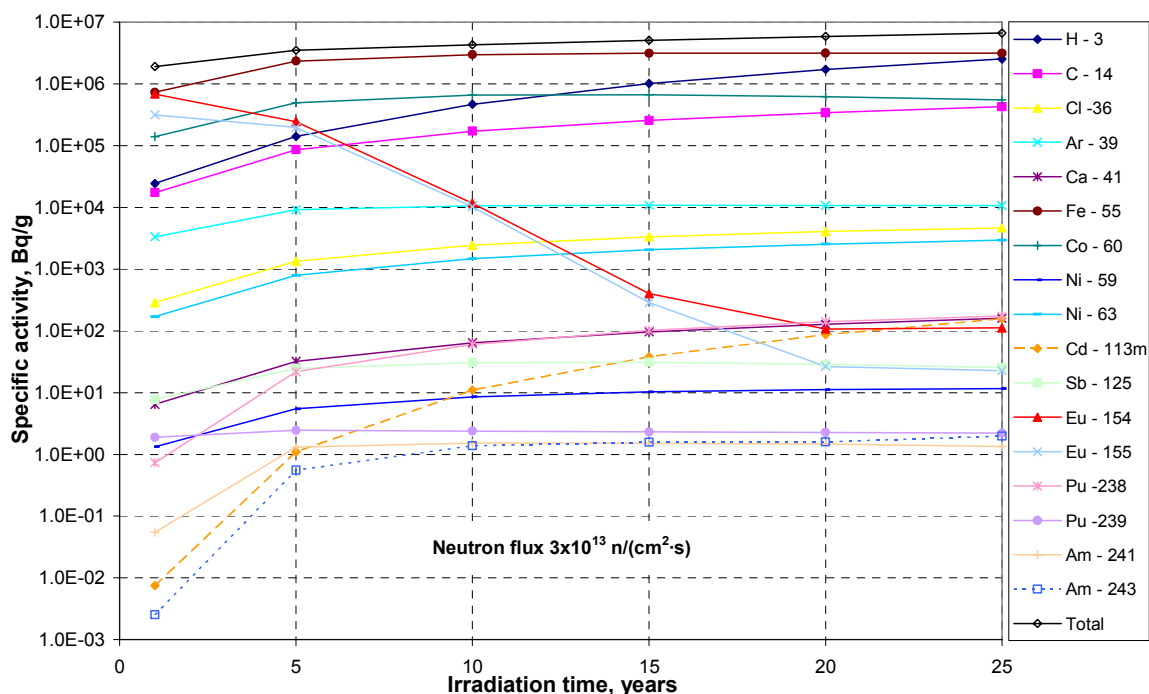


FIG. 4. Induced activity dependence on irradiation time for the main nuclides.

In this case, total activity increases when irradiation time is increasing. However, activity variation with irradiation time of certain nuclides is different. Activity values of ^3H , ^{14}C , ^{36}Cl , ^{41}Ca , ^{59}Ni , ^{63}Ni , ^{238}Pu and ^{243}Am are increasing and activity of ^{155}Eu is decreasing. Activity level of ^{154}Eu is decreasing during approximately 20 years of irradiation time until minimal level is reached. After that, activity level is increasing with increasing of irradiation time. For the remaining nuclides, activity values are increasing until maximal values are reached and after that is decreasing. Maximal activity values of ^{55}Fe and ^{60}Co are approximately after 15 years of irradiation. Maximal activity values for ^{239}Pu and ^{241}Am respectively are after approximately five and 10 years. In this calculation, case maximal activity value does not exceed $6.68 \cdot 10^6$ Bq/g.

Three major processes (radionuclide decay, depletion and formation) determine nuclides concentration variation with the neutron flux and irradiation time. The nuclide depletion and formation rate depends on neutron flux density and irradiation time. There is competition between radionuclide depletion and formation, radionuclide decay and formation. Rate of these processes determines activity (or concentration) variation with time for each radionuclide and depending on which process (or processes) speed is dominant, the activity may decrease or increase during irradiation time.

Activity dependence on cooling time after reactor shutdown for the most important nuclides is presented in Fig. 5.

Neutron flux in reactor core after shutdown is insignificant, so there are practically no activation processes and activity changes are determined by radioactive decay. For radionuclides that have relatively short decay periods — less than six years (^{55}Fe , ^{60}Co , ^{155}Eu , etc.), activity values are decreasing considerably. For nuclides that have relatively long decay periods — more than 75 000 years (^{59}Ni , ^{36}Cl , ^{41}Ca , etc.), activity values are decreasing insignificantly.

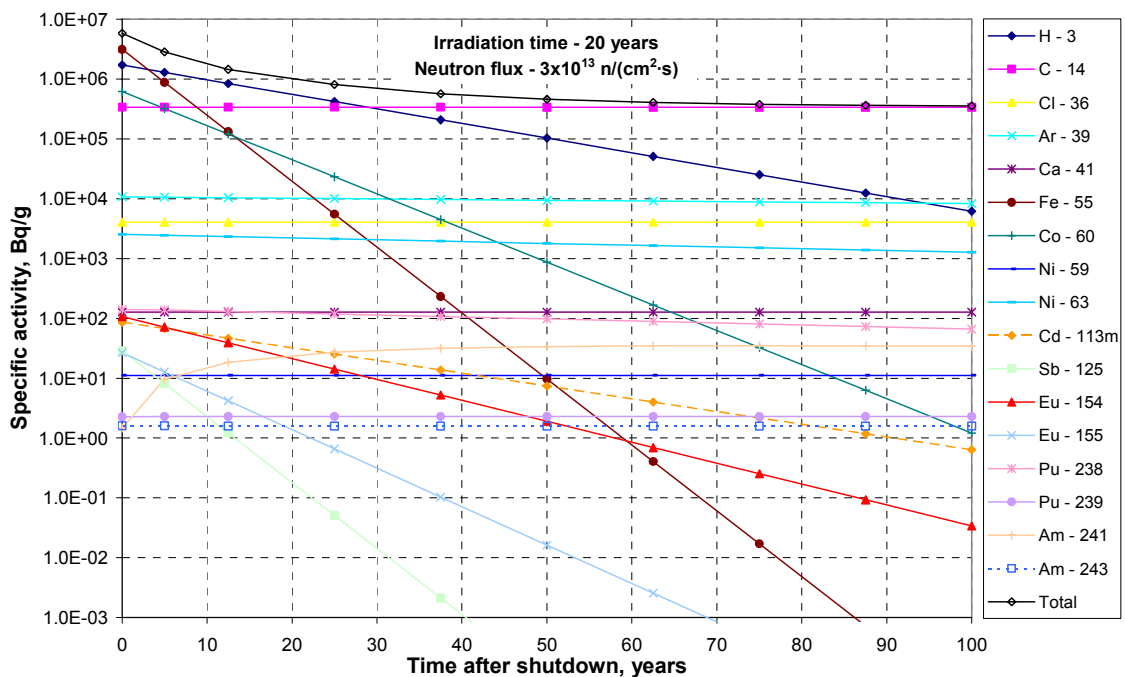


FIG. 5. Induced activity dependence on cooling time for the main nuclides.

Results of induced activity calculations during reactor cooling time using minimal and maximal impurities concentrations are presented in Fig. 6.

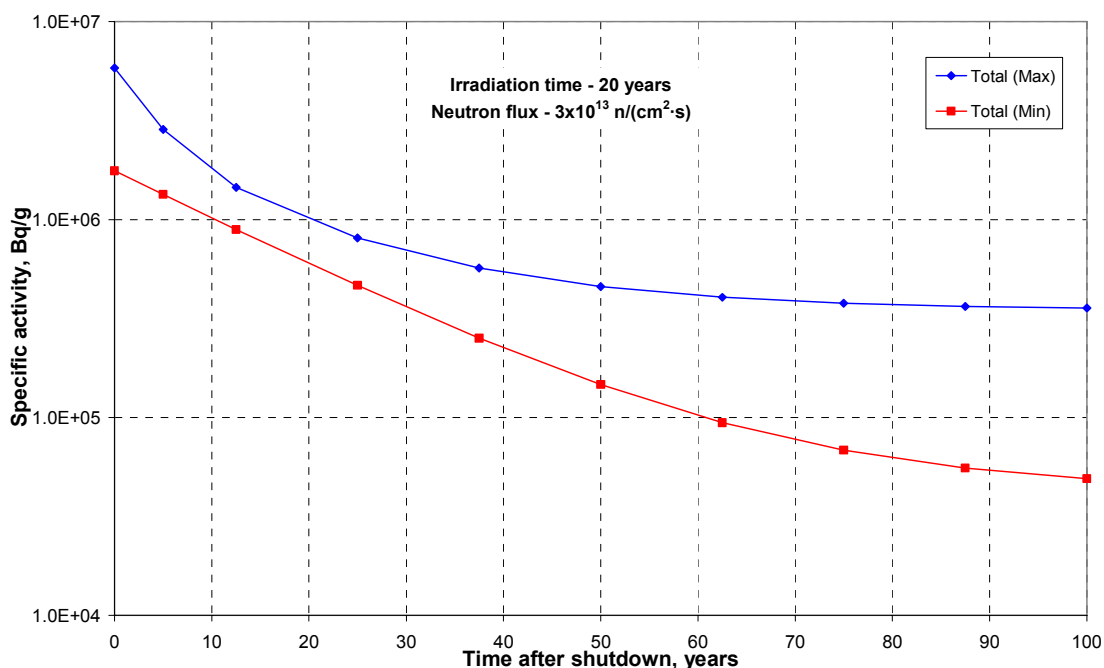


FIG. 6. Induced activity dependence upon impurities concentration and cooling time (Curves Total (Max) and Total (Min) — specific activity levels in graphite respectively when concentrations of impurities are maximal and minimal).

At the time of shutdown high activity levels are determined mostly by short lived nuclides and after five years cooling period the influence of these nuclides becomes insignificant. During 20 years cooling period, ³H, ¹⁴C, ⁵⁵Fe, ⁶⁰Co and ³⁶Cl have the highest activity values. Due to relatively short half-life, influence of ⁵⁵Fe and ⁶⁰Co into total activity decreases significantly during 100 years cooling time and residual activity is defined mostly by ¹⁴C, ³H and ³⁶Cl. Results show that for maximal impurities concentrations activity level at the time of reactor shutdown does not exceed $5.84 \cdot 10^6$ Bq/g and after 100 years it decreases to the level of approximately $3.60 \cdot 10^5$ Bq/g. If concentrations of impurities are minimal, activity level after shutdown is less than $1.76 \cdot 10^6$ Bq/g and decreases to $4.91 \cdot 10^4$ Bq/g after 100 years cooling period.

“Case B”

Main results of the neutron activation analysis for active core graphite blocks (“Case B”) are presented in Fig. 7.

Specific activity level of active core graphite blocks is $\sim 1.94 \cdot 10^6$ Bq/g at the time of final reactor shutdown, and decreases to level $\sim 1.25 \cdot 10^5$ Bq/g after 150 years of cooling (Fig. 7). The most important nuclides during 150 year cooling period from the radioactivity point of view in graphite blocks are ⁵⁵Fe, ⁶⁰Co (short lived) and ³H, ¹⁴C, ³⁶Cl, ³⁹Ar, ⁴¹Ca, ⁶³Ni.

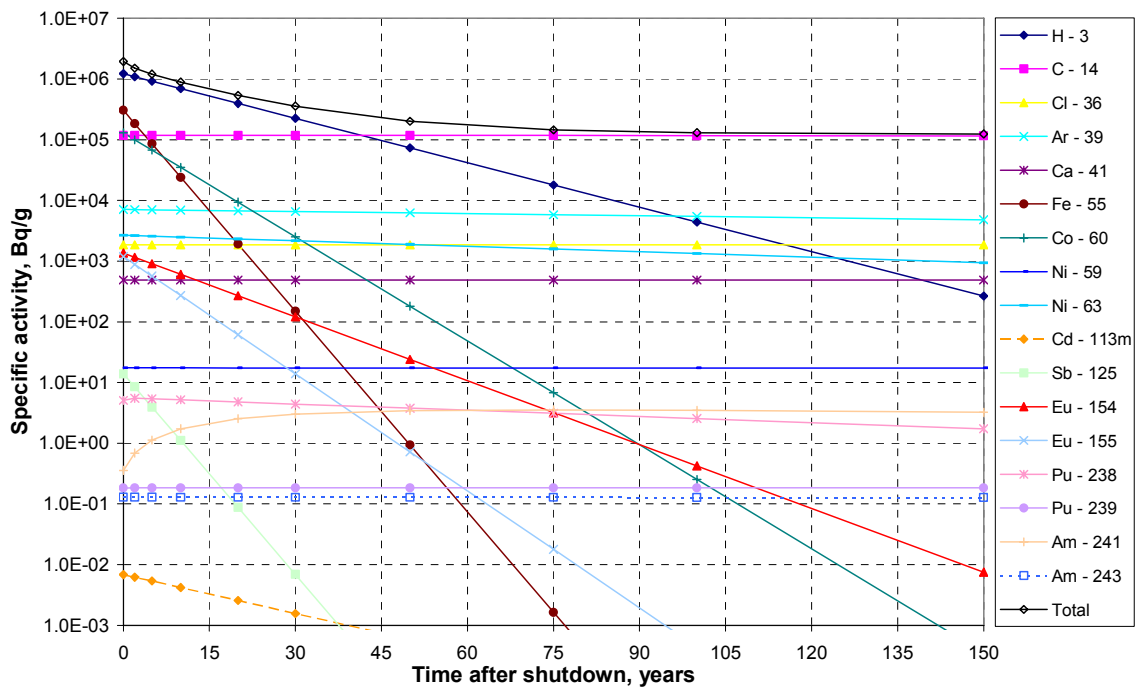


FIG. 7. Induced activity dependence on cooling time for the main nuclides.

2.3. Summary

Performed neutron activation analysis of graphite activation has shown how the induced activity levels depend on neutron flux and irradiation time. Specific activities of most radionuclides and the total specific activity of active core graphite blocks increase, increasing either neutron flux or irradiation time. However, for some radionuclides (¹⁵⁴Eu, ¹⁵⁵Eu, etc.), specific activities decrease, using higher values of neutron flux or irradiation time.

Analysis has also shown that activity level in graphite blocks is very sensitive to initial concentration of impurities. Total graphite specific activity using minimal impurities concentrations is 1.7–7.3 times lower (depending on the time after final reactor shutdown) than using maximal concentrations.

At the time just after reactor shutdown high activity levels are determined mostly by short lived nuclides and after 5–10 years cooling period the influence of these becomes insignificant. During the first 20 years of cooling period, majority of activity is accumulated by radionuclides ³H, ¹⁴C, ⁵⁵Fe, ⁶⁰Co and ³⁶Cl. Due to relatively short half-life, influence of ⁵⁵Fe and ⁶⁰Co on total specific activity decreases significantly during 100 years cooling time and residual activity is accumulated generally by ³H, ¹⁴C, and ³⁶Cl.

Comparing the results of “Case A” and “Case B” (Figs 5 and 7), one can notice that results of both analyses, from the qualitative point of view, are in good agreement despite the modelling differences mentioned above. Main radioactive nuclides in both analyses are the same: ⁵⁵Fe, ⁶⁰Co, ³H, ¹⁴C, ³⁶Cl, ⁶³Ni and ⁴¹Ca.

However, results differ in quantitative form, but this difference was prospective and is understandable. Total graphite blocks specific activity in “Case A” was $\sim 5.84 \cdot 10^6$ Bq/g compared to the value of $1.94 \cdot 10^6$ Bq/g in “Case B”, and during 100 years cooling period it decreases to the values of $3.60 \cdot 10^5$ and $1.31 \cdot 10^5$ Bq/g, respectively. The total specific activity in “Case B” remains about three times lower during all analysed cooling period.

So it is evident that, using impurities content specific only to Ignalina NPP and real reactor operation history, achieved results are less conservative compared to results of conservative analysis in “Case A” (see also Refs [6, 7]).

3. Detailed modelling of the graphite stack activation

The aim of this modelling was to perform a full scale activation modelling of all reactor RBMK-1500 graphite structures. For this purpose, it was necessary to calculate neutron fluxes in all these components numerically, as reliable experimental neutron flux measurement data are available only for active core graphite (moderator). Furthermore, an experimental investigation of impurities in RBMK-1500 reactor graphite specimen was performed. Using results of this investigation (impurities content and concentrations) graphite activation analysis was made, also investigating the uncertainties of such analysis.

3.1. Calculation method and assumptions

The overall calculation scheme used for this modelling state is presented in Fig. 8.

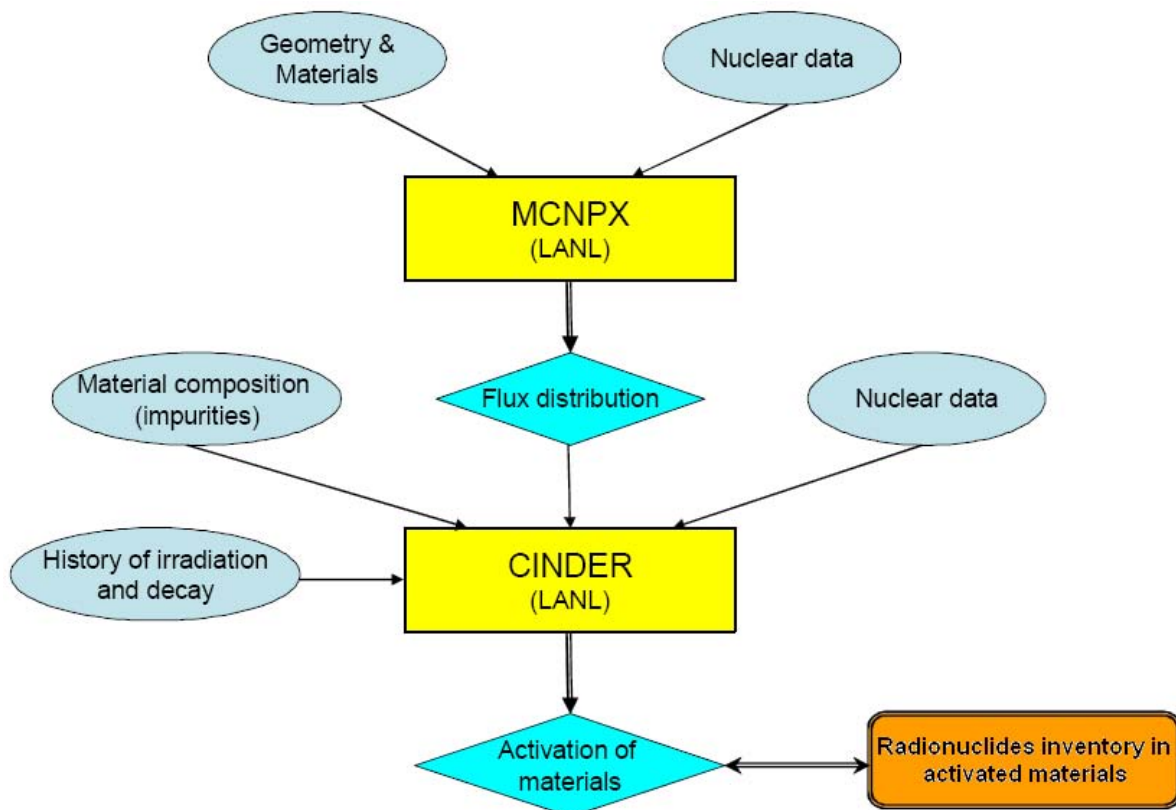


FIG. 8. General activity estimation scheme.

The activation calculations are carried out in two phases: the first phase is the calculation of the spatial neutron flux distributions and energy spectra using MCNPX Monte Carlo code; the second phase is the calculation of activation, radioactive decay and cooling. The MCNPX input data comprise: nuclear data, materials specifications and detailed geometry description. The continuous neutron energy spectrum obtained with MCNPX was divided into 63 energy groups and normalized to a nominal power of the reactor (~4200 MW). The spatial neutron flux is further used as the input data for the calculations in the second (activation) phase. To obtain the irradiation scenario which is close to reality, the history of the power load of Unit 1 during 21 years was used (Fig. 2) by the computer code CINDER’90 in time steps averaged over one year. The code also needs the chemical composition and impurities of materials. Two independent studies for the determination of the RBMK-1500 graphite

impurities have been carried out in the Saclay Research Centre of French Atomic Energy Commission (CEA): gamma spectroscopy based on activation by neutrons and glow discharge mass spectroscopy (GDMS).

The CINDER'90 code uses 63 neutron energy groups and has its own nuclear data library composed mainly of ENDF, JEF and JENDL data libraries. The output of the code is the isotopic composition and radionuclide activity in the irradiated material.

3.2. Results

Analyses of the impurities of the RBMK-1500 graphite

The specimen of the fresh RBMK-1500 graphite taken from the fuel channel sleeve has been investigated experimentally. Table 1 presents the results of that investigation. The graphite specimens were irradiated by the thermal and fast neutron flux in the CEA research reactors ORPHEE and OSIRIS. After irradiation, the specimens were processed and analysed by gamma spectrometry. This method enables to identify the majority of chemical elements, starting with $Z > 11$; however, some important impurity elements such as Li, N, S, Nb and Pb may not be quantified by the gamma spectrometry method.

Table 1. Impurity concentrations of the RBMK-1500 graphite specimen

Elements	Concentration (ppm)	Elements	Concentration (ppm)	Elements	Concentration (ppm)
Li	0.004–0.05 []	Ni	0.39	La	0.15
Be	0.02[]	Cu	0.1*	Ce	0.269
B	0.05*	Zn	0.02	Pr	0.08
N	0.5–70[]	Ga	0.01	Nd	0.11
O	40–197.5[]	Ge	9.0	Sm	0.0213
Na	4.64; 5.0*	As	0.011	Eu	0.0026
Mg	7.0; 0.5*	Se	0.003	Tb	0.0027
Al	9.2; 1.0*	Br	0.025	Dy	0.0032
Si	1.0*	Rb	0.008	Ho	0.0094
P	0.5*	Sr	0.96	Er	0.0053
S	5–52 []	Zr	1.0	Tm	0.0056
Cl	7.6	Mo	0.17	Yb	0.014
Ar	0.14	Ru	0.07	Lu	0.0015
K	1.9; 1.5*	Ag	0.003	Hf	0.0058
Ca	51.9; 2.0*	Cd	0.015	Ta	0.0019
Sc	0.05	In	0.003	W	0.047
Ti	17.4	Sn	0.15	Re	0.0019
V	17.4	Sb	0.004	Au	0.00022
Cr	0.6; 0.3*	Te	0.014	Hg	0.00062
Mn	0.58; 0.2*	I	0.04	Th	0.0079
Fe	18.7; 1.0*	Cs	0.0016	U	0.016
Co	0.019	Ba	2.01		

[] – impurity concentration taken from scientific literature.

* - impurity concentration obtained from GDMS analysis.

Another method used was a GDMS analysis. This method is based on sputtering the atoms to plasma of cathode which is made from the material to be analysed. The atoms of the material then are ionized and, subsequently, are analysed with a mass spectrometer. Although the method is rather sensitive, some elements as Li, N, O, Cl and F may not be quantified because of the absence of Penning ionization in argon.

Both methods enabled to obtain the data on impurities present in graphite. However, for more complete impurity composition, some important elements as Li, N and others, which could not be

quantified by the above mentioned methods, have been taken from scientific literature, mainly on the typical RBMK graphite composition.

Detailed description of this impurity analysis in RBMK-1500 graphite is given in [4][8].

Calculation of the neutron fluxes in graphite constructions of the RBMK-1500 reactor

The model of MCNPX calculations of the neutron fluxes in RBMK-1500 reactor graphite is presented in Fig. 9. The model takes into account the detailed geometrical parameters of the RBMK-1500 reactor. The cell of fuel assembly and graphite column has been modelled as precisely as possible, taking into account data given in the technical description [9]. The calculations have been carried out for the composition corresponding to fresh and irradiated fuel, the burnup of the latter being 10 MWd/kgU. In both cases, the fuel with initial 2.0 % ^{235}U enrichment was used. The horizontal and vertical sections of the RBMK-1500 reactor, as modelled by MCNPX, are given in Fig. 9.

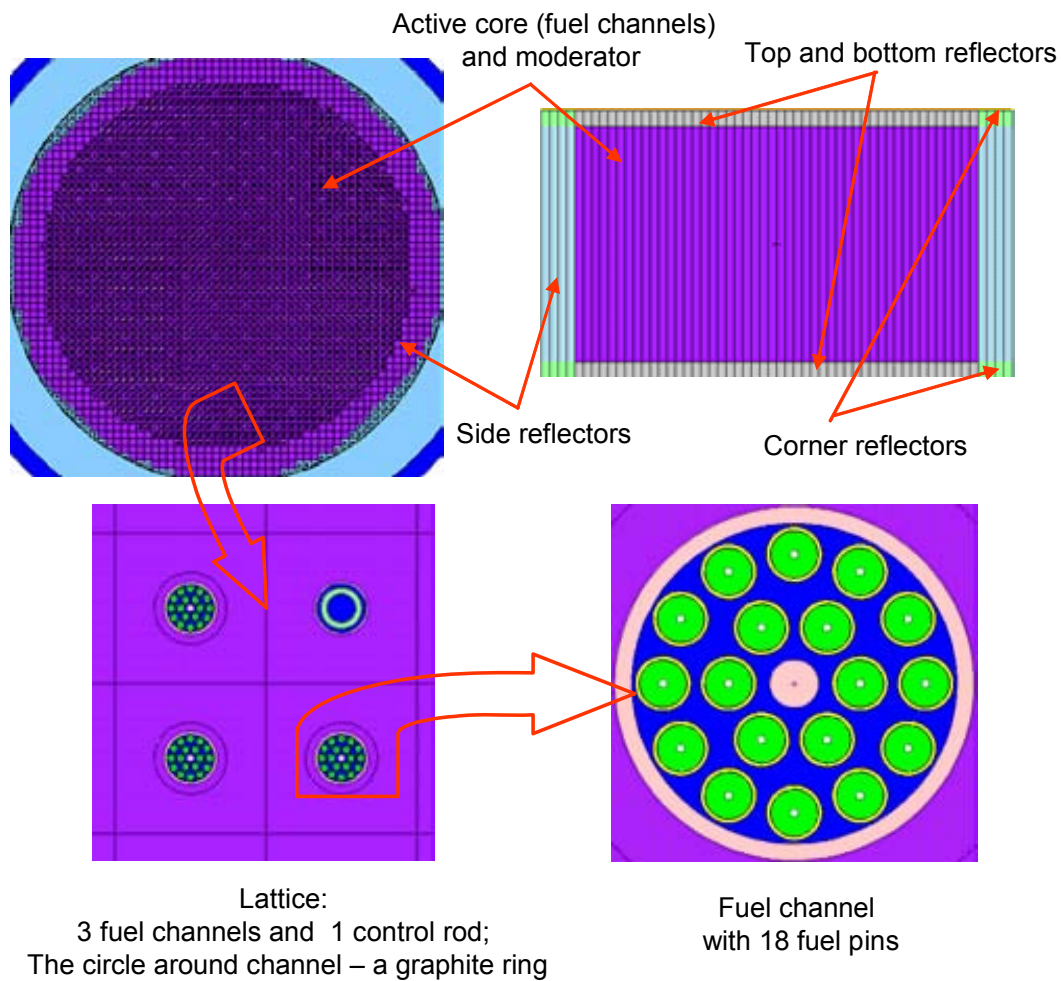


FIG. 9. The MCNPX model of the RBMK-1500 reactor with horizontal and vertical sections, lattice of four elements and fuel channel.

Five graphite constructional zones were identified: the active zone (moderator) of the reactor, the side reflector, the top and bottom reflectors, the part of reactor, where the flux of neutrons is the lowest and nearly fully thermalized (here referred to as the corner reflector), and the fuel channel graphite sleeves, which surround the fuel channel and are designed to fill the space between the channel and moderator (cylinder around the fuel channel). The neutron flux and its energy spectrum were calculated in each of the above mentioned zones. Figure 10 represents normalized distribution of neutron fluxes per unit lethargy in the RBMK-1500 reactor graphite constructions.

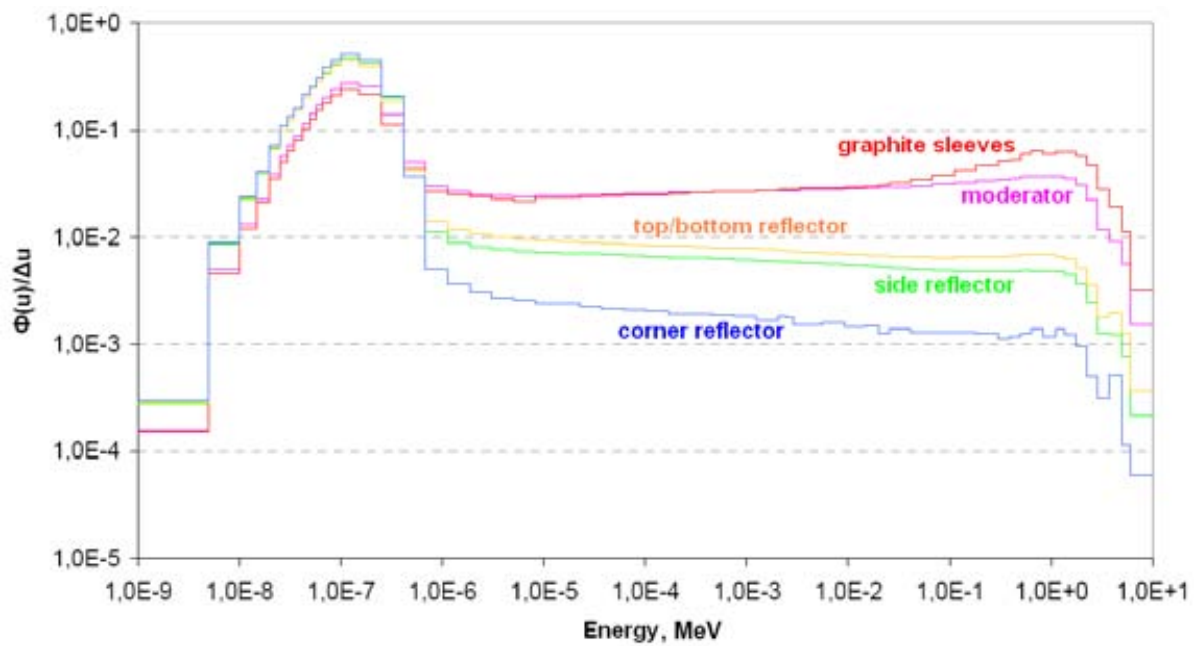


FIG. 10. Radial distribution of the neutron flux in the moderator and side reflector (model dependence).

The fastest neutron flux is observed in the fuel channel sleeves. The part of thermal neutrons is about 48% of the total flux in the sleeves as they are the closest constructional element to the fast neutrons source — the fuel. The thermal neutron flux part is about 56% in the moderator and more than 90% in the reflectors. To evaluate the sensitivity of the neutron flux and its energy distribution in moderator to the fuel burnup and the presence of control rods, three models having the same basic geometry and other parameters have been considered (Fig. 11).

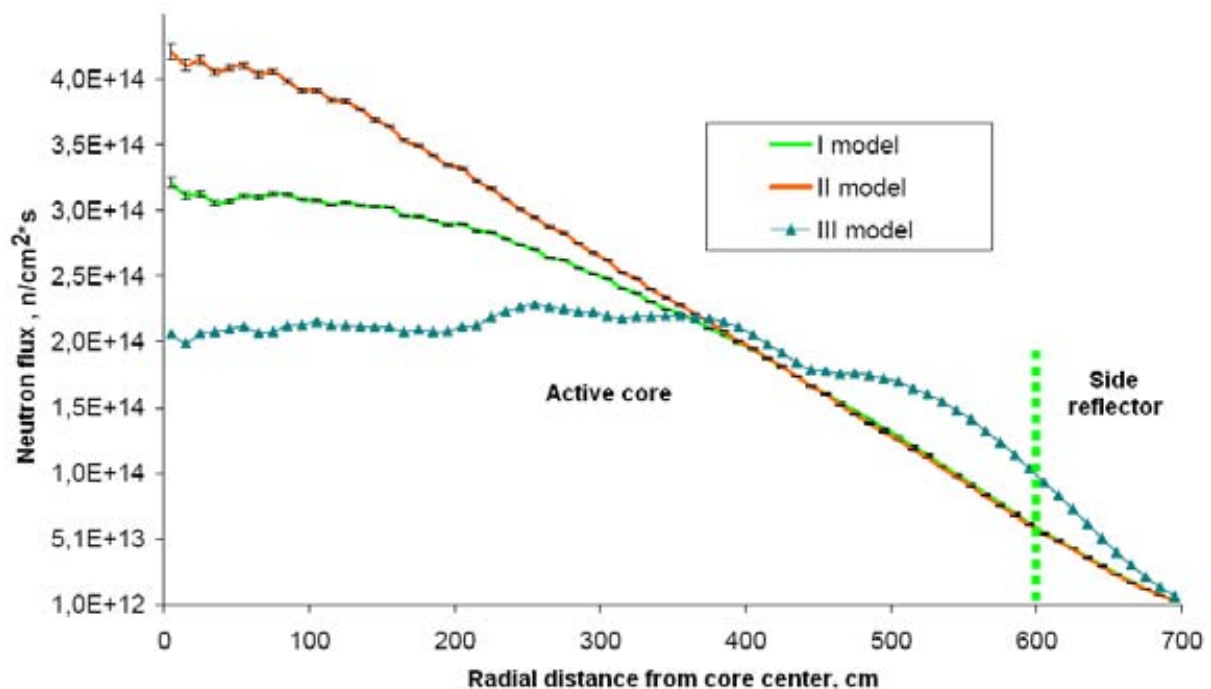


FIG. 11. Radial distribution of the neutron flux in the moderator and side reflector (model dependence).

Fresh fuel and no control rods were used in model I. The fresh fuel was replaced with the fuel of 10 MWd/kgU burnup in model II. Model III has the same burnup as model II, but has both fully and partially inserted control rods in the core. The maximal values of the fluxes obtained in models I and II are in the centre of the reactor and the flux monotonically decreases towards the boundaries of the core (Fig. 11).

A comparison of the neutron energy spectra of models I and II with model III shows that the differences for models without control rods are less than 1% for thermal neutrons and less than 9% for fast neutrons. It allows to conclude that deviations of the neutron flux spectrum in graphite structures due to the fuel burnup and the changing positions of control rods may not lead to a significant error in activation calculations. The fluxes calculated using model III were used for the activation calculations as they represent realistic magnitude of the neutron flux in the reactor core graphite and in reflectors.

Other parameters, which may influence the flux calculations, are the variable density of the water-steam mixture in the fuel channel and the use of higher enriched erbium fuel. The influence of these parameters was also evaluated and it may be concluded that they may not lead to a significant error in activation calculations.

Detailed description on the estimation of the neutron fluxes in graphite constructions of the RBMK-1500 reactor may be found in [4][8].

Activation calculations

The conservative values of measured impurities concentrations (Table 1) were used for the activation calculations with CINDER'90 computer code. The remaining values of impurity concentrations were taken from the scientific literature and averaged.

The result of the calculations of the activity of graphite under irradiation conditions, as described above, is the list of more than 1300 radionuclides with the range of their half-lives from 10^{-7} s to 10^{20} y.

The total specific activity of nuclides in reactor graphite moderator and side reflector as a function of radial distance and the time after the shutdown of the reactor is presented in Fig.12.

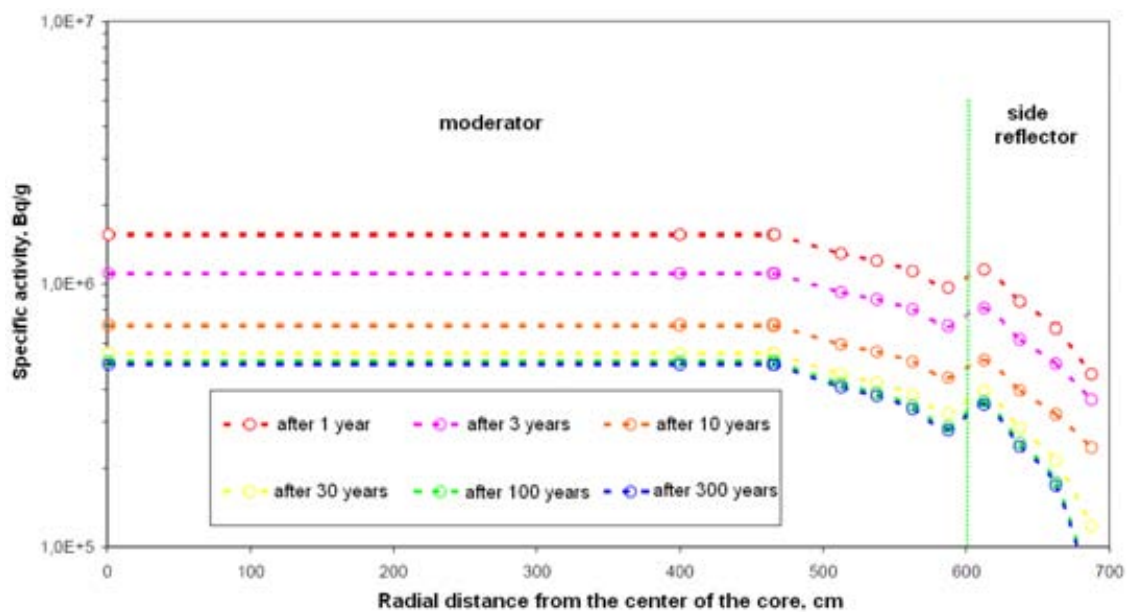


FIG. 12. Total specific activity and its radial distribution in the RBMK-1500 reactor moderator and side reflector as a function of cooling time.

The activity is constant in the central part (plateau) of the reactor core and it decreases towards the periphery of the core. However, in the side reflector at the edge of the core, the total activity increases. It is due to the higher flux of thermal neutrons in the reflector whose contribution to the activation processes is essential. The total activity decreases more sharply after shutdown of the reactor because of the decay of short lived nuclides, while after 10 years of cooling it changes quite slowly for a long time.

Figure 13 shows axial distribution of the total specific activity in each graphite construction of the reactor as a function of cooling time. The reverse axial distribution of the total activity in the side reflector is observed, when it reaches the corner reflector area.

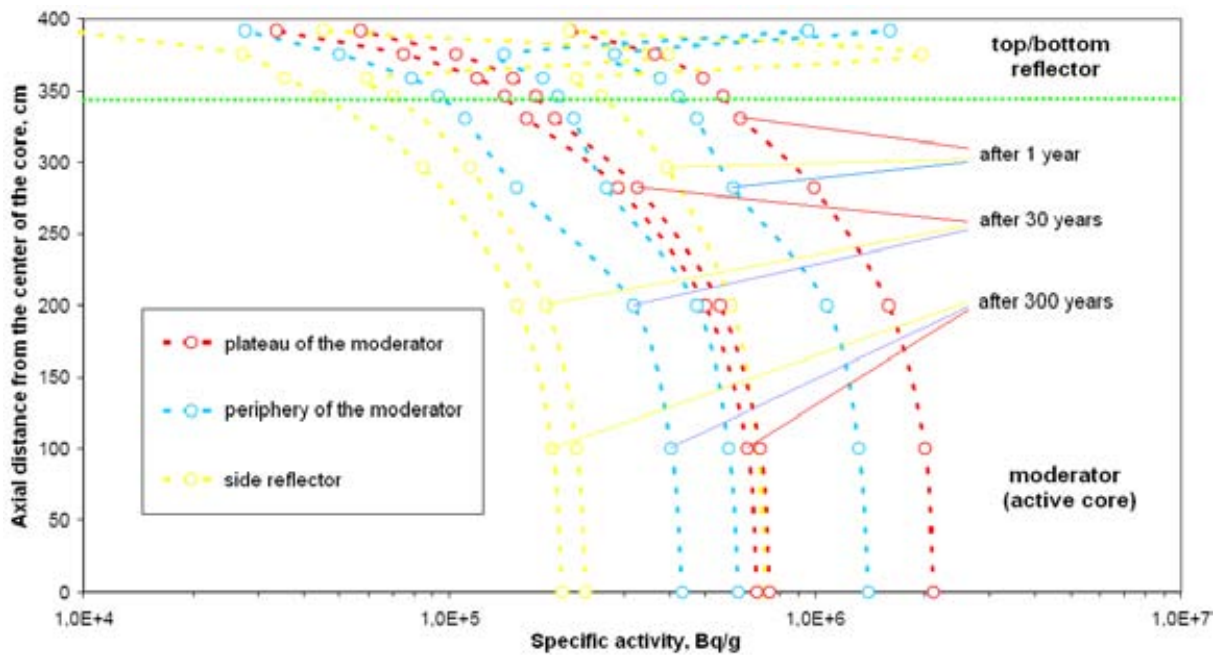


FIG. 13. Total specific activity and its axial distribution in the RBMK-1500 reactor graphite stack as a function of cooling time.

The comparison of irradiated graphite radionuclide composition of moderator and corner reflectors gives the explanation for such inversion, where the radionuclide responsible for the activity in the corner reflector is tritium (^3H). Tritium is mainly produced by the reaction $^6\text{Li}(n,\alpha) = \alpha + ^3\text{H}$. However, in moderator almost the whole ^6Li is burnt out within two years of the reactor operation due to its big neutron capture cross-section. It corresponds to the fluence level of approximately $10^{22} \text{ n}\cdot\text{cm}^{-2}$. Afterwards, only the decay of tritium defines its balance in the graphite structure. But such fluence is not reached in the corner reflector and tritium is being continuously produced during all the time of operation. The same effect is observed for other mother-nuclei with big neutron capture cross-sections when the half-lives of resulting radionuclides are comparable with the operation time of the reactor, e.g. for ^{151}Eu and ^{153}Eu .

The specific activities of main radionuclides, from radiological point of view, in the moderator and in the corner reflector, are given in Fig. 14.

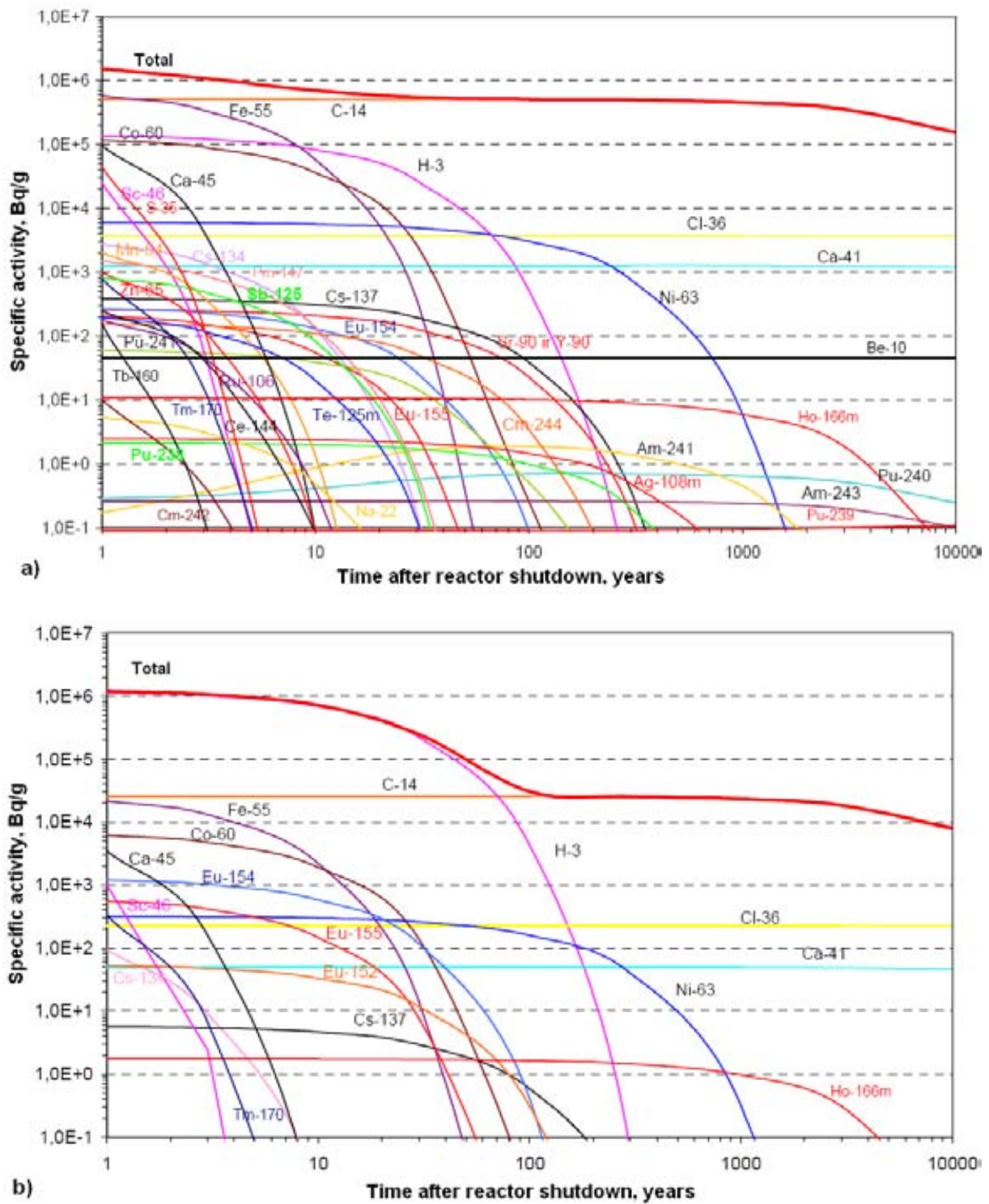


FIG. 14. Specific activities of radionuclides as a function of cooling time:
 a — in the moderator; b — in the corner reflector.

Although ^{14}C and tritium constitute major radioactivity in all the irradiated graphite constructions and are crucial to the long term waste management activities, the role of other radionuclides such as ^{55}Fe and ^{60}Co , etc. has to be properly evaluated, especially for dismantling and on-site waste management purposes.

More details on this RBMK-1500 reactor graphite construction activation modelling may be found in [4][8].

Estimation of uncertainties

The accuracy of such activation calculations is determined mainly by the uncertainties in the effective neutron cross-section data libraries used and by the precision of data on impurity concentrations. The presence of impurities is due to the raw materials involved in fabrication of nuclear graphite and sometimes varies significantly even for the same grade of graphite. The influence of such variations on the results of calculations of the total specific activity is presented in Fig. 15.

The use of maximal key-element concentrations gives the total activity which is by an order of magnitude higher than the total activity in the case of minimal concentrations. Only one key-isotope, namely natural ^{13}C , the concentration of which in carbon is about 1.1%, is practically invariant. Estimations show that for the neutron flux of the RBMK-1500 reactor the production rate of ^{14}C from ^{13}C is equal to the production rate from ^{14}N if the concentration of ^{14}N is about 7 ppm. In fact, the production rate of a radionuclide and the neutron reaction rate per unit of flux may differ from one graphite construction to another due to the difference in spectrum of the neutron flux in these constructions (Fig. 10). Table 2 shows the neutron reaction rates in thermal, epithermal and fast neutron energy regions.

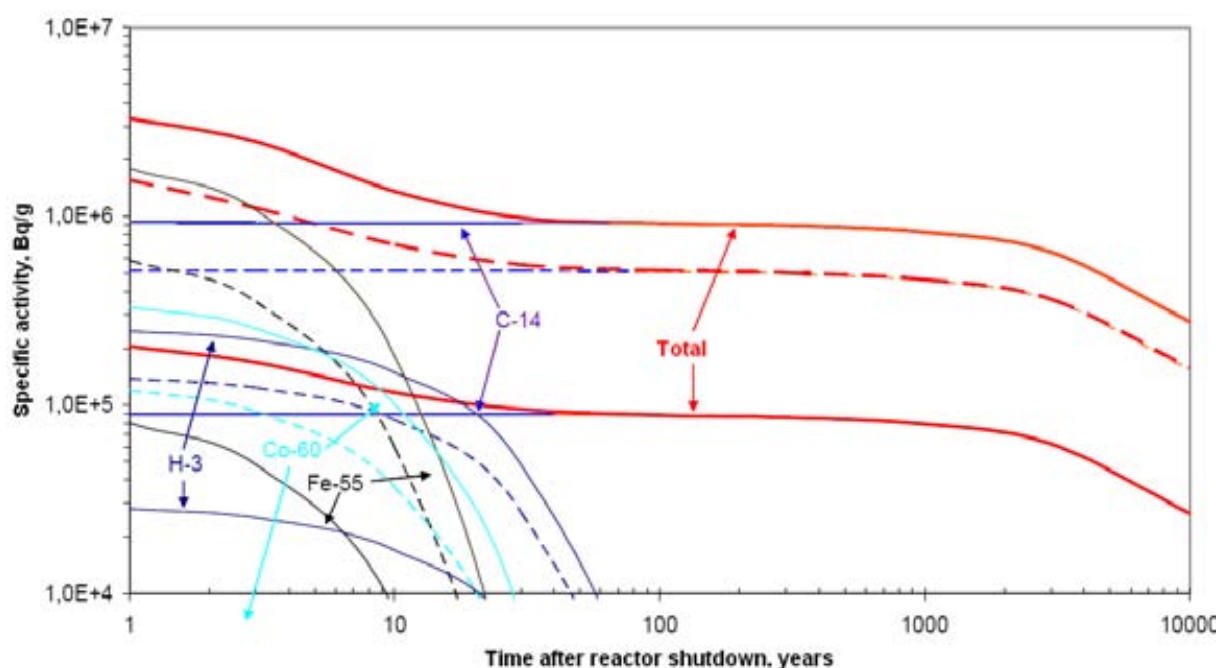


FIG. 15. Calculated total activity in the moderator in the case of maximal and minimal concentration of impurities of key-elements as a function of cooling time.

Although the major activity is a result of reactions on thermal neutrons, some individual radionuclides as ^{60}Co , $^{108\text{m}}\text{Ag}$, ^{134}Cs or ^{154}Eu are produced, in comparable quantities, by reactions with epithermal neutrons.

The uncertainties, which are the result of the use of different effective neutron cross-section data libraries, are less important than those caused by uncertainties of impurity concentrations. Nevertheless, for some individual radionuclides they are not negligible.

Table 2. Relative production rates of some important radionuclides in different neutron energy regions within the moderator

Reaction	Neutron energy region		
	Thermal (55.50%)	Epithermal (32.68%)	Fast (11.82%)
${}^6\text{Li}(n,\alpha) \rightarrow \text{tritium}$	96.47%	3.50%	0.03%
${}^{13}\text{C}(n,\gamma) \rightarrow {}^{14}\text{C}$	87.49%	3.39%	9.12%
${}^{14}\text{N}(n,p) \rightarrow {}^{14}\text{C}$	95.92%	3.48%	0.60%
${}^{35}\text{Cl}(n,\gamma) \rightarrow {}^{36}\text{Cl}$	96.84%	3.16%	0.00%
${}^{40}\text{Ca}(n,\gamma) \rightarrow {}^{41}\text{Ca}$	95.82%	4.01%	0.17%
${}^{54}\text{Fe}(n,\gamma) \rightarrow {}^{55}\text{Fe}$	95.68%	4.19%	0.13%
${}^{59}\text{Co}(n,\gamma) \rightarrow {}^{60}\text{Co}$	84.63%	15.36%	0.01%
${}^{62}\text{Ni}(n,\gamma) \rightarrow {}^{63}\text{Ni}$	96.74%	3.23%	0.03%
${}^{107}\text{Ag}(n,\gamma) \rightarrow {}^{108\text{m}}\text{Ag}$	77.53%	22.16%	0.31%
${}^{133}\text{Cs}(n,\gamma) \rightarrow {}^{134}\text{Cs}$	47.50%	52.43%	0.07%
${}^{151}\text{Eu}(n,\gamma) \rightarrow {}^{152}\text{Eu}$	97.62%	2.38%	0.00%
${}^{153}\text{Eu}(n,\gamma) \rightarrow {}^{154}\text{Eu}$	65.19%	34.75%	0.06%
${}^{154}\text{Eu}(n,\gamma) \rightarrow {}^{155}\text{Eu}$	97.30%	2.69%	0.01%

The best known nuclear data libraries today, ENDF/B-VI, JEF and JENDL, were compared with the original CINDER'90 library. Table 3 gives differences of these libraries calculated for the neutron flux in the RBMK-1500 moderator for thermal, epithermal and fast neutrons. Combining the data from Tables 2 and 3, it may be concluded that significant variation of results for some individual radionuclides may take place because of the use of a certain cross-section data library and a negligible influence of epithermal neutrons. Detailed description of this estimation of uncertainties is available in [4][8].

Table 3. Differences of neutron effective cross-sections using different libraries (related to endf/b-vi or to the library with the note "ref.")

Reaction	Thermal region			Epithermal and fast region		
	JEF	JENDL	CINDER'90	JEF	JENDL	CINDER'90
${}^6\text{Li}(n,\alpha) \rightarrow \text{tritium}$	-0.164%	0.106%	-0.580%	-0.064%	0.119%	-0.757%
${}^{13}\text{C}(n,\gamma) \rightarrow {}^{14}\text{C}$	-	-	-32.00%	-	-	-74.99%
${}^{14}\text{N}(n,p) \rightarrow {}^{14}\text{C}$	-0.558%	-2.995%	95.58%	-1.689%	-4.822%	92.78%
${}^{35}\text{Cl}(n,\gamma) \rightarrow {}^{36}\text{Cl}$	-	Ref.	-0.170%	-	Ref.	2.674%
${}^{40}\text{Ca}(n,\gamma) \rightarrow {}^{41}\text{Ca}$	-	Ref.	0.057%	-	Ref.	0.000%
${}^{54}\text{Fe}(n,\gamma) \rightarrow {}^{55}\text{Fe}$	14.80%	-4.17%	0.126%	15.81%	12.54%	0.117%
${}^{59}\text{Co}(n,\gamma) \rightarrow {}^{60}\text{Co}$	-0.154%	0.111%	0.430%	-0.475%	-0.335%	-1.868%
${}^{62}\text{Ni}(n,\gamma) \rightarrow {}^{63}\text{Ni}$	-0.178%	-1.218%	0.583%	-0.090%	16.89%	0.325%
${}^{133}\text{Cs}(n,\gamma) \rightarrow {}^{134}\text{Cs}$	-1.726%	-1.822%	2.323%	14.41%	3.347%	2.155%
${}^{151}\text{Eu}(n,\gamma) \rightarrow {}^{152}\text{Eu}$	-0.186%	0.319%	-31.21%	-0.313%	-10.56%	-34.53%
${}^{153}\text{Eu}(n,\gamma) \rightarrow {}^{154}\text{Eu}$	-15.85%	Ref.	4.659%	3.036%	Ref.	20.631%
${}^{154}\text{Eu}(n,\gamma) \rightarrow {}^{155}\text{Eu}$	-79.13%	Ref.	-16.99%	119.62%	Ref.	11.05%

3.3. Summary

The radioactivity of all the Ignalina NPP RBMK-1500 reactor graphite constructions was calculated taking into account the power load history of Unit 1 and measured impurities of graphite used in the Ignalina NPP. The calculations were based on computer codes MCNPX and CINDER'90. The modelling procedure involved both neutron fluxes and their total energy spectrum in graphite constructions. It has been found that the spectrum of neutrons in graphite is not influenced significantly by burnup of the fuel or by the position of control rods.

Main radionuclides, which contribute to the total radioactivity, are ^{14}C , ^3H , ^{60}Co and ^{55}Fe . However, their activities differ from one graphite stack zone to another, especially for tritium, as an effect of the burnup of its mother nucleus — Li.

The analysis in this case was performed using different initial content of impurities in graphite, different computer code for activity estimation, different nuclear data libraries, etc. in comparison to analyses performed in “conservative approach” cases. However, comparison of results of “Case B” modelling with the results of analyses performed in this case modelling also shows quite good agreement.

The list of main radioactive nuclides in activated moderator graphite is the same (^3H , ^{14}C , ^{55}Fe , ^{60}Co , etc.) and specific activity values for most of these nuclides are in the same order of magnitude. Total activity concentration in moderator graphite in these analyses is in the order of 10^6Bq/g at the moment of final reactor shutdown, and this value decreases by one order (till the order of 10^5Bq/g) during the first 100 year cooling period.

The principal uncertainty of radioactivity calculations is due to a high variation of impurity concentrations in nuclear graphite. Although the major activity is created by nuclear reactions with thermal neutrons, some radionuclides relevant to radiation protection are produced by epithermal neutrons as well. To avoid underestimation of the activities of these radionuclides, the whole neutron energy spectrum and its variation in different graphite constructions must be taken into account. Comparison of main neutron effective cross-section libraries for the typical neutron flux in the RBMK-1500 graphite shows significant uncertainties for some radionuclides, which implies the need of their update.

4. Conclusions

Some progress was achieved in the characterization of the Ignalina NPP RBMK-1500 reactor graphite, based on the modelling of the irradiation of the graphite structures and experimental investigation of the impurities of the graphite sleeve specimen.

Further investigations and analyses are necessary for the proper characterization of the graphite structures:

- Experimental investigations of irradiated graphite specimens from various Ignalina NPP RBMK-1500 reactor graphite stack zones, in order to characterize graphite radiological experimentally. This is also important for the validation of the numerical results.
- Evaluation of the nitrogen-helium cooling gas migration into the graphite from the graphite stack cooling circuit and its activation into ^{14}C and ^3H .
- Further investigation of fresh (non-irradiated) graphite samples in order to have more representative information on initial impurity content in Ignalina NPP graphite structures.

REFERENCES

- [1] BUSHUEV, A.V., ZUBAREV, V.N., PROSHIN, I.M., SOSTAV, I., sodержanie primesei v grafite promyshlennykh reaktorov, *Atomnaja Energija*, T. 92, Vyp. 4 (2002) 298–302.
- [2] VIRGILEV, Ju.S., Primiesi v reaktornom grafite i evo rabotosposobnost. *Atomnaja Energija*, T. 84, Vyp. 1 (1998) 7–16.
- [3] Ignalina NPP Safety Analysis Report, Ignalina (1996).
- [4] ANCIUS, D., COMMETTO, M., RIDIKAS, D., Activation analysis of graphite for Ignalina RBMK-1500 power reactor and Strasbourg research reactor (RUS), *Proc Int. Conf. on Decommissioning Challenges: an Industrial Reality*, Avignon, France, 23–25 November 2003.
- [5] Power Reactor Information System, Available from Internet: www.iaea.org/programmes/a2/.
- [6] ŠMAIŽYS, A., NARKŪNAS, E., POŠKAS, P., Evaluation of neutron activation processes in RBMK-1500 reactor graphite, *Lithuanian journal of physics* **43** 6 (2003) 499–503.
- [7] ŠMAIŽYS, A., NARKŪNAS, E., POŠKAS, P., Modelling of activation processes for GR-280 graphite at Ignalina NPP, *Radiation protection dosimetry* **116** 1–4 (2005) 270–275.
- [8] ANCIUS, D., et al., Evaluation of the activity of irradiated graphite in the Ignalina Nuclear Power Plant RBMK-1500 reactor, *Nukleonika* **50** 3 (2005) 113–120.
- [9] ALMENAS, K., KALIATKA, A., UŠPURAS, E., Ignalina RBMK-1500, A Source Book, Extended and Updated Version, LEI, Kaunas (1998) 198.

Decontamination of nuclear graphite by thermal methods

J. Fachinger

Forschungszentrum Jülich, Jülich, Germany

Abstract. Contaminated nuclear graphite cannot be stored in low level surface disposal facilities such as Centre de L'Aube, in France, due to the long half life of ^{14}C . Furthermore, the ^{14}C activity of the graphite reflectors from the two German HTR reactors (AVR and THTR) only would already cover more than 90% of the ^{14}C activity licensed for the underground disposal facility Konrad in Germany for non heat-generating radioactive waste. Therefore, alternative waste management strategies must be developed for nuclear graphite. The total burning of nuclear graphite with free release of ^{14}C is problematic due to public acceptance. The solidification of the whole amount of CO_2 would negate the volume reduction benefit of burning. Therefore, a separation of the ^{14}C from the off-gas is required. However, this carbon isotope has the same chemical properties as the ^{12}C from the graphite matrix. Physical separation methods like pressure swing sorption, cryogenic distillation or ultra-centrifugation are not economic for the large amounts of CO_2 . Pyrolysis in an inert atmosphere or steam reforming seems to be a possibility to separate high amounts of ^{14}C . First experiments under an inert atmosphere showed a high selective removal of ^{14}C from graphite. Higher ^{14}C decontamination factors were obtained in a steam atmosphere, but selectivity decreased. Next step will be a combination of these processes to optimize the ^{14}C release rates and high selectivity for an industrial process development.

1. Introduction

Graphite has been widely used as moderator, reflector and fuel matrix in various types of nuclear reactors. At the end of reactor life, activated graphite and carbon installations represent radioactive waste, which requires a special waste management strategy.

Disposal in deep geological formations is one of the most probable ways of radioactive graphite management. However, the large volume of contaminated graphite reduces significantly the cost efficiency of this management route. For example, in case of AVR decommissioning, 230 t of reflector graphite and carbon bricks represent a great volume of low and medium active radioactive waste [1]. This graphite contains significant quantities of radionuclides from neutron activation of impurities and contamination with fission products [2]. Decontamination of the graphite offers the opportunity to separate the majority of the radioactive isotopes from graphite. Thereafter, only a small active residue fraction has to be disposed of and the main mass of graphite can be reused.

The proposed purification procedure is based on graphite calcination and chemical treatment. These procedures allow separating non-volatile and volatile radionuclides by chemical methods. The CO_2 formed can be released to the atmosphere in a controlled way, precipitated as carbonates or reduced to carbon black and transformed into silicon carbide. Chemical methods principally are not capable to separate the carbon isotopes from each other: long lived radioactive ^{14}C and non-radioactive ^{12}C and ^{13}C (1.1%). In principle, the off-gases from incineration could be fractionated in order to recover ^{14}C by physical isotope separation techniques. However, the development of a simplified method for graphite purification from ^{14}C would give an additional economical benefit. Based on safety investigations concerning the behaviour of waste packages containing irradiated graphite (i-graphite) in a fire case, a high temperature treatment of i-graphite can be proposed as suitable process.

2. Graphite samples

Two different graphite types have been used for the following investigations. The radionuclide inventory has been determined and is given in the following table. The “Merlin” graphite was obtained from a thermal column of the research reactor FRJ-1 “Merlin”. The AVR graphite was a drilling sample from the graphite reflector of the prototype high temperature AVR [3, 4].

Table 1. Radionuclide inventory of the graphite samples

	Merlin T10 [Bq/g]	AVR S-GR-5/1 [Bq/g]
H-3	4760	884 000
C-14	449	95 000
Cs-137	0.21	1940
Eu-154	959	560
Co-60	956	27 000

3. Thermal treatment under inert atmosphere

Thermal investigations of i-graphite under inert atmosphere have been performed to study the behaviour of i-graphite in waste packages in case of fire accident after consumption of residual oxygen in the waste package.

A low percentage of the graphite was oxidized to CO and CO₂ despite the inert atmosphere. This could be explained by adsorbed oxygen on the graphite surface or oxygen impurities in the argon used. Figures 1 and 2 show the release of ¹⁴C and ¹²C during the thermal treatment. It could clearly be seen that ¹⁴C is preferentially released. The reason for this effect is the inhomogeneous distribution of ¹⁴C which is related to origin of the ¹⁴C. The most important building process for ¹⁴C is a (n,γ)-reaction of ¹⁴N impurities in the cooling gas. The ¹⁴C build by this route will be adsorbed on the graphite surface. However, the obtained release rates are insufficient for a decontamination process.

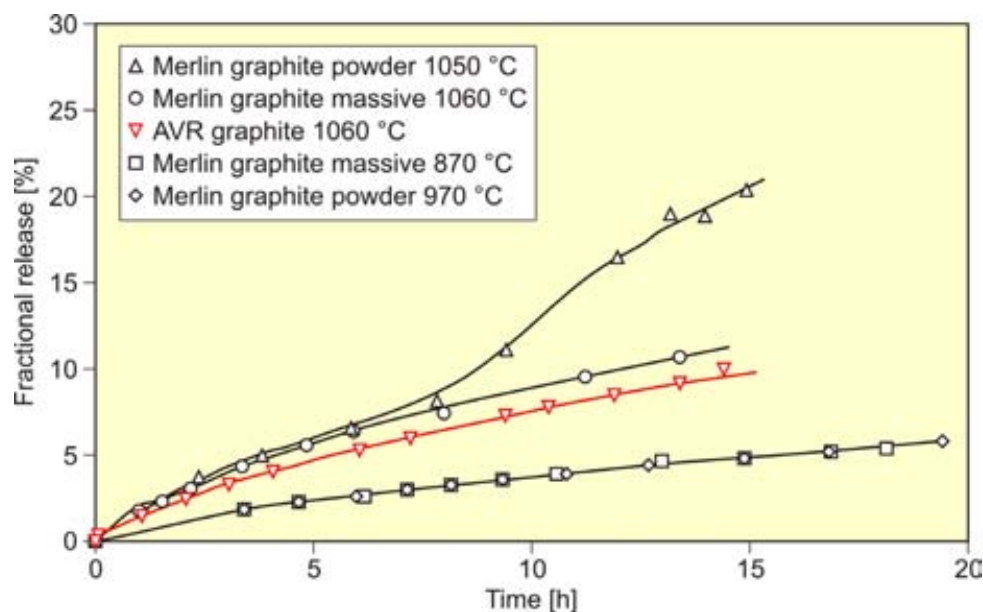


FIG. 1. Release of ¹⁴C from i-graphite under inert atmosphere.

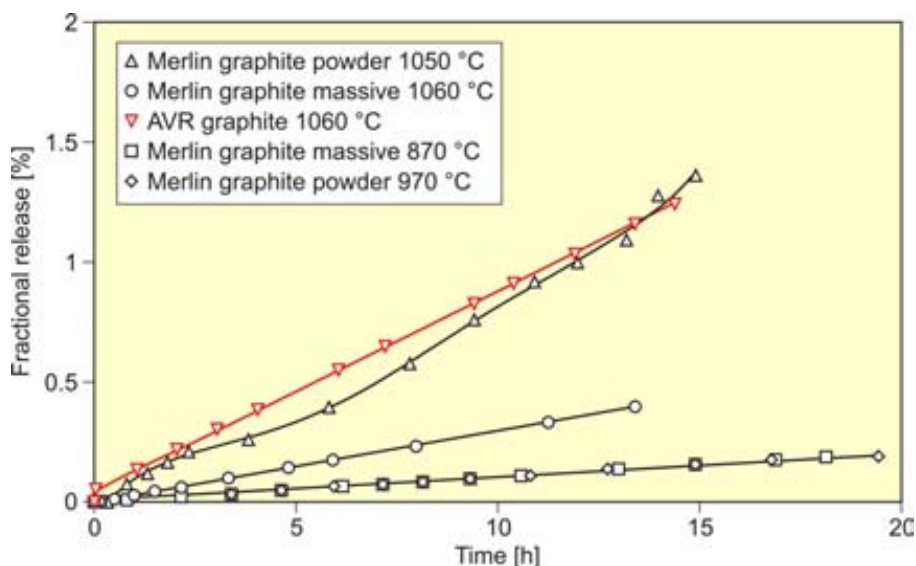


FIG. 2. Release of ^{12}C from *i*-graphite under inert atmosphere.

4. Thermal treatment in presence of steam

Higher oxidation rates of the surface were proposed to increase the release of ^{14}C . One option could be the oxidation by steam. First experiments were performed in argon saturated with water. Figure 3 shows the obtained release rates of ^{12}C and ^{14}C in a steam atmosphere. Up to 80% of ^{14}C could be released. However, the selectivity of the ^{14}C release decreased. Furthermore, the results show a big difference between Merlin graphite and AVR graphite. This indicates that the different graphite structure, the irradiation history and the operation time influence the release behaviour, because all these operational conditions influence the distribution rate between graphite matrix and surface.

5. Proposed process

Based on these results, the following processes (Figs 4 and 5) are proposed for decontamination of graphite.

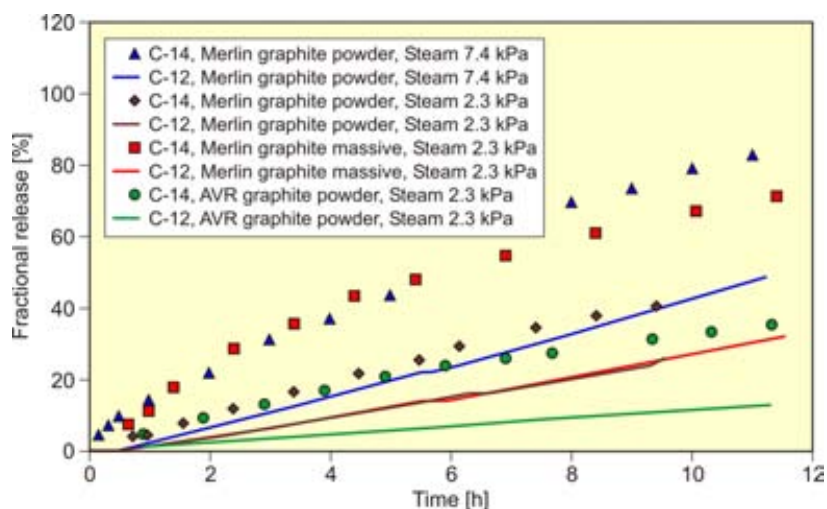


FIG. 3. Release of ^{12}C and ^{14}C in presence of steam.

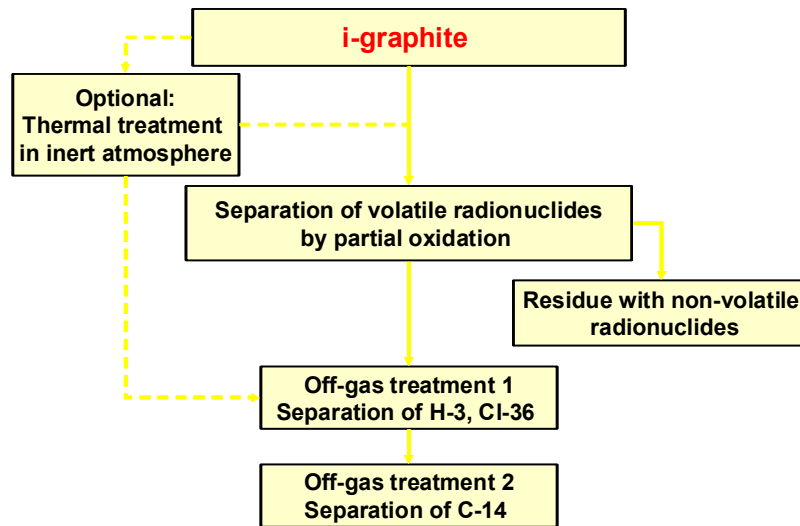


FIG. 4. Process scheme 1.

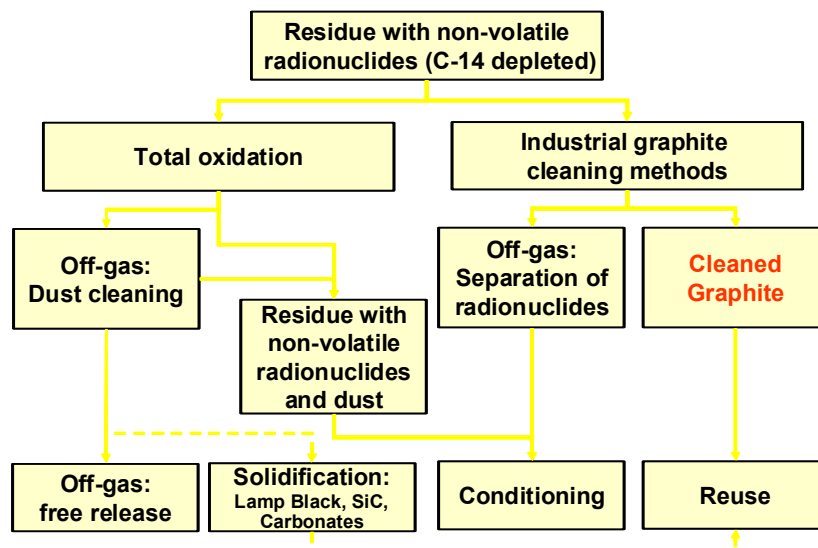


FIG. 5. Process scheme 2.

5.1. Conclusions and outlook

The obtained results prove the principle ability to decontaminate graphite from volatile radionuclides as well as from ^{14}C . However, the process parameters like temperature, vapour pressure and flow rate have to be optimized with respect to the decontamination rate and selectivity.

The separation of ^{14}C is based on the inhomogeneous distribution of carbon isotopes. Therefore, it is necessary to study the different nuclear graphite structures and types as well as the irradiation conditions which are related to the radionuclide distribution.

The decontamination of the non-volatile radionuclides has not been studied yet. However, industrial graphite cleaning processes are proposed as suitable option. The total oxidation can be considered as backup solution.

In general, the adaptation of the processes to industrial scale is proposed with industrial partners. However, a lot of lab scale investigations are necessary before a scale-up can be started.

REFERENCES

- [1] MILLINGTON, D.N., et al., Report on the International Regulation as regards HTR/VHTR Waste management; Deliverable D-BF1.1 of the Raphael Project, EC Contract 516508.
- [2] BRENNECKE, P., Anforderungen an endzulagernde radioaktive Abfälle (Vorläufige Endlagerbedingungen, Stand: April 1990 in der Fassung von Oktober 1993) — Schachanlage Konrad, BfS-ET-3/90-REV-2, Salzgitter (October 1993) 51.
- [3] Expertenworkshop Rückbau AVR am 20/21.09.2001 in Köln — Ergebnisbericht, Entsorgungskonzept für radioaktive Reststoffe aus dem Rückbau AVR, p 5.
- [4] BISPLINGHOFF, B., LOCHNY, M., FACHINGER, J., BRÜCHER, H., Radiochemical characterization of graphite from Jülich experimental reactor (AVR), Nuclear Energy **39** 5 (2000) 311–331.

GLEEP graphite core removal and disposal

M. Grave

Doosan Babcock Energy Ltd., Gateshead, United Kingdom

Abstract. The Graphite Low Energy Experimental Pile (GLEEP) was located at Harwell, United Kingdom. Stage 3 decommissioning that involved removal, processing and packaging of the graphite pile was contracted by UKAEA to Doosan Babcock Energy Ltd (formerly Mitsui Babcock). This paper focuses on the graphite removal but also notes related work to remove the bioshield and other materials allowing eventual return of the site to a field.

1. Introduction

Doosan Babcock Energy Ltd was awarded the contract by UKAEA for Stage 3 decommissioning of the Graphite Low Energy Experimental Pile (GLEEP) that was located at Harwell, United Kingdom. The project was high profile because GLEEP was the first nuclear reactor to operate in Western Europe.

Prior to the Stage 3 contract fuel had been removed and concerns related to both the residual radionuclides and their impact upon waste disposal costs had been addressed. Consequently the paper discusses:

- GLEEP construction and operational history
- The UKAEA needs and goals
- Stage 3 scope of work including the project objectives
- The HP and Waste Management controls
- The graphite handling process and preparation for disposal
- Site management and lessons learned
- Related activities
- Programme and performance

History

The GLEEP reactor was established to study neutron scattering and nuclear fission physics for the UK Nuclear Power Programme. It was built and commenced operation in 1946–1947 and was shut down in 1990. During this period, it operated for a short period of about 18 months at 80 kW (100 kW design capability). For most of its life, it operated at around 3 kW. Due to a very stable neutron flux at the core centre it was of value as an international standard. Decommissioning commenced in 1994. Construction records obtained from the Public Records Office proved great benefit in planning the reactor dismantling process.

For experiments and production of radioisotopes for hospitals, a 10 m length of carriages supported on a light alloy track could penetrate the reactor core in a thermal column.

A photograph and a layout of the reactor are shown in Figs 1 and 2, respectively.

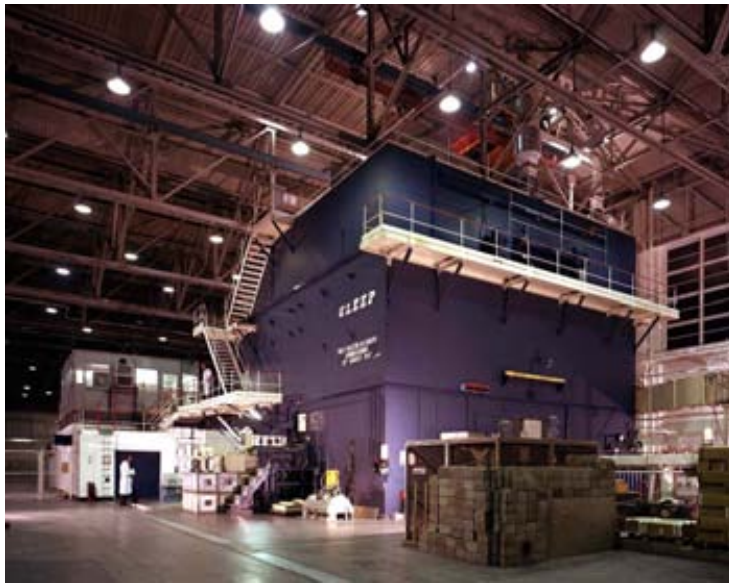


FIG. 1. General view of GLEEP.

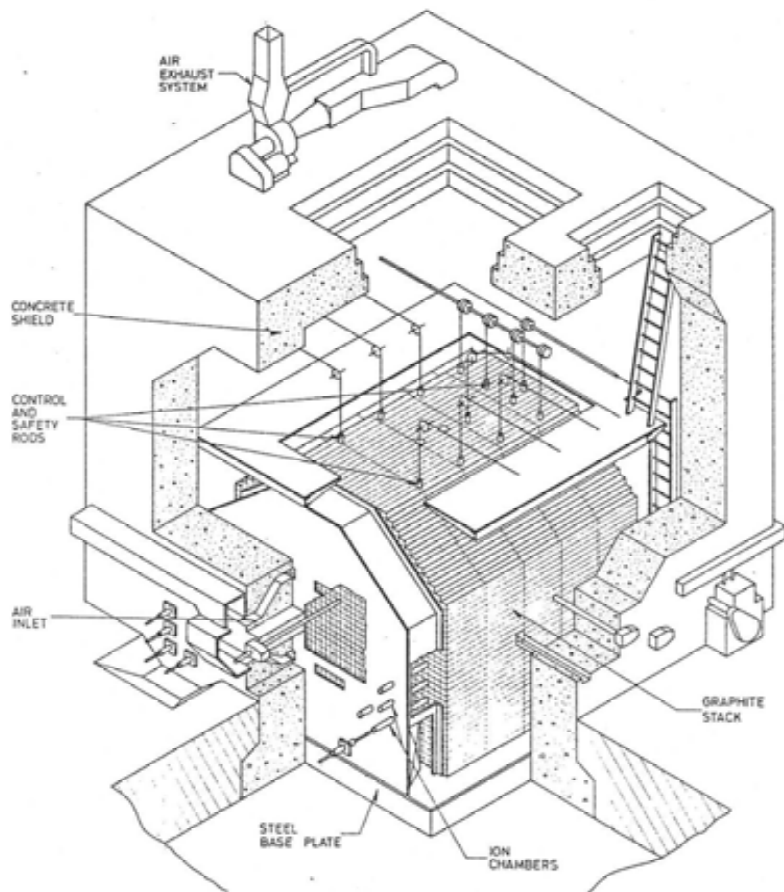


FIG. 2. Cross-section of GLEEP.

Stage 1 and 2 decommissioning

Stage 1 commenced in 1994 with the removal of the fuel and control rods from the reactor and was undertaken by AEAT. The fuel and control rods (99% of the radioactive inventory) were consigned to Harwell. The train that had been used for experiments was also removed.

Stage 2 comprised care and maintenance during which period the reactor remained in its hanger until the decision to remove it in 2003 was taken. With the exception of the items removed in Stage 1, the state of the reactor during Stage 2 is as shown in Figs 1 and 2. As well as the bioshield and the core, there remained the thermal column with the track upon which the train had accessed the core, and a local empty storage pit. The drainage systems, sumps and foundations of the reactor remained unchanged. Locally, the hanger also contained offices and a former coating facility. The offices were suitable for use by the site team during the project.

General hazards included the need to be aware of asbestos in buildings of this age and to acknowledge the structural conditions of the hanger. For the latter, noise and vibrations during reactor dismantling operations (particularly the bioshield) and the limited clearance between the hanger roof support steelwork and the top of the bioshield were of importance. The hanger structure was in generally good condition.

Towards the end of Stage 2, UKAEA held a competition for five bidders who were shortlisted from a total of 17 interested organizations. Firstly, indicative functional specifications were prepared under the terms of the Engineering and Construction Contract (Option C). The goal was to give prospective contractors the opportunity to be innovative and optimize the decommissioning procedure bearing in mind costly waste routes. Secondly, the final contract specification was developed with the preferred contractor as a preliminary phase of the Stage 3 contract.

2. Stage 3 decommissioning

2.1. UKAEA objectives

UKAEA needed to evaluate:

- (1) continued care and maintenance of the reactor, or
- (2) removal of the reactor, or
- (3) removal of the reactor and hanger.

The decision was to clear the site as waste routes for the graphite and other wastes were available, the land on which the hanger resided was suitable for redevelopment and continuing maintenance costs of the hanger were significant. During the work, it was important to avoid contamination of the hangar due to the decommissioning activity itself.

2.2. Stage 3 decommissioning issues

Contractor selection was considered important not only for the usual reasons of safety, quality and cost, or because of the ministerial and media attention noting the historical relevance of GLEEP, but also because of the many constraints that required a flexible and innovative approach. The key issues were as follows.

The distribution of radioactivity in the core and bioshield was predicted by UKAEA but not known in detail to those tendering. Emerging data arising from sampling and analysis during the Stage 3 activity would affect the decommissioning method. A flexible approach was therefore demanded to ensure that waste volumes were well managed.

Reverse of the manual construction methods for the graphite core would not be possible because lifting regulations (more recently introduced) prevented manual handling of graphite blocks nominally

41 kg in weight and 13 500 in number. The large number of blocks led to the need for a production line approach. The graphite blocks were not all identical being in several size groupings. Sampling of individual graphite blocks was required for inventory monitoring purposes and to ensure that correct waste routes were used with respect to both graphite condition and cost of route.

UKAEA sought a pragmatic fit-for-purpose approach and it was noticeable that focusing prospective safety case writers on this objective at the tender stage was challenging and was reflected in the range of safety case quotations received. In the event, UKAEA led the safety case preparation as well as its submission.

A record of the decommissioning work was required in accordance with UKAEA practices as UKAEA uses decommissioning data accumulated for parametric decommissioning project estimation and calculation of liabilities. Time-lapse photography was also to be used.

The challenge to the prime contractor also required the selection of innovative and responsive sub-contractors. In the event, Doosan Babcock chose handling subcontractors carefully as the production line approach demanded this. Briar Group had developed drill and tap techniques for Windscale AGR graphite removal and this could be adapted for use for graphite removal and sampling in the GLEEP core. R S Cranes were used for other out-of-core graphite handling operations. Callaghan Demolition Ltd was chosen for the bioshield demolition, disposal of conventional wastes and protection of the hanger.

2.3. Stage 3 scope of work and end point

The upper level scope of work to be undertaken by Doosan Babcock Energy Ltd and its team of subcontractors included:

- Removal of the graphite core, the subject of this paper
- Demolition of the reinforced concrete bioshield
- Handling and packaging of all radioactive and non-active wastes
- Cleanup of subreactor drains, sumps and foundations and storage pit.

Also included were the associated planning, contribution to safety cases, demonstration, sampling and analysis, mobilization of the team with training, implementation, demobilization and records.

Three safety cases were prepared for the project as follows:

- Radiological protection
- Reactor graphite removal and processing
- Removal of the biological shield

The physical end point of the project was defined as the removal of internal steelwork, graphite blocks, sub-base steelwork, demolition of the concrete bioshield, removal of sumps and drains and all wastes segregated, packaged and removed from the hanger. The dismantling and demolition processes were to be controlled by an agreed methodology to avoid impact upon the hanger of contamination, structural damage or unacceptable emissions to the surrounding areas.

The radiological end point for decommissioning was defined as follows:

Levels of contamination on hard non-porous surfaces on land and in buildings below 0.4 Bq/cm² (alpha) and 4.0 Bq/cm² (beta) averaged over an area of 0.3 m² taking into account background levels due to normally occurring radioactive material in construction material. Enhancements above these levels need to be shown to be due to NORM and agreed with the Project Manager. Where any measurement exceeds 0.1 Bq/cm² (beta) averaged over an area of 0.3 m², a swab should be taken to demonstrate that contamination is fixed. The contractor will agree the background levels to be used for the works with the project manager during production of the DSC.

2.4. Stage 3 organization

The UKAEA team responsible for the work included the overall project management team, commercial manager, RPA, HS&E personnel and supporting site services. UKAEA undertook a surveillance role with the exception of the safety case for which they took responsibility for preparation and submission and for site services that provided transport, storage and other miscellaneous supporting services.

Doosan Babcock Energy Ltd as prime contractor undertook all other activities as discussed above. The team on-site included:

- A site operations manager responsible for day-to-day control of the workforce, liaison with UKAEA and subcontractors, and most importantly ensuring absolute focus of every site team member on health, safety and environment.
- Especially, in the early days of the project, a site-based manager who had led the tender preparation team assisted in project management and technical issues to ensure close fit with UKAEA objectives.
- A radiation protection advisor with deputy to ensure not only the proper supervision of the workforce but also key to the management of wastes on this project.
- Suitably qualified and experienced HP monitors, tradesmen, and decommissioning and decontamination operators who implemented the work.
- An experienced demolition subcontractor to deal with the bioshield and associated excavation and concrete crushing activities and clean waste disposal.
- From time to time, other specialist subcontractors often already working at Harwell were engaged for specific tasks, e.g. asbestos removal.

3. Health physics

3.1. Health physics understanding and development of graphite inventory

The graphite pile contained a total of 167 GBq of which over 95% came from tritium and carbon-14. This relatively low level meant that it was possible for operators to enter the bioshield and remove the graphite core whilst wearing light protective equipment. Typical dose rates in the area were in the range background to 80 $\mu\text{Sv/h}$. The specific activity in graphite blocks ranged from 60 Bq/g to 1800 Bq/g and could be attributed largely to the above isotopes, though other isotopes were present, such as cobalt-60. Without wishing to detract from the importance of the personnel protection issues, it can be seen that the presence of tritium and carbon-14 impacts significantly on the disposal of the waste graphite.

UKAEA provided Doosan Babcock with detailed computer-based drawings identifying the position of every graphite block placed in the 40 layers forming the GLEEP core from which an identification and labelling system was derived. The exact position of every graphite block was therefore known as was its subsequent disposition. The labelling and recording (described in a later section) enabled records to be retained of the radiological data for each block. Initial monitoring and core sampling was at the point of removal of each block from the core. One data sheet was obtained for each group of 16 blocks that were removed concurrently in a single bin from the reactor core together with core samples. Before each group of 16 blocks was eventually crushed and placed in four 200 L drums (i.e. four crushed full sized graphite blocks per drum), monitoring for alpha and beta contamination and gamma dose rate was undertaken outside the bioshield. These monitored blocks were placed on pallets in groups of 16 and wrapped in cling film for temporary storage prior to crushing. Additional data was obtained because the drill and tap method used to secure and lift each block led to the opportunity to

obtain an individual core sample for every block within the reactor. These samples were analysed by an independent laboratory.

3.2. Health physics controls for graphite working

Supervised and controlled area designations were established and audited to the UKAEA site procedures. Alternative working controls developed as the project progressed. The cumulative dose for graphite removal and management was limited to 7 mSv by forward planning and open discussions with the site team. All ideas and suggestions for efficient working practices were considered. This was possible because suitably qualified and experienced decommissioning operatives and other tradesmen with extensive experience of site working practices in the areas of erection and dismantling had been selected. Detailed methodology and training prior to the graphite removal ensured all work was carried out in accordance with ALARP.

Alpha and beta air sampling and analysis were carried out within the reactor biological shield and at positions throughout the hangar area. Tritium-in-air analysis was carried out within the biological shield and passive tritium monitoring carried out throughout the hangar. All temporary extract systems were vented to atmosphere via an existing stack. In-situ particulate and tritium monitoring was carried out throughout the project. All survey data was entered onto the site database, reviewed by UKAEA and no detectable airborne activity resulting from the removal processes was recorded.

3.3. Health physics controls for graphite and secondary waste

Graphite blocks were crushed individually and stored in 200 L drums. There were 13 500 graphite blocks each weighing nominally 41 kg. On completion of the crushing process, each drum was subjected to a 14-point gamma radiation survey, and all results were recorded onto a logging sheet and transferred to the site database.

Various secondary wastes accumulated from the graphite removal processes (paper oversuits, gloves, polythene wrapping, etc.) were bagged and stored under controlled conditions. Disposal was via UKAEA waste routes.

3.4. Day-to-day control of project — radiological protection

Best management practice required that all personnel were issued with digital dosimeters for the duration of the removal process, and a daily personnel dose chart was maintained and kept as part of the site database. Additionally, contamination controls were established at the start of works by considering detailed methodology and training ensured that personnel were aware of the possibility of changes in working conditions as the project developed. Dressing procedures and strict contamination controls were enforced at the early stages of the graphite removal and proved appropriate as no contamination events were recorded.

Health physics personnel carried out a routine and interactive health physics monitoring regime daily and weekly including work area surveys. All survey reports were collated and reported, and will form a useful lessons learned information for future projects.

In view of the importance of the health physics processes, use of a health physics team comprising suitably qualified and experienced persons was considered to be of high priority, and all the monitoring personnel were consequently selected and employed by Doosan Babcock and their CVs submitted to UKAEA for approval.

3.5. Health physics lessons learned

The pre-planning and personnel selection stages of the works were very time consuming, but the benefit was to get it right first time in terms of quality, health, safety and environmental issues.

A specific problem with working with graphite was the possible ingress of graphite particles into the internal components of the selected monitoring instruments. Consideration needs to be given to this in care and maintenance of the health physics instrumentation.

4. Operations

4.1. Management of graphite waste route

Total accountability for each graphite block removed was achieved by logging individual blocks and ensuring traceability of the data right through to the crushing and drumming process. Detailed analysis carried out by an independent laboratory and historical data enabled activity fingerprints to be produced for activity assessments. This was facilitated because the drill and tap method used for safe lifting of each graphite block resulted in core samples being available for each block. All waste transfers were carried out in accordance with UKAEA requirements. Drummed crushed graphite was transferred to storage areas on the Harwell site in accordance with existing UKAEA procedures. A positive teamwork approach between UKAEA and Doosan Babcock to resolve waste issues encouraged the success in ensuring that site requirements were met and that UKAEA will be in a strong position to demonstrate to waste disposal authorities the traceability of the GLEEP waste.

4.2. Final disposal of graphite — client responsibility

Doosan Babcock responsibility ended with the handling of the crushed graphite in drums and the associated records to UKAEA. It should be noted that there were two waste routes considered, either disposal to the Low Level Waste Repository in half-height ISO container or thermal treatment for which crushing was desirable to facilitate the process. The thermal route was subsequently the preferred option.

4.3. Graphite removal

The graphite removal activity comprises three processes:

- (1) The physical process for removing the blocks safely, efficiently and quickly from the reactor core;
- (2) The waste management process for processing the graphite to the point where it can be handed over to the client for storage/disposal;
- (3) The documentation process that supports this process to assure traceability of waste.

Removal of blocks from core

Three solutions were considered: manual sliding of graphite blocks into a lifting bin, vacuum lifting, and drill and tap (Fig. 3). The second and third solutions were preferred. In the event, both techniques were used, but drill and tap was the preferred technique for initial graphite block handling in the reactor, and vacuum lifting was retained as a reserve and also assisted lifts outside the bioshield. The vacuum lifting fail-safe condition was to lower a graphite block to the ground.

Drill and tap had also been used for handling graphite in the Windscale AGR and had proved very successful. The specialist mechanical handling company was engaged by Doosan Babcock to supply and advise on the system for GLEEP. The spin-off advantage of drill and tap was that, because every block required three holes drilled in it, core samples could be obtained from the debris, collected by a vacuum cleaner (Fig. 3) and taken away for radiochemical analysis. Handling operations for the drill and tap machine in the core area were carried out using a remotely controlled x-y plotter machine in Fig. 4.



FIG. 3. Drill and tap machine and collection of graphite sample.



FIG. 4. Graphite block handling.

The core contained 13 500 blocks of various dimensions. The pile was constructed from individual blocks stacked in layers. Each graphite block was 184 mm^2 . There were three lengths which were 737 mm (predominant), 368 mm (some of them) and 552 mm (a few). The average density of the graphite was 1.64 g.cm^3 . Each full 737 mm block weighed approximately 41 kg, the others weighed proportionately less. A small number of half bricks were also present and abestos was found between some layers of bricks. The removal process had to accommodate the weight of these blocks, the access, which was done top down using existing access into the bioshield (Fig. 5), and the removal in a reasonable timescale.

Man access to the graphite core was initially performed by using a basket lowered in by crane from the top until sufficient graphite had been removed to reach the thermal column. Thereafter, access was performed through the side of the bioshield.

Graphite waste management

Removal from the reactor involved removing 16 blocks at a time in a bin (Fig. 5). The bin was lifted out of the reactor using a pillar/swivel crane installed on top of GLEEP and the crane lowered the bin down the side of the bioshield to the hangar floor, where the bin was emptied using the vacuum lifter, and the blocks were wrapped in cling film and temporarily stored on pallets. Later, they were transferred to the shredder located in the same area (Fig. 6) where they were unwrapped and placed on a roller table before being driven by hydraulic ram into a shredder and crushed. The vacuum lifting device was also used at this point of the process. The shredded graphite was loaded into 200 L drums that were then sealed and palletted prior to transport to UKAEA's storage area. Additional monitoring was also carried out in the shredding/wrapping area.

The standard waste shredding machine was fitted with improved cutters and included a grading plate that ensured that the graphite pieces were less than 50 mm in size before deposition in the 200 L drums. The machine had a variety of interlocks and safety devices, and included sealing to limit the spread of dust.

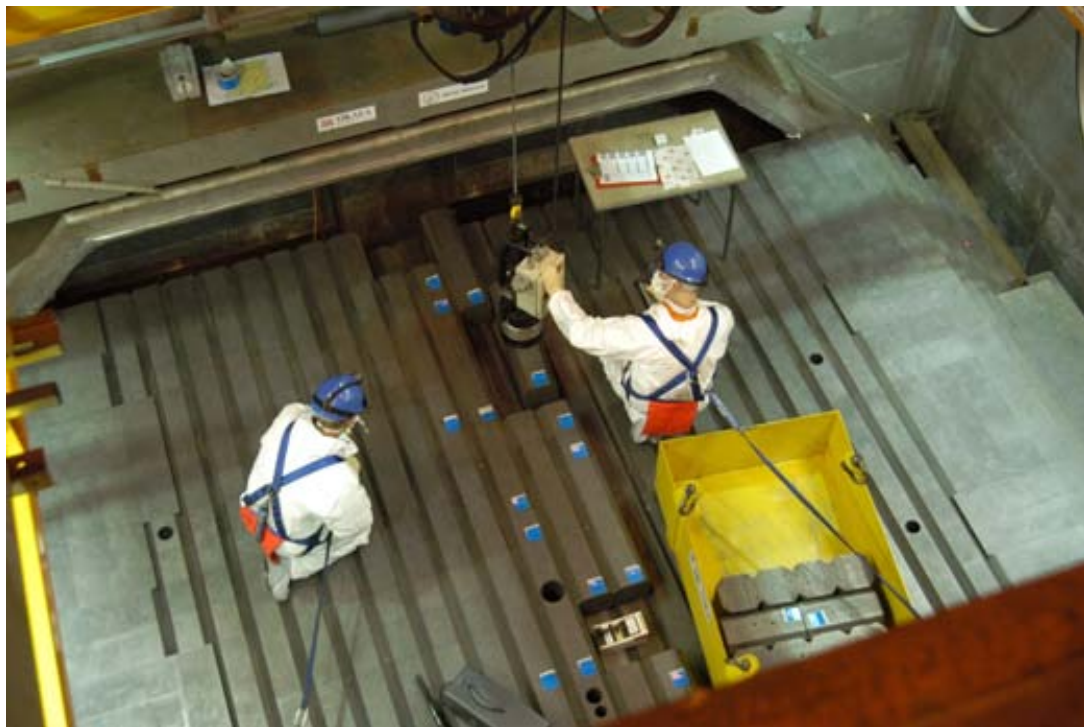
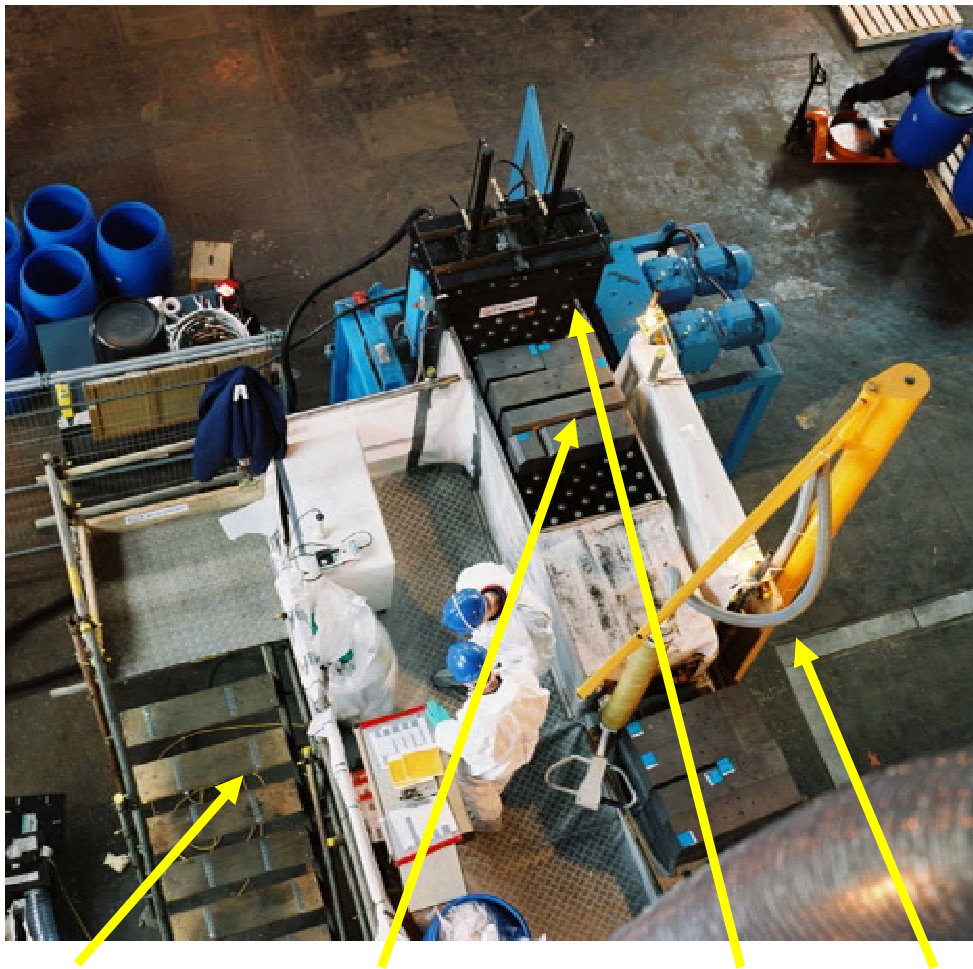


FIG. 5. View of top access into reactor showing bin and top of core.



Monitoring table Half blocks on roller table Shredder Vacuum lifter

FIG. 6. Aerial view of the block crushing station.

Waste traceability

The labelling, documentation and recording procedure is summarized in Table 1.

Table 1. The labelling, documentation and recording procedure

Step	Action	Note
1	Issue office issues document pack in robust plastic envelope.	Includes: <ul style="list-style-type: none"> • Labels • Logging sheet • Pallet number
2	Deliver document pack to GLEEP core area	
3	Identify blocks and take sample from drill and tap residues	Drill and tap needed for lifting block
4	16 identified blocks loaded into bin together with all documentation and samples	Bin lifted out of core area by crane and placed on hanger floor
5	Each block placed on an identified pallet and samples removed to transfer fume cupboard	16 blocks per pallet stored and then taken to crushing area
6	Documentation returned to issue office for transfer to A4 document pack	
7	A4 document packs collected from issue office and taken to crushing area	
8	Block labels transferred to 200 L drums and drum label attached to drum	4 blocks crushed and placed in the 200 L drum, then sealed Block logging sheet returned to issue office
9	All drums weighed and 14 point radiological survey Data recorded	Issue office sends and receives the logging sheet with the data recorded.
10	Logging sheet info entered onto database and UKAEA waste transfer documentation now complete	Activity assessments on each batch of drums also carried out
11	Waste review acceptance received and recorded, and cross-referenced to location of waste in UKAEA waste store	
12	Integration of drum labelling data and database entries	
13	Deliver drums to allocated position in waste store	Logging sheet stored in site filing system

Each of the above steps was covered by an appropriate quality procedure.

4.4. Site management and lessons learned for graphite removal

In summary, the important management issues on this work related to the management systems and records, the promotion of teamwork and specific site experience.

Management systems and records

Site organization required a highly skilled team from management through health physics to the implementing workforce, both Doosan Babcock employees and the subcontractors. Site organization development commenced pre-tender and continued to the end of the project. Close interface with the client, the subcontractors and Doosan Babcock's own team at all stages contributed to a successful project outcome.

The quality assurance system used enabled UKAEA to demonstrate and substantiate the waste management process in terms of source, inventory, condition, packaging and disposition of the packaged waste. This was necessary to enable the final disposal choice for the graphite, which for GLEEP was thermal treatment.

Teamwork

The team was considered to comprise the employees of UKAEA, Doosan Babcock and the sub-contractors. The combined experience of the team members covered the following:

- Knowledge of GLEEP's design and operational history
- Assessment of graphite contaminant inventory
- Safety case preparation
- Harwell site working
- Quality assurance, health, safety and environmental management systems
- Safe working in radioactive environments
- Handling of materials
- Lifting and processing operations
- Demolition
- All aspects of the waste management process
- Innovative transfer of experience across UK nuclear sites

Proactive application/team involvement in workforce safety

Despite the relatively limited radioactive inventory, the decision to select the most highly skilled team was justified as it demonstrated to the public, those responsible for safety and those for funding that UKAEA and its contractors had managed the process professionally and close to time and budget. Such teamwork requires confidence in the expertise, willingness to work together to resolve problems and appropriate contract conditions such as the Engineering Construction Contract.

Site experience

The experienced site team was able to manage change and had to respond to the following:

- As layers of graphite were progressively removed, an access route alternative to top entry was reached (the thermal column), giving the opportunity to speed up the graphite removal process.
- Graphite blocks covered a much wider weight range than expected and specifications for lifting operations needed to be aware of this.
- UKAEA was able to use lessons learned to the benefit of its overall graphite reactor decommissioning programme. Windscale AGR experience in lifting graphite was fed into GLEEP and one reason for maximizing data gathering from the GLEEP graphite was to feed on to Windscale Pile decommissioning.
- The GLEEP core was built from two types of graphite, Canadian graphite and British graphite. The Canadian graphite was purer and was used for the central layer, and British graphite was used for the upper and lower layers.
- Asbestos seals found in the core came as a surprise, but it is never a surprise that asbestos might turn up in these old plants and so the problem could be easily addressed by being aware of an asbestos removal contractor already working in radioactive areas on Harwell site.
- One does not normally have to receive at least four visits from television and the Energy Minister who wishes to crush the last graphite block, but it was recognized that such interest

might occur, and the site team welcomed the interest in the project and took time-lapse photography as it is expected interest will continue for some time.

- The use of drill and tap for lifting and to obtain samples was a particular useful example of kill two birds with one stone. And this duality gave the technique an advantage over the vacuum lifting process, which was used outside the reactor.
- The standard paper shredder, but modified to deal with the properties of graphite, proved to be an extremely simple and effective crushing device.
- The amount of attention paid to handling the graphite blocks to assure operator safety proved well worthwhile as an excellent safety record was maintained.

5. Other work

Whilst not the subject of this paper, for completeness it should be noted that the project went on to remove the 11.4 m² by 12.5 m high and 1.65 m thick reinforced concrete bioshield. Four metres of the bioshield was below floor level and the core was supported on a steel plate. Beneath, there were drains and sumps for fire suppression water and foundations. There was an adjacent redundant fuel storage pit. There was non-uniform distribution of mainly tritium activity in the bioshield with maximum concentrations arising close to the inner surface of the concrete and on the centre line of the reactor core. Other radioactive isotopes present were cobalt-60, europium-152, europium-154 and iron-55.

The wastes produced in disposing of the bioshield are summarized in Table 2. The methods, criteria of evaluation and choice of demolition technique are given in Table 3. Figure 7 shows demolition in progress, Figs 8 and 9 show the demolished concrete before and after crushing for use as in-fill, Fig. 10 shows subreactor excavations and Fig. 11 the packaged crushed graphite waste awaiting transport for storage prior to its eventual thermal treatment.

The waste quantities produced during demolition of the reactor, not graphite, are summarized in Table 2, and the techniques considered, criteria for selection and final decision given in Table 3.

A paper describing the removal of the bioshield may be found¹.



FIG. 7. Demolition in progress.

¹ Grave, M.J., Buffery, J., McNaughton, P., Hayward, R., Dobriskey, M., Decommissioning of GLEEP: Demolition and Waste Management of Concrete Structures and Foundations. Tenth International Conference on Environmental Remediation and Radioactive Waste Management. September 4–8, 2005, Scottish Exhibition and Conference Centre, Glasgow, Scotland.



FIG. 8. Concrete prior to crushing.



FIG. 9. Concrete after crushing.



FIG. 10. GLEEP excavation.



FIG. 11. Packaged graphite awaiting transport to store.

Table 2. Demolition waste quantities

Waste quantities achieved
<ul style="list-style-type: none"> - 230 t of free release steelwork - 2300 t of concrete - Concrete crushed to <25 mm for road building - 160 t of low level waste (<12 GBq/te beta/gamma and <4 GBq/te alpha)
LLW Management
<ul style="list-style-type: none"> - Process in hangar into half-height ISO containers - Disposed to LLW repository by UKAEA - Miscellaneous items HHISO (items weighed, recorded and photographed in position)
Bulk items (not LLW)
<ul style="list-style-type: none"> - Into builders skip (weighed, monitored, fingerprint check)

Table 3. Selection of demolition methods

Techniques considered
<ul style="list-style-type: none">- Planing- Gas-canister bursting- Conventional demolition breaking- Not preferred — water jetting and diamond wire
Criteria of evaluation
<ul style="list-style-type: none">- Distribution of activity in concrete- Presence of reinforcement and steel structure- Hardness of the concrete- Management of waste volume- Reuse of the concrete
Decision
<ul style="list-style-type: none">- Low radioactivity levels — no need for planning- Concrete generally too soft for gas-canister- Conventional breaking preferred

6. Programme and performance

The tender start date was October 2002 with contract award in May 2003. To facilitate programme, safety approvals for graphite removal and demolition were undertaken separately and graphite removal approval was achieved in November 2003; the core was removed in May 2004 and the overall project completed at site in November 2004. The case history was completed in January 2005. The project was completed one week ahead of schedule. A target cost contract was used against an activity schedule with a pain/gain share mechanism with adjustment both positive and negative for compensation events. Allowing for the adjustments the contract comes in within +5% of the target value.

7. Conclusions

Graphite was removed from the reactor by a mechanized process, crushed and stored in 200 L drums.

Simple proven mechanical techniques eliminated the need for manual handling.

The project objectives, quality assurance, safety, programme and cost were achieved by selecting a hand picked team and by learning from the workforce.

Management of records was a high priority and was simply achieved.

Teamwork under appropriate contract conditions benefited the project, the client and the contractor.

The graphite handling process was designed to assist the client access more economic and effective graphite disposal means.

ACKNOWLEDGEMENTS

This paper draws upon several papers presented by authors of UKAEA and Doosan Babcock Energy Ltd. The inputs of P. McNaughton, M. Dobriskey, B. Hayward of Doosan Babcock Energy Ltd, Gateshead, UK, and J. Buffery of UKAEA, Harwell, UK are acknowledged. The project was funded by the UK Department of Trade and Industry.

Review of the characterization of nuclear graphites in UK reactors scheduled for decommissioning

A.N. Jones[†], L. McDermott, J. Marsden, T.J. Marrow

Materials Performance Centre, University of Manchester, United Kingdom

Abstract. The United Kingdom (UK) graphite moderated reactors will produce somewhere in the region 90 000 t of irradiated nuclear graphite after operation ceases. Therefore, radioactive graphite core dismantling and the management of radioactive graphite waste are important issues in the UK. There are potential concerns associated with several radioactive isotopes in this material; these are namely ^3H , ^{14}C , ^{36}Cl , ^{60}Co , ^{152}Eu and ^{137}Cs . One isotope of importance is ^{14}C , which is produced during irradiation through the transmutation of the ^{14}N . ^{14}C has a long half-life of 5730 years and there are environmental concerns related to possible release of this isotope during decommissioning. Recent research has indicated that it may be possible to reduce the activity of the radioactive graphite waste [1, 2]. If applied, this would lead to the reduction in volume of intermediate level waste. This paper addresses the types of UK nuclear graphite and carbon waste, which have very different microstructures and different quantities of isotopic impurities. Waste management programmes, for the development of treatment and recycling and long term safety assessments for final disposal, require further detailed assessment of the data and comprehension of the structure and localization of the isotopic containment. The paper describes issues surrounding the decommissioning of the UK nuclear graphite and identifies possible methods for impurity removal treatment.

1. Introduction

Graphite has been used as a neutron moderator and neutron reflector in more than 100 nuclear power plants worldwide and in many research and plutonium production reactors [3]. There are approximately 42 nuclear power stations in the United Kingdom (UK) (18 still operational), which when closed will produce somewhere in the region 90 000 t of irradiated graphite waste [4]. Graphite was chosen as the material of choice for a nuclear moderator due to its ability to slow down the neutrons produced by the nuclear fission reaction, as a result of its high scattering cross-section and low cross-section for neutron capture. In order to achieve the best performance from the graphite, it requires the highest possible density and the greatest degree of purity. Other properties such as good mechanical strength [5], machine ability, high thermal conductivity and low thermal expansion are also important [6, [7].

As well as acting as a neutron moderator or neutron reflector, graphite is also used for other features of reactor cores such as shield-wall graphite. It is also used for fuel channel liners (Chapelcross), fuel sleeves (AGRs and Hunterston A), fuel support struts (Berkley), Windscale boats and dowels. The core volumes can amount to over 3000 t of graphite material in the largest reactors (e.g. the later Magnox reactors).

There are four main sources of UK graphite waste: (1) the former UKAEA gas cooled reactors (Table 1). Windscale Piles, British Experimental Pile Zero (BEPO) and Graphite Low Energy Experimental Pile (GLEEP, now dismantled), plus a large quantity of operational waste from the Windscale Piles. There is also the High Temperature OECD Dragon Reactor at ex-UKAEA Winfrith [8]. This graphite included grades such as AGXPT, AGXP, Welland etc. (2) Magnox reactors

[†] Correspondence author

(Table 2). Pile Grade A (PGA) used as a moderator and Pile Grade B (PGB) used in the reflectors (in fact PGB consists of several grades). (3) Advanced gas cooled reactors (AGRs) (Table 3), in which Gilsocarbon was used as a moderator and various grades were used as a reflector. (4) Significant numbers of fuel sleeves, manufactured from either PGA (early Magnox sleeves) or VFT coke graphite and NITTETSU coke graphites (AGR fuel sleeves and later Magnox sleeves).

Table 1. Former UKAEA gas cooled reactors (all shut down)

Reactor	Site	Type	Power MW(th)
GLEEP	Harwell	Graphite moderated air cooled	0.05
BEPO	Harwell	Graphite moderated air cooled	6.5
PILES 1 and 2	Windscale	Graphite moderated air cooled	160
WAGR	Windscale	Graphite moderated CO ₂ cooled	110
DRAGON	Winfrith	Graphite moderated He cooled	20

Table 2. Magnox reactors

Station	Reactors	Start of operation	Total electrical power (MW)	Shutdown	Expected closure
Calder Hall	4	1956–1959	200	2003	
Chapelcross	4	1959–1960	200	2005	
Berkley	2	1962	276	1988–1989	
Bradwell	2	1962	246	2002	
Hunterston A	2	1964	300	1990	
Trawsfynydd	2	1965	390	1993	
Hinkley Point A	2	1965	470	2000	
Dungeness A	2	1965	440	2006	
Sizewell A	2	1966	420	2006	
Oldbury on Severn	2	1968	434		2008
Wylfa	2	1971	950		2010

Table 3. Advanced gas cooled reactors

Station	Reactors	Total electrical power (MW)	Start of operation	Graphite manufacturer
Hinkley Point B	2	1220	1976	AGL
Hunterston B	2	1190	1977	AGL
Dungeness B	2	1210	1984	AGL
Heysham, 1	2	1150	1984	BAEL
Hartlepool	2	1110	1985	BAEL
Torness	2	1250	1988	UCAR
Heysham 2	2	1250	1989	UCAR

2. Characterization of UK graphites

Characterization of radioactive graphite waste is complicated due to many variables between nuclear plant design and operational conditions [9]. Not only has nuclear grade graphite been sourced from a variety of locations, the effects of other variables such as operational lifetimes, reactor assembly, core temperature, fuel, coolant composition, graphite radiolytic weight loss and shutdown periods on the microstructure and its properties must be considered.

2.1. UK's nuclear graphite manufacturers

It is well documented that nuclear graphite is manufactured from petroleum or natural pitch cokes [10]. Non-irradiated (virgin) nuclear graphite is a polygranular crystalline material that has an initial density in the range 1.6–1.8 g cm⁻³. This can be compared with a theoretical graphite crystal density of 2.265 g cm⁻³, the difference being due to internal porosity in the manufactured structure [11]. The type and size of coke used and the manufacturing route largely determine the virgin graphite material physical properties. Typical virgin material properties for the UK Pile Grade A (PGA) and Gilsocarbon graphites are shown in Table 4. PGA was the graphite used in the Magnox reactors, and was produced from a petroleum coke, which is a by-product of oil refining industry. The PGA coke has needle-shaped coke particles. The PGA blocks were produced by an extrusion process, which tended to align the needle coke particles; thus the crystallographic basal or layer planes tend to lie parallel to extrusion axis, giving rise to the anisotropic properties of PGA graphite.

In comparison to PGA, Gilsocarbon is a “more robust” graphite, especially developed for the AGRs. The final polycrystalline microstructure of Gilsocarbon is determined by the structure of the coke, the binder and also by the manufacture process. The naturally occurring asphalt pitch-coke was mined from Gilsonite veins, found between Colorado and Utah, USA [12]. The coke particles have an “onion skin” structure and the blocks were produced by a moulding process, which aimed to give a random coke orientation. This leads to the generally near-isotropic Gilsocarbon graphite properties. Gilsocarbon graphite has a higher density and strength compared to PGA and a lower porosity, which gives a lower radiolytic oxidation rate. Figure 1 shows cross-polarized optical micrographs and scanning electron micrograph (SEM) images of PGA and Gilsocarbon graphites typically used in the UK reactors.

Table 4. Typical virgin properties of Pile Grade A (PGA) and Gilsocarbon nuclear graphites

Property	Units	Pile Grade A graphite (Anisotropic)	Gilsocarbon graphite (Isotropic)
Density	g cm ⁻³	1.74	1.81
Thermal expansion coefficient (20–120°C)	K ⁻¹	0.9E6 * 2.8E6 **	4.3 × 10 ⁻⁶
Thermal conductivity (20°C)	W.m ⁻¹ K ⁻¹	200 * 109**	131
Young's modulus (20°C)	GPa	11.7 * 5.4**	10.85
Strength tensile	MPa	17 * 11**	17.5
Strength bend	MPa	19 * 12**	23
Strength compression	MPa	27* 27**	70
Electrical resistivity	M ohm cm ⁻¹	620 * 1100*	900

* Denotes parallel to the layer planes.

** Denotes perpendicular to the layer planes.

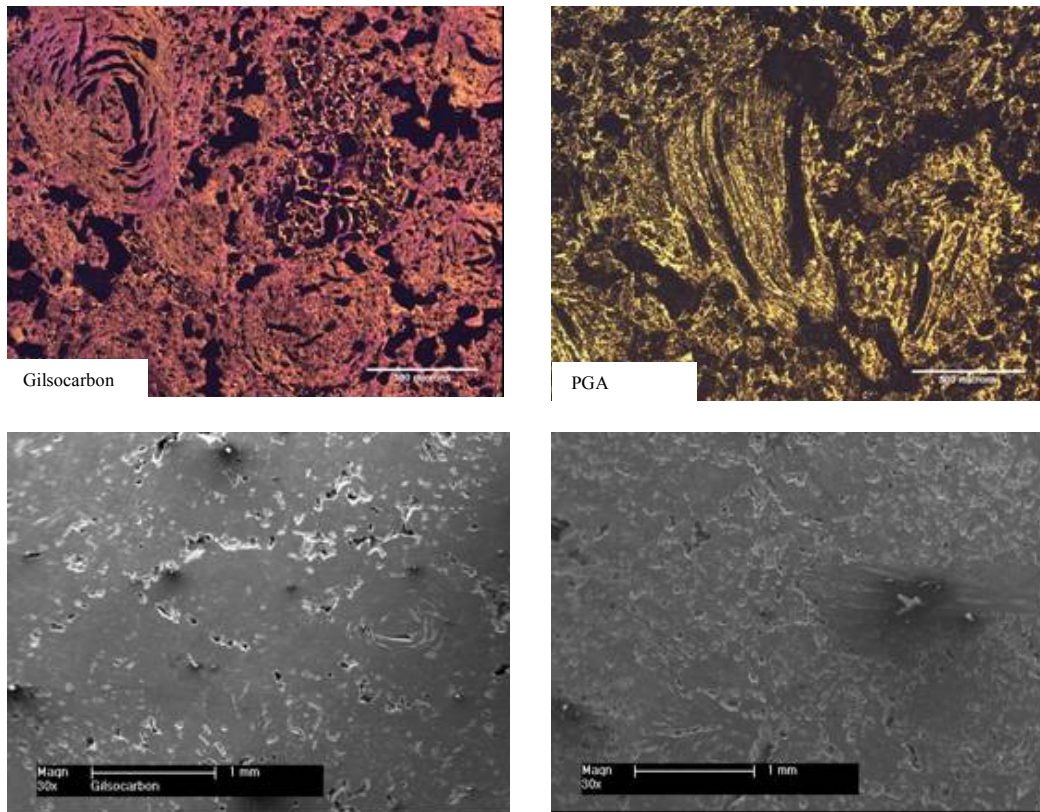


FIG. 1. Cross-polarized optical micrographs (scale bar 500 μm) and SEM images (scaled bar 1 mm) of typical Gilsocarbon and PGA graphites used in the UK reactors.

Although both Gilsocarbon and PGA graphites are extremely pure, with impurities measured in parts per million (ppm), purity is an important factor that needs to be taken into account when decommissioning these reactors. However, it is unlikely that decommissioning was seen as a major issue when these reactors were designed. The PGA used in the Magnox reactors, which use natural uranium fuel, was deliberately chosen for its purity whereas the higher rated AGRs, which use uranium oxide fuel, did not require such a stringent purity specification. The result is that the activity of irradiated Gilsocarbon graphite tends to be higher than that of PGA graphite, due to traces of ^{60}Co from the activation of impurities and from the transmutation of ^{59}Co for example.

There were two main UK manufacturers of nuclear graphite¹:

- (1) Graftech — previously, British Acheson Electrodes Ltd (BAEL), which then became Union Carbide Corporation (UCAR)
- (2) SGL — previously Anglo Great Lakes (AGL), later amalgamated with Pechiney in France)

BAEL was based in Sheffield; AGL in Newcastle-on-Tyne; both companies no longer manufacture graphite in the UK and the factories no longer exist.

2.2. Variables within the UK manufacturers

The UKAEA was responsible for the graphite supply to all the Magnox reactors, under the direction of C. Hinton. All Magnox Pile Grade A is understood to have been produced from the same coke supply in Pernis, Netherlands. However various binder and impregnation pitches are likely to have been used

¹ There was also a prototype graphite manufacturing plant at UKAEA Harwell, which operated for a few years [44]

in the graphite manufacture. Pile Grade B was used for the Magnox reflectors. In the first eight dual power plutonium and power production Calder Hall and Chapel Cross reactors, this was the same grade as used in the Windscale Pile cores; however, shortages in graphite supplies for the new range of “civil” power producing reactors led to the reflector graphite being manufactured from various sources depending on what was available at the time [13].

Gilsocharbon graphite was all manufactured from Gilsonite pitch-coke [12]. The AGR fuel sleeves were produced from various pitch coke graphites. This was first manufactured by both GrafTech and SGL (and their predecessors), with the machining of the AGR sleeves carried out by BNFL [15]. However, now only SGL still produces and machines fuel sleeves. Initially, the AGR fuel sleeve graphite was manufactured from VFT coke graphite from Germany. Later, however, this was discontinued and replaced by NSCC coke from Japan. This is still used to date.

2.3. Neutron flux rates

UK graphite will have been irradiated to various fast neutron doses by end of generation. These are estimated to range between 0.1×10^{20} n cm⁻² equivalent DIDO nickel dose (EDND) and $\sim 200 \times 10^{20}$ n cm⁻² EDND [16]. Additionally, the graphites have been irradiated in various coolant gas compositions (air, helium, carbon dioxide and mixed coolants such as CH₄ + H₂ + CO). In certain cases, the coolant gas may have included impurities, which arose failed fuel or reactor accidents. Examples of this are the Windscale Piles [15] and Chapelcross [19]. Some graphite in storage silos and also in Windscale Pile 1 may have been wet at some time. Some irradiated graphite operational waste is stored under water (AGR fuel sleeves at Windscale for example).

2.4. Radiolytic oxidation and stored energy within nuclear graphite

Radiolytic oxidation occurs when carbon dioxide reacts with ionizing radiation to produce an oxidizing species [20] These reactive oxidizing species absorb on a graphite surface, and lead to graphite oxidation. The rate of radiolytic oxidation of the graphite depends on the gamma energy absorbed by the carbon dioxide within the pores of the graphite. Graphite exhibits various degrees of radiolytic oxidation, which may be up to $\sim 40\%$ weight loss from the virgin state. This will have lead to degradation of the graphite properties, including hardness, strength and thermal conductivity. In the Dragon high temperature helium cooled reactor, at UKAEA Winfrith, where the graphite operated in an inert atmosphere, such radiolytic oxidation is not an issue.

For the Windscale Piles and in BEPO (Harwell), the irradiated graphite waste contains significant levels of stored (Wigner) energy. The rate of release of stored energy on heating has been known to exceed the specific heat of graphite, thus the release of stored energy can be self-propagating under certain circumstances. In Magnox reactor graphite, the rate of release of stored energy does not exceed the specific heat of graphite due to the higher operating temperature. Hence, even though there is a significant amount of stored energy in some of the Magnox graphite, the release of this energy has been shown not to be self-propagating [25][27]. Stored energy is not an issue in the AGR graphite wastes, as these operate at higher temperatures.

2.5. Mechanical property changes in irradiated graphite

During the operational reactor lifetime, nuclear graphite is subjected to fast neutron irradiation. Under fast neutron irradiation, some of the properties of graphite change significantly from the virgin values; important irradiation-induced changes to graphite properties are component dimensional changes and changes to Young’s modulus [28], strength, coefficient of thermal expansion (CTE) and thermal conductivity [6] This issue is complicated further as the graphite properties (with the exception of CTE) are also changed by the process of radiolytic oxidation, as discussed above.

3. Radioactive graphite waste

Graphite is used for neutron moderation, and some of the impurities will be activated as a result of nuclear fusion reactions which occur at the relatively high temperatures of reactor operational conditions. Particular concerns associated with disposal of irradiated graphite waste include the presence of several radioactive isotopes; these are namely ^3H , ^{14}C , ^{36}Cl , ^{41}Ca , ^{55}Fe , ^{63}Ni , ^{60}Co , ^{152}Eu , ^{90}Sr , ^{133}Ba and ^{137}Cs , and some transuranics [31]. Table 5 gives details on the types of radiation and typical half-life for the radioisotopes found in nuclear graphite. The significance of these isotopes depends on their quantity, half-life and free neutron kinetic energy. These are shown in Figs 2 and 3. Most activity is contributed by ^{14}C and ^3H (tritium). Carbon-14 is a long lived beta emitter with a half-life of 5730 years; it is produced by three nuclear reactions between $^{14}\text{N}(\text{n},\text{p})^{14}\text{C}$ and $^{13}\text{C}(\text{n},\gamma)^{14}\text{C}$ that are contained in the graphite moderator and ^{17}O . Tritium has a half-life of 12.3 years and is mainly produced from the neutron activation reaction $^6\text{Li}(\text{n},\alpha)^3$. Very small amounts of ^3H probably occur also from $^3\text{He}(\text{n},\text{p})^3\text{H}$ and $^2\text{H}(\text{n},\gamma)$. Tritium is a low energy beta emitter, leading to issues of detection and contamination. The environmental problems related to these isotopes are due to the possible release of radioactive methane gas or other harmful organics whilst decommissioning [31].

Table 5. Types of radiation and half-lives for the radionuclides in nuclear graphite

Radioisotope	Radiation energy				Half-life (years)
	α	B	γ	E	
^3H		√			12.3
^{14}C		√			5730
^{36}Cl		√			300 000
^{41}Ca				√	130 000
^{60}Co		√	√		5.3
^{85}Kr		√			10.8
^{94}Nb		√	√		20 000
^{95}Nb		√	√		0.096
^{133}Ba			√	√	10.5
^{134}Cs		√	√		2.06
^{137}Cs		√	√		30.2
^{152}Eu			√	√	13.3
^{154}Eu		√	√	√	8.5
^{155}Eu		√	√		4.96
^{238}Pu	√				87.75
^{239}Pu	√				24 390
^{240}Pu	√				6537
^{241}Am	√		√		433
^{241}Pu	√	√			14.89

Other active contributory isotopes include ^{60}Co and ^{36}Cl [32]. Carbon-60 is a significant activation product when decommissioning a reactor core as it has a short half-life of 5.3 years, emitting both beta and gamma radiation. Chlorine-36 has a half-life of ~300 000 years; it is present as a daughter product of krypton (produced by fission of U and Pu [33] and from trace amounts in the atmosphere) and is produced by neutron activation of $^{35}\text{Cl}(\text{n},\gamma)$, which remains from the purification of graphite in the manufacturing process. The long half-life of ^{36}Cl (with its subsequent low specific activity), combined with the relatively low energy of its beta particle and small amount of gamma radiation, limits the hazards associated with this radionuclide.

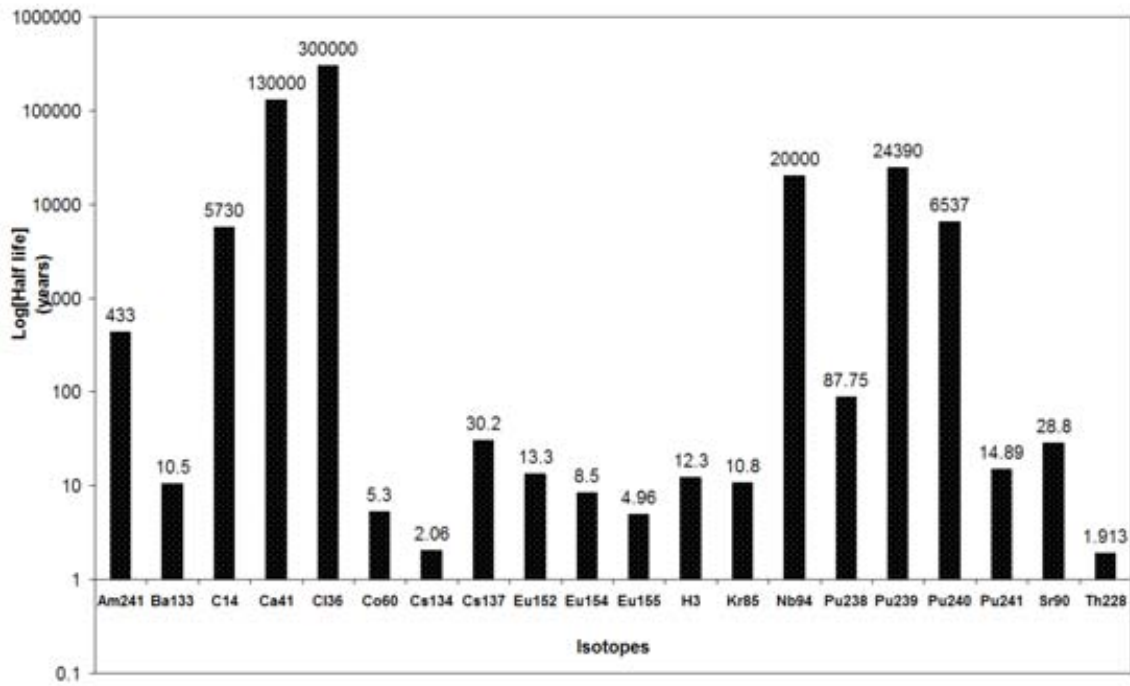


FIG. 2. Common radioisotopes found during decommissioning.

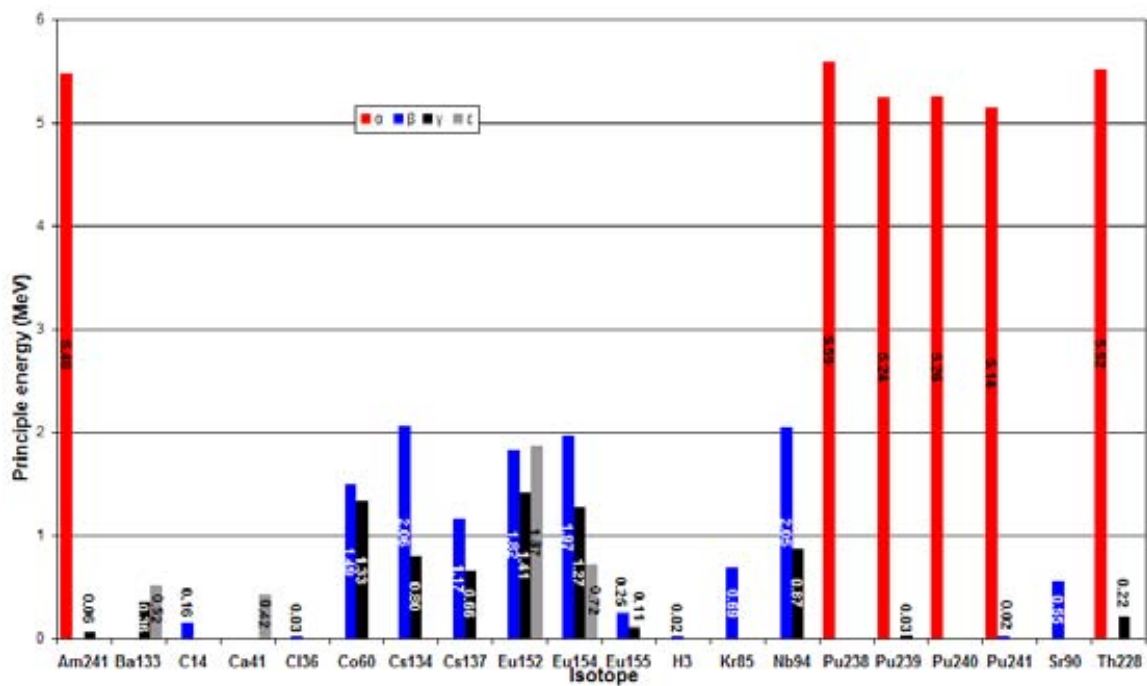


FIG. 3. Principal particle energies of various radioisotopes relevant to decommissioning.

4. Treatment and isotopic immobilization of nuclear graphites

The main issue associated with the disposal of irradiated graphite is the large volume of relatively low active waste to be dealt with [34]. Current data released by the Nuclear Decommissioning Authority (NDA) [36] reports that 56 000 t Magnox, 25 000 t AGR plus graphite[37] from other sources including Windscale piles and test reactors will lead to 90 000 t of nuclear waste graphite in the UK. This does not include the effects of oxidation weight loss, which will affect a proportion of this graphite. The favoured option, to date, for the 90 000 t of irradiated nuclear graphite waste is deep geological disposal. The NDA has calculated that the NDA-owned graphite would be in excess of 50 000 m³, with packaged volumes in excess of 100 000 m³ (dependent on packaging factor volume). This volume would take up two thirds of a proposed UK deep repository.

Therefore, to evaluate the possibility of reducing costs, it is important to consider alternative methods. These include various methods of encapsulation, and alternative routes for disposal [38], reprocessing [39] and decontamination [40]. A number of innovative techniques have been suggested, such as thermal treatment under inert and oxygen conditions [41] or with reactive gases [42], chemical leaching [1], ¹⁴C sequestration for future reprocessing (using ¹⁴C separation techniques) [41] and the potential microbial treatment.

Present work under development at the University of Manchester includes thermal treatment and leaching to ascertain methods to accurately determine the activity of radioisotope nuclides in nuclear graphite. This work is initially concentrating on the activity of ¹⁴C and ³H. The aim is to understand the type and quantity of impurities in both unirradiated and irradiated graphite. Future research will focus on questions such as graphite isotopic concentration and differences between the surface and the matrix.

5. Conclusions

The types of UK graphite waste are diverse. Categorization based on only one or two grades of graphite as definitions of 'UK graphite' can be misleading due to the variation of raw material suppliers, and the varying manufacturers and operational histories.

The irradiation history and irradiation damage processes, including radiolytic weight loss, which lead to dimensional and property changes including thermal conductivity and strength, are quite well understood and can be quantified.

More information regarding the initial impurity and final radioisotopic inventory of irradiated graphite waste is required. A better understanding of how these impurities are bound within the microstructure of the irradiated graphite waste is also required. This understanding is needed to make informed decisions regarding the disposal of this waste; in order both to devise waste treatments and reduce the activity and to assess the stability of the irradiated graphite waste for a selection of disposal options.

ACKNOWLEDGEMENTS

This work was carried out as part of the TSEC programme KNOO and as such we are grateful to the EPSRC for funding under grant EP/C549465/1.

REFERENCES

- [1] HOU, X., OSTERGAARD, L.F., NIELSEN, S.P., *Analytica Chimica Acta* 535 (2005) 297.
- [2] COSTES, J.R., DE TASSIGNY, C., VIDAL, H., *Waste Management* 10 (1990) 297.
- [3] KELLY, B.T., *Carbon* 20 (1982) 3.
- [4] INTERNATIONAL ATOMIC ENERGY AGENCY, *Nuclear Graphite Waste Management, Proceedings of a Technical Committee Meeting held in Manchester, United Kingdom, 18–20 October 1999*, IAEA, Austria, Vienna (1999).
- [5] PRESTON, S.D., MARSDEN, B.J., *Carbon* 44 (2006) 1250.
- [6] ZOU, Z., FOK, S.L., MARSDEN, B.J., OYADIJI, S.O., *Engineering Fracture Mechanics* 73 (2006) 318.
- [7] MITCHELL, B.C., SMART, J., FOK, S.L., MARSDEN, B.J., *J. Nucl. Mater.* 322 (2003) 126.
- [8] SHAW, E.N., *Europe's Nuclear Power Experiment — History of the OECD Dragon Project*, Pergamon Press, Oxford (1983).
- [9] MARSDEN, B.J., WICKHAM, A.J., *Nuclear Decommissioning 1998*, Professional Engineering Publishing, London (1998) 145.
- [10] U.C.C. Inc., *The Industrial Graphite Engineering Handbook*, Parma, Copyright © 2001.
- [11] KELLY, B.T., *The physics of graphite*, Applied Science Publishers, London (1981).
- [12] KRETCHMAN, H.F., *The Story of Gilsonite*, American Gilsonite Company, Salt Lake City (1957).
- [13] POCKOCK, R.F., *Nuclear Power*, The Gresham Press, Old Woking (1977).
- [14] PRINCE, N., SIMONS, C.R., HART, J.D., in N.E.G.o.t. IME (Editor), *Graphite Structures for Nuclear Reactors*, London (1972) 1.
- [15] ARNOLD, L., *Windscale 1957*, London (1992).
- [16] SUTTON, A.L., HOWARD, V.C., *J. Nucl. Mater.* 7 (1962) 58.
- [17] BOCHIROL, L., BONJOUR, E., *Carbon* 6 (1968) 210.
- [18] KELLY, B.T., MARTIN, W.H., NETTLEY, P.T., *Philosophical Transactions of the Royal Society of London. Series A, Mathematical and Physical Sciences* 260 (1966) 37.
- [19] WEIR, C.G., *Chapelcross Melt-Out and Recovery Operations Active Working on Reactors*, London (1971).
- [20] BEST, J.V., STEPHEN, W.J., WICKHAM, A.J., *Progress in Nuclear Energy* 16 (1985) 127.
- [21] JOHNSON, P.A.V., BLANCHARD, A., KELLY, B.T., *Carbon* 20 (1982) 141.
- [22] JOHNSON, P.A.V., SCHOFIELD, P., BLANCHARD, A., KELLY, B.T., *Carbon* 20 (1982) 141.
- [23] STANDRING, J., ASHTON, B.W., *Carbon* 3 (1965) 157.
- [24] KELLY, B.T., *Progress in Nuclear Energy* 16 (1985) 73.
- [25] TELLING, R.H., EWELS, C.P., EL-BARBARY, A.A., HEGGIE, M.L., *Nat. Mater.* 2 (2003) 333.
- [26] THROWER, P.A., *Carbon* 6 (1968) 211.
- [27] WÖRNER, J., BOTZEM, W., PRESTON, S.D., “Heat treatment of graphite and resulting tritium emissions” in *Nuclear Graphite Waste Management, Proceedings of a Technical Committee Meeting held in Manchester, United Kingdom, 18–20 October 1999*, IAEA, Austria, Vienna (1999).
- [28] KON, J., KATASE, M., MURATA, K., Ishihara A., *Carbon* 6 (1968) 207.
- [29] HALL, G., MARSDEN, B.J., FOK, S.L., SMART, J., *Nuclear Engineering and Design* 222 (2003) 319.
- [30] LI, H., MARSDEN, B.J., FOK, S.L., *Nuclear Engineering and Design* 232 (2004) 237.
- [31] HOU, X., *Applied Radiation and Isotopes* 62 (2005) 871.
- [32] HOU, X., OSTERGAARD, L.F., NIELSEN, S.P., *Anal. Chem.* 79 (2007) 3126.
- [33] SHUKOLYUKOV, Y.A., MESHNIK, A.P., PRAVDIVTSEVA, O.V., VERKHOVSKII, A.B., *Atomic Energy* 63 (1987) 903.

- [34] QUADE, U., et al., “Packing requirements for graphite and carbon from the decommissioning of the AVR in consideration of the German final disposal regulations”, Technologies for Gas Cooled Reactor Decommissioning, Fuel Storage and Waste Disposal, IAEA, IAEA-TECDOC-1043, Vienna (1998) 275-286.
- [35] HOLT, G., “The decommissioning of commercial Magnox gas cooled reactor power stations in the United Kingdom”, Technologies for Gas Cooled Reactor Decommissioning, Fuel Storage and Waste Disposal, IAEA, IAEA-TECDOC-1043, Vienna (1998) 71-84.
- [36] NDA Public Release Report on Graphite Quantities, June 2007.
- [37] ANTUNES, A.F., LOBO, A.O., CORAT, E.J., TRAVA-AIROLDI, V.J., MARTIN, A.A., VERISSIMO, C., Carbon 44 (2006) 2202.
- [38] C.o.R.W.M. <http://www.corwm.org/pdf/FullReport.pdf>, in, CoRWM 2006.
- [39] IZUMI, J., et al., Adsorption 11 (2005) 817.
- [40] INTERNATIONAL ATOMIC ENERGY AGENCY, Characterization, Treatment and Conditioning of Radioactive Graphite from Decommissioning of Nuclear Reactors, IAEA, IAEA-TECDOC-1521, Vienna (2006).
- [41] TAKESHITA, K., NAKANO, Y., SHIMIZU, M., FUHII, Y., J. Nucl. Sci. and Techn. 39 (2002) 1207
- [42] PODRUZHINA, T., in FZJ Report Jülich, 2004.
- [43] HIPPO, E.J., MURDIE, N., KOWBEL, W., Carbon 27 (1989) 331.
- [44] PRICE, M.S.T., YEATS, F.W., in Industrial Carbon and Graphite, London (1957) 111.
- [45] XIAOWEI, L., JEAN-CHARLES, R., SUYUAN, Y., Nuclear Engineering and Design 227 (2004) 273.

Graphite dust explosibility in decommissioning: A demonstration of minimal risk

A.J. Wickham^a, L. Rahmani^b

^aPrivate Consultant, Powys, United Kingdom

^bArbresle Ingénierie, L'Arbresle, France

Abstract. This paper reviews the available information on the explosibility of graphite dust, which is a potential issue in the decommissioning of reactors with graphite components. It concludes, mainly on the basis of experimental studies in the United Kingdom and France, that the probability of initiating a dust explosion in graphite-containing debris materials during any realistic dismantling operation is exceedingly low as graphite is only very weakly explosible, even in totally favourable conditions, and that any likely impurities will act as inerters.

1. Introduction

Memories of the accident at Chernobyl and of the Windscale Pile 1 fire in 1957 have served to place in people's minds the possibilities both that graphite components from a reactor might present a fire hazard during decommissioning and that dust generated from graphite might present an explosibility hazard. The first point may readily be dismissed on the basis of a vast literature of graphite oxidation behaviour, but the second point has demanded careful attention ahead of the expected decommissioning of former graphite-moderated nuclear plants. Whilst the present work concentrates upon activities in the UK in support of Windscale Pile decommissioning and in France in support of the dismantling of UNGG plant, colleagues in Italy (SoGIN and contractors) and Japan have also contributed very usefully to studies of the dust behaviour.

The perceived problem has arisen in part because pure graphite dusts, once considered to be inexplorable, are now classified following the introduction of the ISO standard test and similar investigations as 'weakly explosible'. Reactor dismantling activities which are perceived by regulators or safety officials as potentially hazardous include, but are not necessarily limited to, flame-cutting operations on adjacent steelwork, the presence of flammable gases within the vessel arising from malfunctioning cutting equipment, etc. Any potential hazard during a particular dismantling activity can be eliminated by removing one of the conditions which must simultaneously be satisfied in order for a dust explosion to take place. However, it is even better if it can be shown that no explosion is actually possible anyway under the severest practical conditions.

Using representative graphite materials ground to appropriate particle size distributions, independent programmes of work have taken place in the UK (utilizing specialist facilities at the University of Leeds) and in France in collaboration with the laboratories of the Centre National de Prévention et de Protection (CNPP) at Vernon (France). In each case, standard explosibility parameters have been determined (deflagration index, maximum rate of pressure rise, minimum explosible concentration etc.) using standard test procedures involving chemical igniters. The UK also studied the effect of impurities (verifying independent results from Italy and Japan), ageing and agglomeration of dusts, the secondary explosion risk in relevant geometries, and undertook kinetic studies utilizing a methane-gas driver. In France, the additional studies involved replication of full scale pipework containing suspended dusts at relevant concentrations and a high energy ignition source, which demonstrated

using high speed photography that the graphite was self-extinguishing (as predicted) in comparison to the violent effects of 'standard' test materials such as flour.

A thorough analysis of all available data leads to the conclusion that the probability of initiating a dust explosion in graphite-containing debris materials during any realistic dismantling operation is exceedingly low as graphite is only very weakly explosible, even in totally favourable conditions, and likely impurities act as inerters. Thus, on the basis of what is now a rather large body of evidence, there need be no concerns about the risk of a disruptive graphite dust explosion when planning for decommissioning.

2. Background

A useful starting point is the basic list of conditions which must be satisfied if a dust explosion is to take place [1]. Strictly, the propagation of a flame front through a suspended dust cloud is sub-sonic and, therefore, the event is a *deflagration* rather than a *detonation*.

Six basic conditions must be satisfied simultaneously before a dust deflagration can be initiated:

- (1) The dust must be combustible (the presence of volatile constituents is an important factor here).
- (2) The dust must be airborne, implying a need either for a turbulent gas flow or for some physical disturbance which allows the dust to fall freely through an oxidizing gas.
- (3) The particle size must be optimized for flame propagation.
- (4) The dust concentration must fall within the explosible range (i.e. neither too high nor too low).
- (5) An ignition source of sufficient energy to initiate flame propagation must be in contact with the dust suspension (a high temperature surface may be sufficient for this, whilst a naked flame or electrical spark are obvious sources).
- (6) The atmosphere must contain sufficient oxygen to support combustion (this allows the possibility to provide an inert atmosphere local to the scene of any cutting operation if there is cause for concern about the reactivity of any adjacent materials).

An additional requirement, if a disruptive or damaging event is to result, is that the dust suspension must be in a confined space which inhibits the relief of the pressure rise resulting from the ignition. It is useful to expand upon two of these conditions:

Particle size

In carbonaceous materials it is to be expected that the explosion hazard increases as the particle size is reduced. Field [1] shows, for a typical dust (polyethylene), that a decrease in particle size brings about

- (1) a decrease in the minimum ignition energy;
- (2) a decrease in the minimum explosible concentration;
- (3) an increase in maximum explosion pressure (this is very sensitive to size and falls very sharply at larger particle sizes);
- (4) an increase in the maximum rate of pressure rise.

It is difficult to define a particle size where the material is free from hazard, but it appears to be the general experience that particle sizes in excess of 500 μm are in general unlikely to initiate a dust explosion, although they may participate in secondary explosions.

Particle concentration in the suspension

The explosibility hazard of a dust suspension passes through a maximum with concentration in the same manner as the explosibility limits in a gas mixture. At very low concentration, the separation of the particles is too great for a flame to propagate, especially when radiative heat losses are taken into account. This lower explosion limit is also dependent upon particle size and the combustibility of the material. Field [1] cites minimum explosible concentrations for a selection of carbonaceous dusts although none are directly applicable here: Pittsburgh coal is quoted at 55 g.m^{-3} and polyethylene at around 10 g.m^{-3} . Schriftenreihe des Hauptverbandes... [2] quotes 60 g.m^{-3} for charcoal and lampblack of small particle size.

The upper explosion limit is considered to be determined by the situation where the particles are so closely packed that the access of air is inhibited and flame propagation is again quenched. The heat capacity of the material is also relevant. This limit is considered [1] to be of the order of $5\text{--}10 \text{ kg.m}^{-3}$ for many materials.

Between these limits, the maximum explosion pressure is biased towards the lower concentration ranges, and the maximum rate of rise even more so. The most severe effects are not usually found to equate to the stoichiometric mixture because particulate material is usually left unburned in a dust explosion. Consequently, the most severe effects are usually felt in suspensions where the dust is at 2–3 times the stoichiometric concentration.

The particular situations in the UK Piles and the French UNGG reactors have been evaluated against these principles, with particular attention paid to the effects of particle size, the presence of various contaminants to the graphite dusts, and the potential for the initiation of secondary explosions in connected regions of the reactor compartments, should an initial event disturb dusts in an adjacent area. The results will apply equally to other types of graphite-moderated reactors.

3. UK studies

In the UK Windscale Piles, which were air-cooled, the only carbonaceous dust which should be present is that arising from nuclear-grade graphite, and high purity graphite has historically been classified as ‘non-explosible’ [1]. However, the application of modern standards to the classification of dusts has somewhat changed the perspective. The standard ISO test [3] uses a chemical igniter of 10 kJ in a spherical vessel of approximately 1 m^3 , and the chemical energy added is sufficient to result in a weak explosion in nuclear graphite when the dust concentration and particle size range are favourable. Fig. 1 shows a version of this equipment.

It is important to understand the characteristics of graphite dust likely to be encountered in the Windscale Piles in detail, especially in regard to the effects of possible impurities and potential catalysts which might be present, particularly in Pile 1 which was the scene of the core fire in 1957 [4]. In addition, it was considered prudent to investigate the propagation of pressure waves and the possibility of secondary explosions using the ‘connected-enclosure’ facilities at the University of Leeds which can be configured to represent approximately the relative volumes of parts of the Windscale Piles gas circuits.

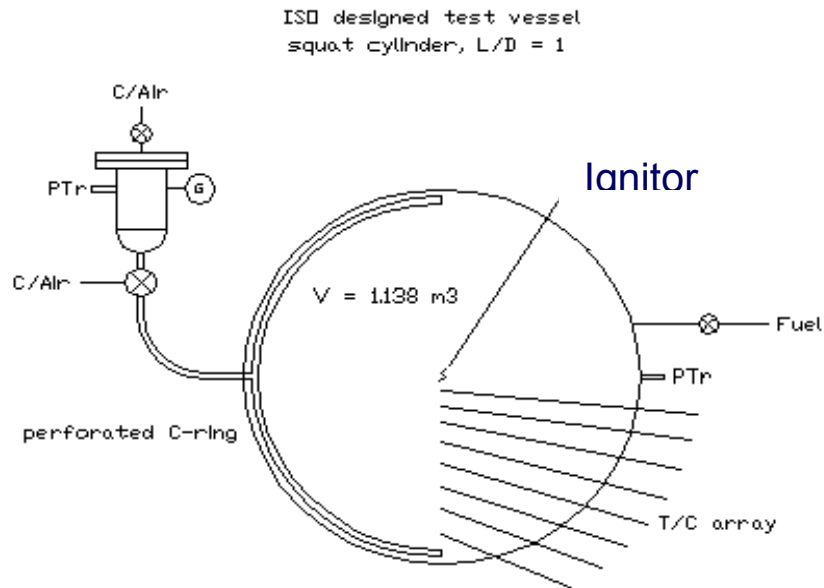


FIG. 1. Standard ISO test arrangement as used at Leeds.

Such equipment is capable of producing detailed information about pressure changes with time following ignition of a sample, and also information about the progression of the resulting flame front through the suspended dust, utilizing data from the internal thermocouples. Figure 2 shows a typical response: the dust is injected with a pulse of air which returns the internal pressure in the vessel to one atmosphere, and ignition then takes place.

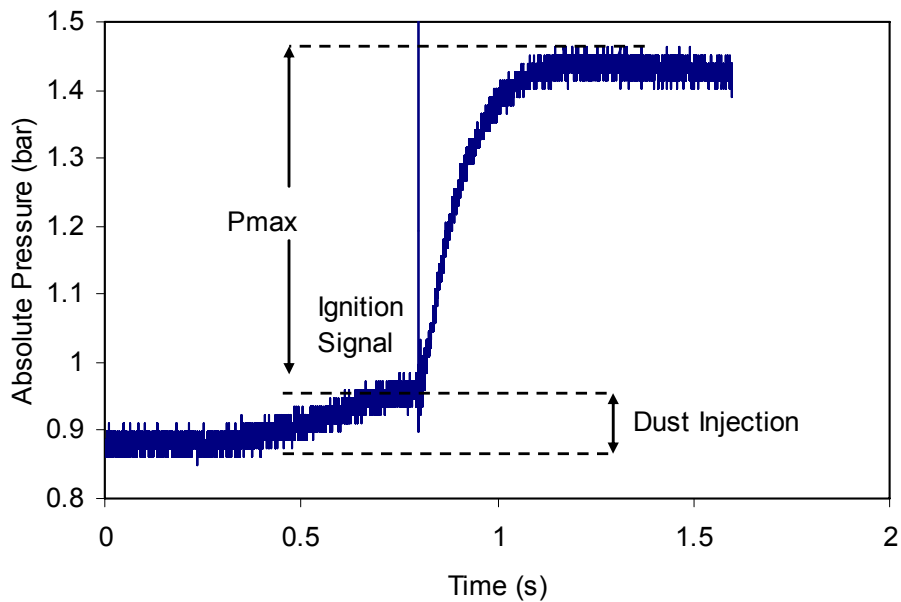


FIG. 2. Typical time/pressure plot for a dust deflagration.

3.1. Experimental results

3.1.1. Basic study

The UK work utilized PGA graphite characteristic of the Calder Hall Magnox reactors, the nearest currently available material to the AGXP graphite used in the Piles. The work has revealed an unexpected influence of particle size, with only the very finest particles ($< \sim 5 \mu\text{m}$) participating actively in combustion whilst larger particles behave as heat sinks and thus serve to suppress flame propagation. This results in a rather low reactivity of typical graphite dust samples, to the extent that a methane ‘driver’ has been utilized to produce the explosions necessary to study the full range of behaviour and to evaluate more detailed kinetics.

A major feature of the present work is the ability to study the possibility of the initiation of secondary explosions and the effects of propagation of the pressure pulses between connected enclosures whose volumes are in approximate proportion to the volumes of the various reactor void-space areas. This is especially important in a reactor such as the Windscale piles where there is no pressure vessel.

Although the work confirmed that the graphite dust was weakly explosive under the ISO test conditions, there were a number of important subsidiary findings:

- (1) Use of several different igniter energies and other types (e.g. 1–15 kJ pyrotechnic, continuous 4 J arc) illustrated that no explosion occurred at any graphite concentration up to 450 g.m^{-3} in air unless at least 4 kJ energy input from the chemical igniter was available, and that even then a large fraction of the graphite powder, initially present in the size range of $2\text{--}25^1 \mu\text{m}$, did not participate in the explosion but rather behaved as a heat sink, which reduces the possibility of secondary explosions to a very low probability indeed: an initial ‘hot fireball’ was necessary for a flame to propagate at all.
- (2) In the older ‘Hartmann Bomb’ type apparatus (as used for the majority of test results cited in [1]), no ignition occurred with two types of 15 kJ igniters.
- (3) Only the finest particle sizes participated in the explosion, and it was separately noted that the samples tended to agglomerate quickly with storage (over a period of weeks following preparation) such that these fine particle sizes were no longer present in later tests: agglomerated masses were typically 1 mm diameter.
- (4) In order to get meaningful data on graphite-dust behaviour, most of the tests had to be ‘driven’ to explosion by the addition of methane gas, and the known characteristics of methane combustion then ‘subtracted’ from the total behaviour in order to provide data on graphite: the most reactive graphite concentration in the presence of methane was at 55 g.m^{-3} , but this requires a correction to be valid for graphite alone, and the figure then approaches the stoichiometric concentration of 105 g.m^{-3} .
- (5) The maximum overpressure was generated at a dust concentration of 440 g.m^{-3} and was found to be extremely sensitive to the powder injection conditions and to the ‘age’ of the powder (essentially the agglomeration effect mentioned in ‘3’).
- (6) The estimated peak deflagration index² (standard measure of flame propagation) was around 61 bar.m.s^{-1} with an upper-bound value of 106 bar.m.s^{-1} , the difference reflecting the difficulty of extracting meaningful data for a substance so unwilling to participate directly in an explosion: this is a very low result in comparison with most explosible dusts.

¹ There is a significant peak in the size distribution at around $6 \mu\text{m}$.

² The deflagration index, K_{st} , is the product of the maximum rate of pressure rise and the cube root of the volume of the vessel in which the explosion test is conducted: thus, for a standard spherical vessel of 1 m^3 , as recommended for the ISO test, the index reduces to the maximum rate of pressure rise.

- (7) Overpressure calculations following explosions were specific to the Windscale Piles geometry, but were low (0.2 bar): this defines the necessary capabilities of the structure (and any connected enclosures subject to pressure waves or to secondary explosions) to withstand the consequence of the worst case (highly pessimistic) scenario of an explosion.

These findings are illustrated in Figs 3, 4, 5 and 6 and summarized in Table 1.

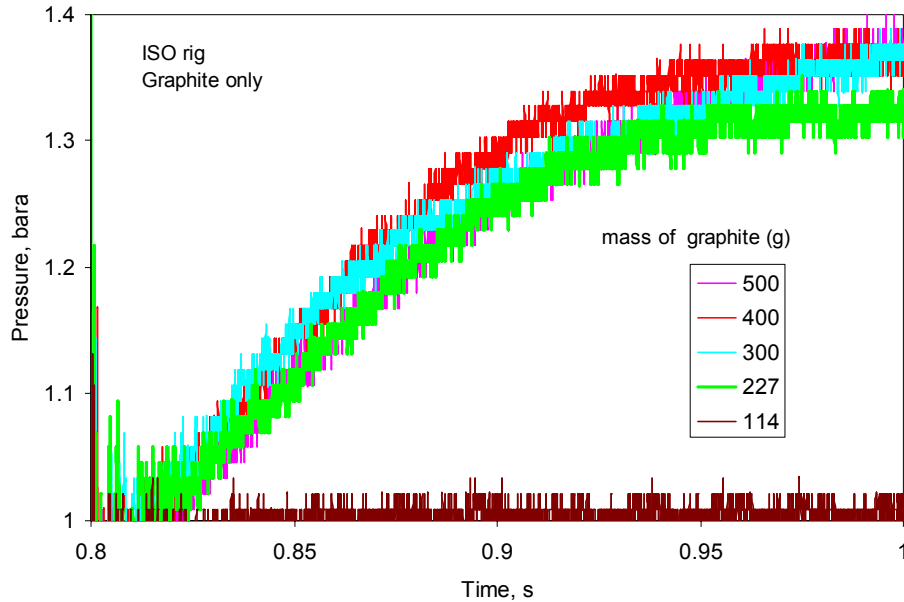


FIG. 3. Graphite powder behaviour in the ISO vessel.

Table 1. Summary of ISO-rig test data obtained at the University of Leeds

	Measured peak (graphite alone)	Predicted peak from methane- driven tests	Predicted concentration for peak (g.m^{-3})	Corrected concentration assuming 60% unburnt (g.m^{-3})	Measured concentration for peak (g.m^{-3})
K_{st} (bar.m.s^{-1})	14	61	86	215	450
P_{\max} (bar)	0.5	5.7	278	695	450
from flame speed tests			313	783	

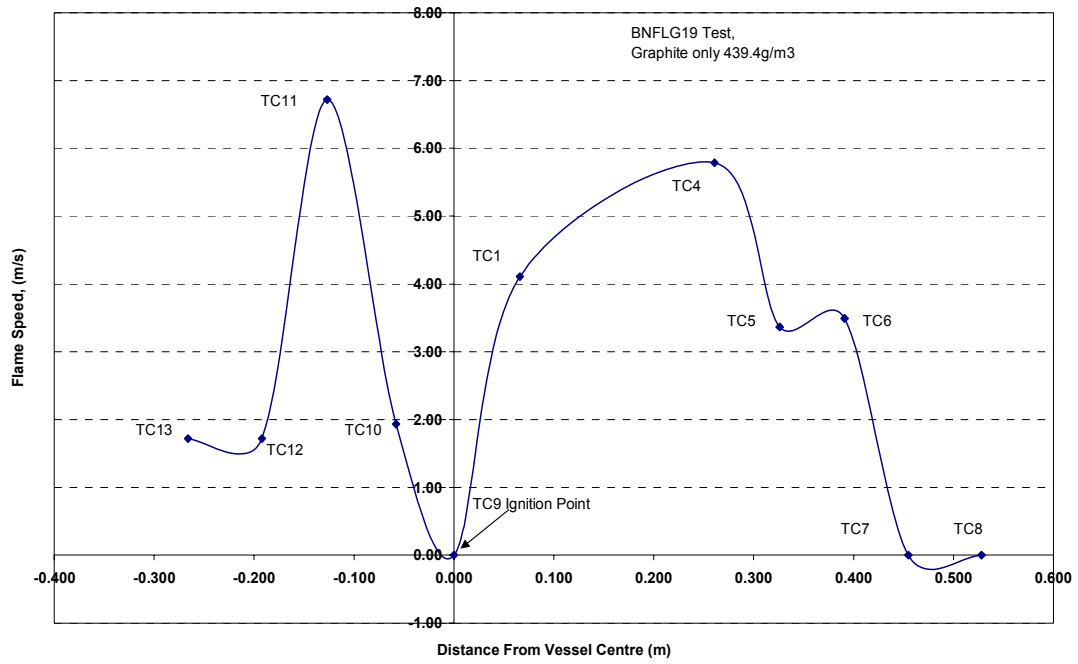


FIG. 4. Flame speed derived from arrival time at thermocouples within ISO vessel.

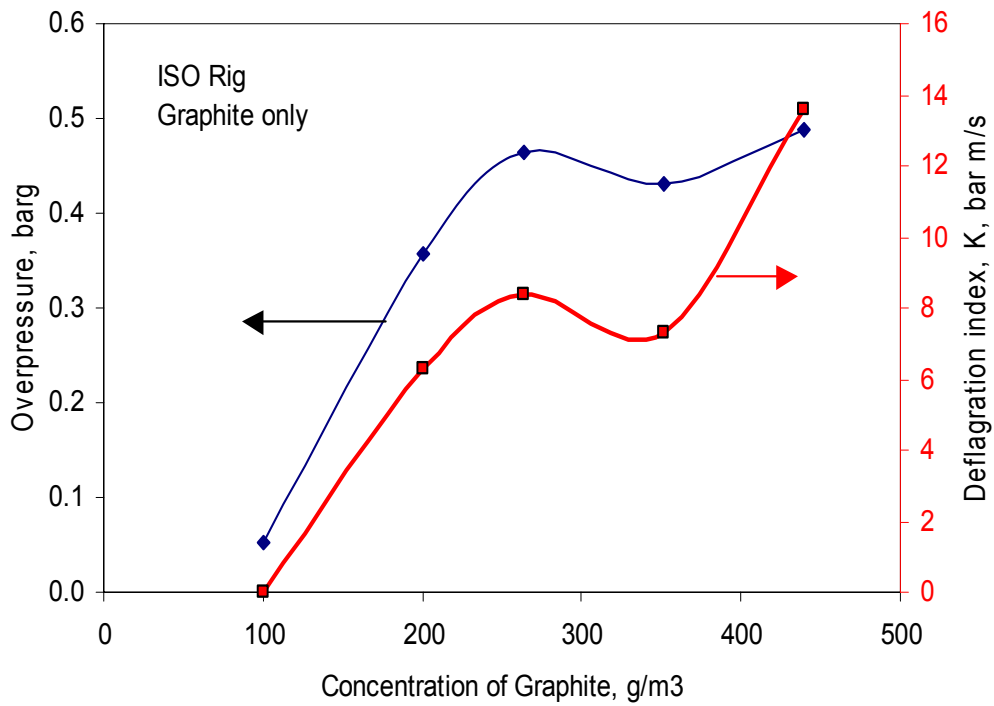


FIG. 5. Typical data from PGA graphite behaviour in the ISO test.

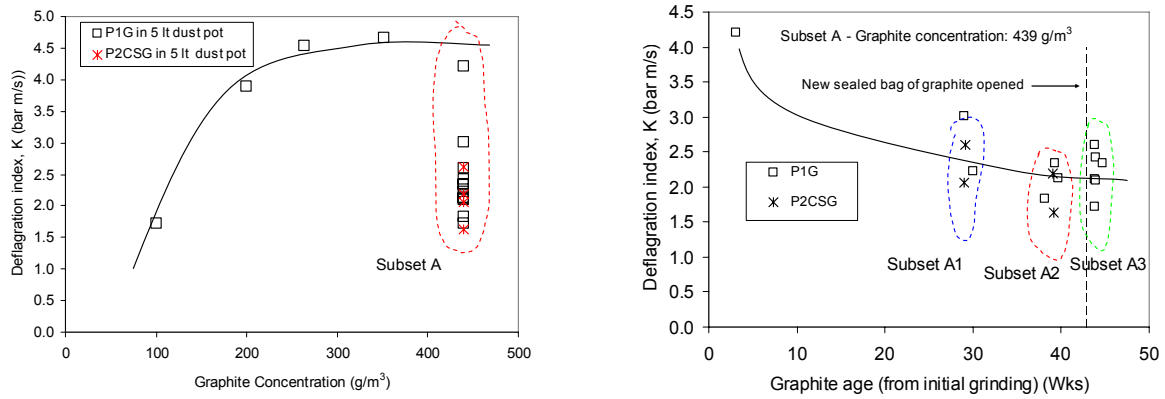


FIG. 6. 'Ageing' of graphite powder due to agglomeration, with large drop in reactivity.

Overall, these are highly satisfactory results, confirming the difficulty with which pure nuclear graphite dust can be made to participate in a dust explosion and thus the relative ease with which it is possible to engineer in safeguards in decommissioning activities such that the simultaneous requirements for a dust deflagration cannot occur.

Connected enclosures

The connectivity of various void spaces within the Windscale Pile 1 reactor was represented in the study by a series of connected enclosures in which the relative volumes were at a scale of 1/2500 as illustrated in Fig. 7.

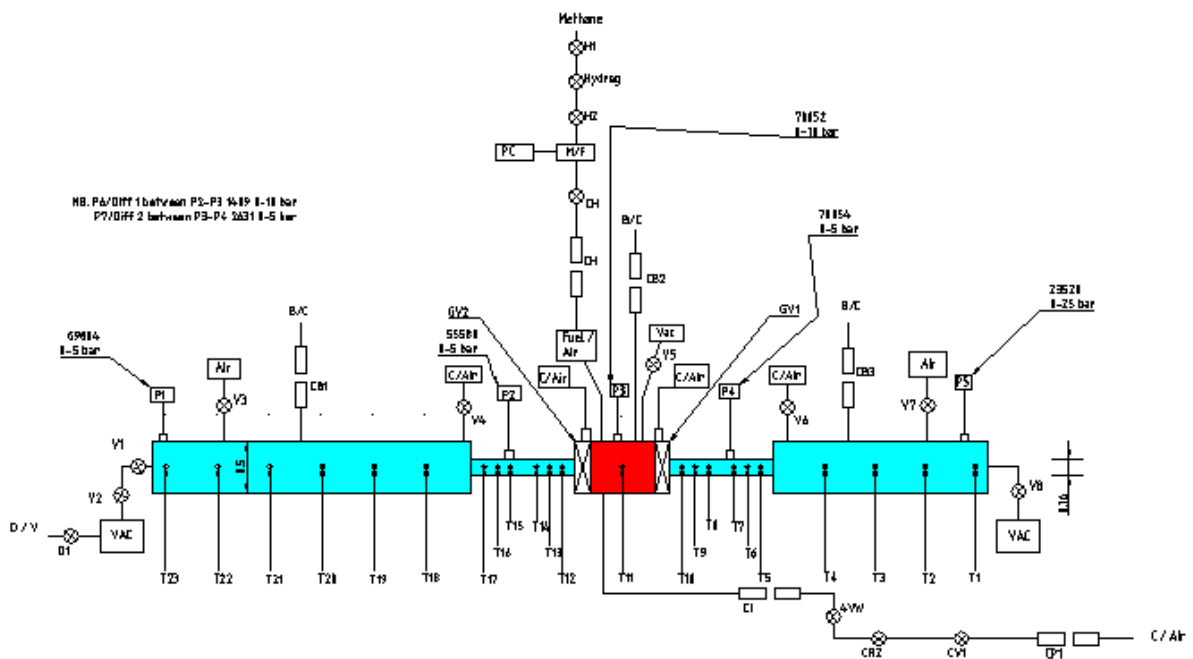


FIG. 7. Schematic of connected enclosures representing Windscale Pile 1.

The red region represents a possible void space within the core resulting from the fire: other work presented in this conference now suggests that this region is extremely unlikely to be present [5].

The perceived risk which was investigated was the mobilization of dusts in a secondary part of the circuit as a result of a pressure pulse derived from a primary explosion elsewhere in the system. This might be sufficient to set off a secondary explosion or, alternatively, the pressure wave arriving from the primary explosion might be sufficient to cause secondary damage in its own right. In the event, it

proved impossible to sustain any significant explosion with pure graphite dusts, nor to propagate any secondary explosion in this system, even when the primary explosion was ‘driven’ by methane.

The effects of impurities

In the Windscale Piles, contamination of the cores with lead is known to have occurred. Lead was used as a filler and spacer material in isotope-cartridge holes and elsewhere within the cores, despite the core temperature being sufficient to melt this metal. Lead is known to be one of the most effective catalysts for graphite oxidation in air [6], an observation more recently confirmed for PGA graphite as used in UK Magnox reactors and in the current tests.

However, catalysis is important in bulk graphite only when the overall reaction rate is controlled by reaction kinetics, and not when it is controlled by diffusion considerations or by the available supply of oxygen. In the case of fine powder, the situation is potentially more complex.

Lead was mixed with the graphite powder in the form of the oxide Pb_3O_4 at 1000 wppm. The surprising result was that it had no detectable effect on the explosibility characteristics of the graphite. The implication of this is that the oxidation is equivalent to the ‘Mode III’ (gas-transport-controlled) oxidation of bulk graphite, where catalysis is ineffective. This seems inconsistent with expectation since, with the graphite in powder form at very small particle sizes, one might assume that the access of oxygen was at maximum efficiency and that the reaction would indeed be ‘Mode I’ (kinetic controlled) in which catalysis should play a significant role, speeding up the exothermic reaction and the release of heat, and thus facilitating flame propagation.

The implication is that the oxide particles and the graphite particles were effectively behaving independently, despite the employment of ‘opposed jet milling’ which is expected to give an intimate mixture, with the lead oxide thus behaving as an inert diluent. Whilst this issue is not properly resolved, the result of the test was deemed to give adequate comfort for the decommissioning programme and therefore the problem has not been further pursued.

A second impurity, which could be present in Windscale Pile 1 from fire-damaged nuclear fuel, is aluminium oxide Al_2O_3 . The study has shown that this, in 25% admixture, appears to lower the overpressures and reactivity somewhat, although the results remain within the scatter of the pure-graphite data as illustrated in Fig. 8. Here again, the impurity has no significant effect.

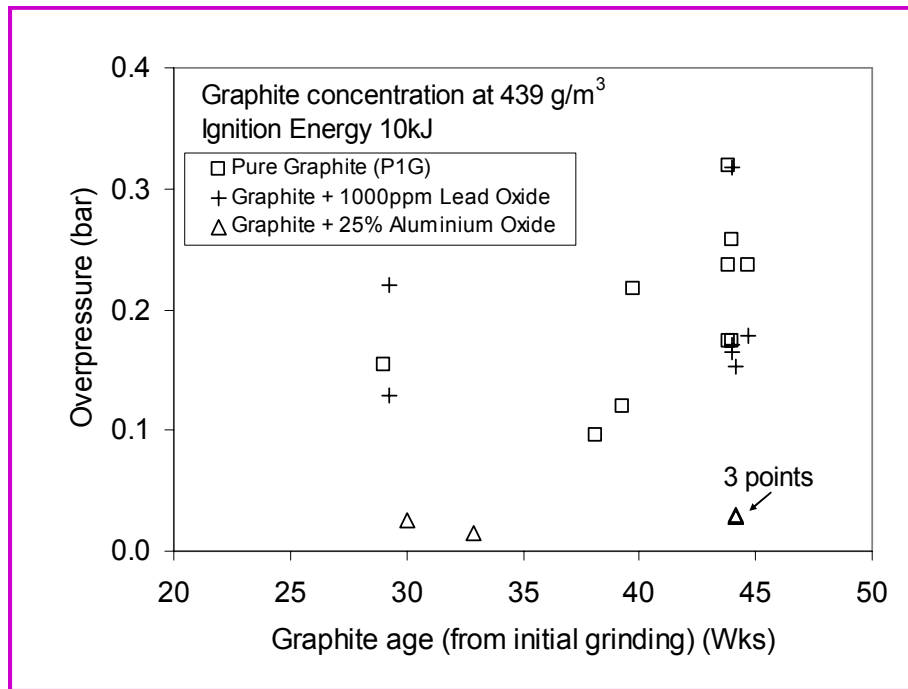


FIG. 8. Insignificant effects of lead oxide and aluminium oxide impurities, superimposed upon the 'ageing' effect.

Admixture of flammable dusts with materials which are already fully or partially oxidized should be expected to contribute to a general reduction in explosibility potential, otherwise described as 'inerting'. This phenomenon has been known for many years, with the assessment of the inert content of dusts in coal mines being an important part of the assessment of explosion hazards [7] for routine safety assessments. The general reactor dust burden in a gas cooled system is likely to arise from corrosion products of metal structures and will thus be in the form of oxides incapable of further oxidation — this effect is demonstrated by recent work by the Italian decommissioning agency SoGIN, in which reactor dusts removed from the Latina Magnox reactor after nearly 30 years of operation were found to be inexplorable in the ISO test whereas pure unirradiated graphite was, as found by other workers, weakly explosible (M. Sturvi, personal communication). The concrete dusts drawn into the Windscale Piles through the concrete air ducts are likely to have a similar inerting effect.

Generally, therefore, one may conclude that impurities in graphite dusts encountered in reactor decommissioning are unlikely to represent an additional explosibility hazard and are more likely to be beneficial, acting as 'inert' materials and reducing the potential for any explosion.

4. French studies

The principal French studies into graphite dust deflagration are documented in reports from INERIS (Institut National de l'Environnement Industriel et des Risques) [8] and from CNPP (Centre National de Prévention et de Protection) [9]. The initial INERIS studies were undertaken to support the proposed long term storage of the graphite cores within the pressure vessels of the reactors: subsequently, the issue has been more comprehensively addressed with specific reference to decommissioning activities.

INERIS studies

These studies commenced with an evaluation of the auto-ignition risk using thermogravimetry, determination of K_{st} , and evaluation of the particle size and water content of the pulverized sample. In the preamble, note is made of an unreferenced theory attributed to Frank-Kamenetskii which relates

the ‘characteristic dimension’ of the powder (which might be an average particle size) to a function of the oxygen concentration and a ‘shape factor’, possibly the agglomerated form of the deposit on the surface, along with the activation energy for the oxidation reaction and some other property-dependent constants. The value of this citation in the present context, without further identification of the appropriate parameters, is doubtful.

In common with the studies already discussed, Ref [8] also includes in its introduction a comprehensive review of the conditions necessary for the establishment of a dust deflagration. One point of note is a comment that the lower explosible concentration limit for a dust is usually of the order of 50 g.m^{-3} , although this appears more of a general observation than a specific reference to graphite. Particular note is made of the ability of a hot surface to act as an ignition source, whilst it is also noted that a ‘minimum electrical energy for ignition’ can be defined for every (powdered) substance.

Granulometry

The graphite for the INERIS studies was provided in the form of a triangular bar by EdF. This was initially crushed to provide pieces of nominal dimension 50 mm, and these were then ground under nitrogen to give a sample of dust specified as $<0.1 \text{ mm}$.

Approximately 7% of the material was sub- $5 \mu\text{m}$, significantly less than that found in the material used in the later stages of the UK work. By monitoring the weight change in the material held at a temperature of 104°C , it was determined that the moisture content was lower than 0.1%.

Differential thermal analysis (risk of auto-ignition)

The determination was made in a standard suspension thermobalance between 25 and 800°C , with a rate of temperature rise of 5 K.min^{-1} . An inert substance was also present, in order to allow the generation of heat by exothermic reaction in the graphite sample to be determined by difference between temperature sensors in the two materials. Three runs were conducted in which the behaviour of the graphite powder was compared with powdered carbon fibres and powdered coke, as illustrated with Table 2.

Table 2. Runs comparing risk of auto-ignition

<i>Sample</i>	<i>Furnace temperature at onset of weight loss</i>	<i>Furnace temperature at first sign of exothermic reaction</i>	<i>Furnace temperature at which differential temperature between sample and inert reference reached 50 K</i>	<i>Maximum rate of temperature rise in sample</i>	<i>Weight loss after ‘combustion’</i>
Graphite powder	600°C	540°C	602°C	90 K.min^{-1}	$\sim 0\%$
Powdered carbon fiber	595°C	530°C	595°C	400 K.min^{-1}	$\sim 0\%$
Powdered coke	400°C	280°C	395°C	90 K.min^{-1}	37%

The conclusions of [8] with respect to graphite powder are that it has approximately the same ‘reactivity’ as carbon fibre and very much less than coke, which is nonetheless categorized as ‘low reactivity’. Since INERIS has much greater experience of coke behaviour than nuclear graphite, it suggests in [8] that a relationship for the auto-ignition of coke-dust deposits based upon the Frank-Kamenetskii theory could be used “with a very large margin of security” if applied to graphite.

Explosion parameters

INERIS employed a standard 20 L vessel for these determinations, using a pair of chemical igniters of total energy 10 kJ. The individual energy of one igniter, 5 kJ, is rather quaintly compared with the energy afforded by striking all of the matches in a box simultaneously. The experiments recorded maximum overpressure and $(dP/dt)_{max}$ for a range of concentrations of graphite dust: we calculate K_{st} ³ from the latter utilizing the vessel volume of 0.02 m³ as illustrated on Table 3:

Table 3. Experimental results and calculated values

Dust concentration (g.m ⁻³)	60	125	250	500	750	1000	1250	1500
Maximum overpressure (bar)	0	5.3	6.7	5.8	4.4	4.1	4.3	3.6
$(dP/dt)_{max}$ (bar.s ⁻¹)	0	35	250	235	170	60	265	50
K_{st} (bar.m.s ⁻¹)	0	9.5	67.8	63.8	46.1	16.3	71.9	13.6
(calculated by present authors)								

Reference [8] identifies the minimum explosible concentration of graphite dust as lying somewhere between 60 and 125 g.m⁻³, the maximum overpressure occurring at a graphite-dust concentration of 250 g.m⁻³, and the maximum rate of rise, or K_{st} , corresponding to a dust concentration of 1250 g.m⁻³. The result at 1250 g.m⁻³ concentration might, however, be considered anomalous, since the data break from a clear trend which sees all parameters otherwise peak at around 250 g.m⁻³ concentration.

The Italian work also covered concentrations up to 1250 g.m⁻³ and found no such second peak in $(dP/dt)_{max}$; indeed, it confirms that the peak in both reported parameters occurred at a concentration of around 250 g.m⁻³ as found here for the maximum overpressure and as inferred from the remaining data for $(dP/dt)_{max}$. We therefore consider that, on balance, the true maximum rate of pressure rise was found at 250 g.m⁻³ and that the result at 1250 g.m⁻³ is an experimental anomaly. However, it is worth also reconsidering the data from the University of Leeds in Fig. 5. Here, too, maxima in both parameters were found at around 250 g.m⁻³ although there is a suggestion, albeit based upon one determination at 450 g.m⁻³, the highest concentration used in the UK work, that a subsequent rise in parameters, especially K_{st} and hence in $(dP/dt)_{max}$, might have occurred.

Therefore, whilst the possibility cannot be entirely dismissed that the INERIS result at 1250 g.m⁻³ is genuine, it breaks a clear trend in data for which there is a precedent and there is no logical explanation for encountering one such high $(dP/dt)_{max}$ result in this fashion.

A comparison is also given of typical literature values of K_{st} and the maximum overpressure found for graphites from a variety of sources which, in general, support the view that typical figures are around 70 bar.m.s⁻¹ and 5.5–6.5 bar, respectively. These data only allowed the minimum ignition energy to be placed somewhere in the range 100–10 000 Joule.

On the basis of the results obtained at INERIS, this graphite dust is classified as weakly explosible (classification St_1) under the French standard VDI 3673, and gives about the same reaction as carbon-fiber powder which was studied in parallel to this work.

Additional information

Ref [8] includes a short bibliography of mainly French documents (although early work in support of the UK WAGR is mentioned) from which some useful information may be cited here. A CEA report [11] predicts a total of 16.7 t of deposits (polymers of carbon suboxides of an uncharacterized nature) arising from radiolytic reactions in the coolant of the Saint Laurent A1 reactor. UK experience in Magnox reactors would suggest that the majority of this material is closely associated with graphite and would not be ‘loose’ within the reactor circuit. This quantity of deposits is approximately 0.63%

³ Whilst the French definition of K_{st} does not differ from the standard usage, it may be helpful to note that the definition appears in the official recommendation VDI 3673 (October 1983), but that it is cited as K_{max} in the experimental standard AFNOR U 54-540 (December 1986).

of the weight of the graphite blocks, and ref [11] concurs with the UK view to the extent that the maximum mass of deposit on some graphite surfaces reaches 5.37%, presumably from monitoring tests. Thus, although this total quantity of reactive deposit may sound alarming in ‘dust’ form, and its chemical reactivity is likely to be higher than that of ‘pure’ graphite, it does not necessarily represent a significant explosibility risk.

EdF have separately assessed a settled powder content of 277 kg on and around the floors of the steam generators which occupy the lower half of the Bugey 1 reactor vessel, according to [8]. EdF additionally advise that this powder has a size range between micrometric and centimetric; some of it is carbonaceous, some metallic. The graphitic part is thought to arise mainly from splitting of biological protection blocks as a result of the corrosion of steel inserts. A rationalized extrapolation on all surfaces in the reactor of the observations made on the accessible bottom raised the figure to a few (about 4) t of dust.

A second CEA note [12] reviews potential risks of pyrophoricity of graphite dusts and debris when removed from the storage ponds in which fuel-element graphite sleeves from the St. Laurent A reactors were deposited, and found no risk. Other technical notes mentioned in [8] cover issues of Wigner energy and graphite purity, but they are of only minor interest in the present context.

The summary of [8] does not elaborate on possible mechanisms for the generation of graphite dusts (e.g. from friction in fuel-handling chutes), commenting only upon the possible toppling of graphite blocks and noting (without reference) that it takes more than three times the energy to pulverize graphite than it does to pulverize granite to the same granulometry. On the other hand, it makes extensive reference to the suspension of existing dusts and potential sources of ignition energy, and also correctly identifies the role of materials such as metal oxides in inerting the effect of a deflagration through absorption of heat.

Three residual uncertainties were identified in the view of the INERIS laboratory:

- the influence of the particle size distribution and the chemical composition of the dusts likely to be encountered on surfaces within the reactor vessel;
- the minimum energy for ignition of a graphite dust cloud;
- the energy of mechanical sparks which might be generated during handling and dismantling operations, and their effect on any suspended graphite deposits.

In the context of [8], namely the ‘safe-storage’ of the reactor cores within their original pressure vessels for an extended period, attention was also drawn to the risks of secondary (dust) explosions should an explosive gaseous atmosphere be generated, and of the creation of potentially explosible dust clouds by falling objects.

Programme in association with CNPP

EdF-CIDEN made a commendable decision to explore the dust-deflagration issue further by seeking to replicate a real engineering situation with suspended graphite dust and a considerable ignition energy, with the objective of providing a convincing practical demonstration of the essentially benign nature of graphite dust. This programme was undertaken by the CNPP in association with an EdF site at Moret-sur-Loing (“Les Renardières”), near Paris.

Phase 1

As a first step, CNPP conducted some additional basic studies [9] to confirm the initial INERIS results. The basic combustibility of graphite dusts was compared with that of graphite, utilizing a simple ceramic ‘boat’ and a muffle furnace. The samples were as follows:

- solid graphite;
- graphite dust in the range of 100–400 μm ;
- graphite dust <45 μm ;
- graphite dust <15 μm ;
- graphite dust (70%) with iron dust (30%), all <45 μm .

The last item was included to mimic the possibility of rupture of a powder-torch hose during cutting of components within the reactor.

In each case, the temperature of the furnace was raised from ambient to 900°C at a rate of 3–4 K.min⁻¹ and the extent of mass loss noted. As these conditions, in an essentially free supply of air, would be expected to result in significant oxidation of bulk graphite, let alone dusts, it is perhaps unsurprising that these materials all suffered significant mass loss, with some 32% loss from the solid graphite, and total oxidation of the samples with particle sizes of 45 μm or less. Just 54% mass loss, however, occurred in the case of the mixture with iron powder, but this could result from total loss of the carbon if the iron is oxidized to Fe₂O₃.

Overall, these test results are unsurprising. A significant oxidation rate was first observed with the dust at a temperature of around 580°C.

CNPP also conducted tests with graphite dust preheated to 850°C, following which they then utilized (i) an oxy-acetylene torch, and (ii) dropping molten metal. The first caused the dust to become suspended and ignite, which is essentially unsurprising, whilst the molten metal had no effect.

With dust at ambient temperature, a sample was then saturated in hydraulic oil following the French absorption standard NF T 90-361. It is to be noted that the reporting of this work in [9] is erroneous, and the correct ratios of oil to graphite are 173:100 by weight for the graphite of 100–400 μm granulometry and 215:100 for that of 45 μm material. Thus, the dusts became aggregated with more than their own mass of oil under the specified conditions (essentially immersion for 20 minutes followed by draining for 30 minutes). The oil-soaked dusts of each of the specified granulometry were then each subjected to the flame of a “camping-gas” burner, and to particles of molten steel produced by a blowtorch, by arc welding and by a grinder. Each of these processes, except for the grinder, produced some ignition of the oil-soaked material. With the camping-gas burner, applied for 30 seconds, it was slow: with the other methods producing molten metal, there was extinction in less than 10 seconds, except for the intermediate particle size (<45 μm) which took up to one minute. The reason for this is not understood. Propagation of the flame beyond its initial area was negligible.

The final test done in this preliminary CNPP work was to inject dusts into a vertical cylinder containing an open flame at the base, in order to compare the behaviour of graphite dusts of various granulometries with that of iron dust and the standard maize flour. The dusts were blown from a 100 g heap in small ‘puffs’ into a cylindrical aperture in the side of the bottom of the cylinder using an air gun. The initial flame height was approximately one third of the height of the cylinder, which was a 60 cm long sleeve with a triangular opening at the base.

There were three thermocouples at different heights within the cylinder. Only the lowest of these recorded changes of significance. From an initial temperature of 670°C, graphite of all three granulometries and the graphite/iron mixture produced a temperature increase to 750°C, whilst iron powder alone produced 800°C and maize flour 900°C. Flames were emitted from the top of the cylinder only with the iron powder and, more significantly, with the flour: graphite/iron, approximately 30 cm in height above the top of the cylinder; iron alone, approximately one metre; and maize flour, 1.2 m.

Whilst these initial CNPP tests do not constitute a suitable matrix of tests to provide an envelope for assessing the behaviour of the graphite dusts comprehensively, they are in accord with the observations from other laboratories. Reference [9] concludes that graphite dusts of fine granulometry

may be inflamed under certain conditions (e.g. oil soaking) and that suspended dust at a concentration of at least 60 g.m^{-3} may be inflamed if a sufficient energy source is present. Nevertheless, the dusts are low in reactivity with air in comparison with iron powder and maize flour.

Phase 2

This second phase of the CNPP work, documented in detail in [10], was itself conducted in two stages. The first covered the development of an opacity methodology for the determination of dust concentration in air, and the second, the utilization of high speed photography to study the propagation of flame fronts in a ‘semi-confined environment’ — a transparent pipe of size comparable to realistic situations likely to be encountered in decommissioning a commercial reactor — essentially with the objective of proving that, even if a major ignition source were present and a suspension of fine graphite dusts occurred, a flame front moving along a pipe of typical plant dimensions would be self-extinguishing. This final study was developed with the recognition that routine studies in equipment such as the ISO vessel, although important, were not directly representative of the conditions to be encountered in reactor decommissioning.

The development of the opacimeter was also conducted in a plexiglass tube, vertically mounted and with a capacity of 200 L as illustrated in Fig. 9.



FIG. 9. CNPP apparatus for the determination of the relationship between opacimeters and graphite dust concentration.

The vertical tube was mounted on a closed plexiglass base and the upper end was closed by a further transparent plate. Graphite dust was introduced by a pulse of air delivered to a reservoir of graphite dust such that it was discharged around a circular tube at the base of the plexiglass tube. The injection system was extremely efficient and the average concentration of dust in the vessel could be calculated accurately. The tube was fitted with an upper and a lower opacimeter, each consisting of opposed light emitters and receivers linked to a simple electronic measurement system. The test allowed the determination of the relationship between the dust concentration and the light transmitted, which is the difference from 100% of the opacity value.

For the opacimeter studies, UCAR graphite grade GS45E⁴ was used to prepare a powder of which 90% was <49.53 μm (30% lay between 25 and 45 μm , 31% between 10 and 25 μm , and 29% <10 μm). The density of the settled but unpacked powder was 0.34 $\text{g}\cdot\text{cm}^{-3}$.

After ‘zeroing’ the output of the opacimeter, the valve was adjusted to blow in the dust, and the gas pressure was maintained for 10 seconds to ensure the best possible mixing of the dust with the air inside the tube. Numerous injections were made, exploring the best separation of the emitters and receivers, which was eventually set at 10 cm for the formal calibration tests. Some systematic differences were observed between the readings of the upper and lower opacimeters, the lower one consistently showing a greater reduction in light transmission than the upper one, indicative of a slightly higher dust concentration in the lower part of the tube, explained in [10] in terms of the mode of dust injection. The maximum recorded relative difference was 27% at a mean dust concentration of 25 $\text{g}\cdot\text{m}^{-3}$. There was also a modest scatter in all data which was, however, not sufficient to obscure this systematic difference. A ‘global’ average of all measurements, including both detectors, was utilized in forming the relationship between concentration and opacity.

The formal calibration utilized dust concentrations of 25, 50, 100 and 150 $\text{g}\cdot\text{m}^{-3}$. At this highest concentration, it was clear that the instrumentation was approaching saturation, and this represents an upper concentration limit for this detector system unless it is possible to place emitter and receiver much closer together. The relationship in Fig. 10 was obtained:

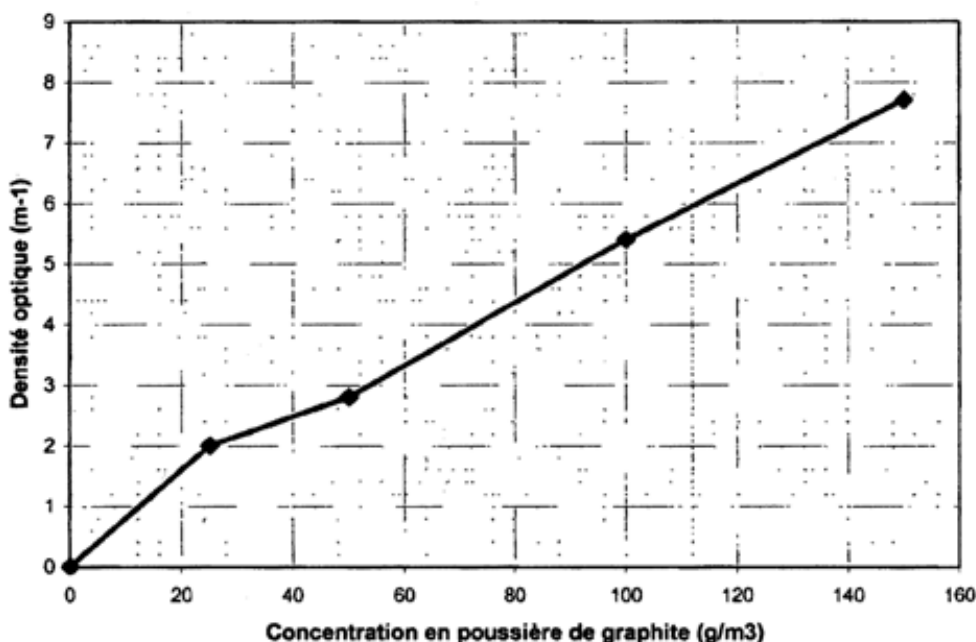


FIG. 10. Opacimeters with 10 cm separation between emitter and receiver: relationship between graphite dust concentration and optical density.

Two opacimeters were incorporated into the design of the large horizontal plexiglass tube used for the major part of the experimental programme as illustrated in Fig. 11.

This tube was a little over 4 m in length, approximately 50 cm in diameter and with an internal volume of 742 L. In this case, a two section dust-injection system was employed to ensure an even distribution of material throughout the tube. In each half of the tube, a metal channel was placed containing evenly distributed graphite dust. Across the top of each channel passed a perforated pipe, the air pulse emitted

⁴ This grade of graphite is not utilized in any French reactor system nor, indeed, in any of the others facing decommissioning in the other nations participating in this comparison. However, this is not regarded as significant in terms of the performance of the dust.

from it blowing downwards onto the channel of graphite dust, rapidly raising a quasi-uniform dust cloud. At one end of the tube was the ignition system, which is discussed below. At the opposite end of the horizontal tube, a pressure-relieving filter system was installed.

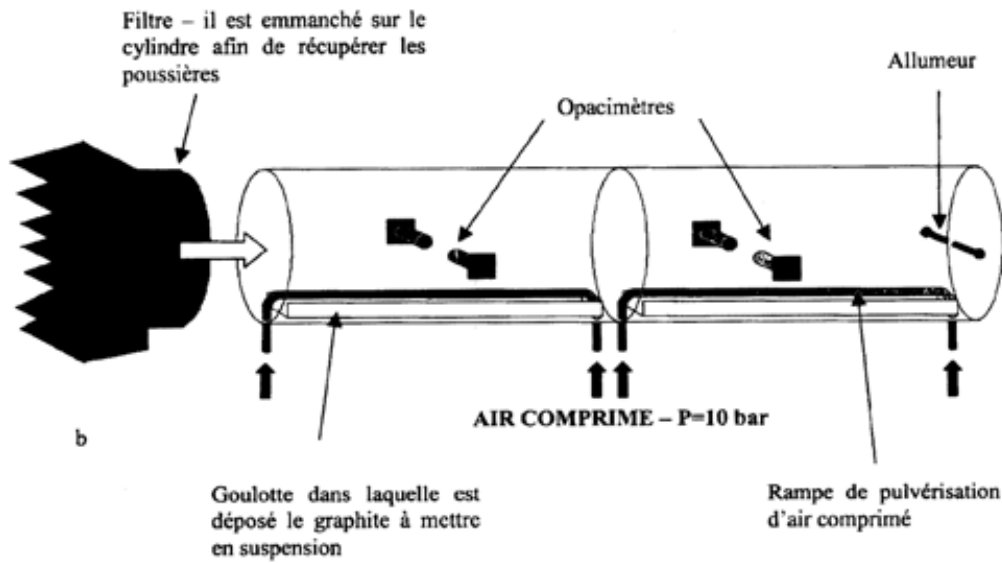


FIG. 11. The CNPP flame-propagation apparatus, showing the position of the igniters ('Allumeur'), graphite-dust channels ('Goulottes'), air-injection system, pressure-relieving filter and opacimeters.

The electrodes consisted of graphite covered with copper at a spacing of 16 cm, disposed 35 cm from the closed end of the plexiglass tube as illustrated in Figs 12 and 13. The arc was initiated between the electrodes with the aid of a fusible silver filament. The arc was driven from a 430 V AC source at 14 kA, for durations of 10, 20 or 30 milliseconds, corresponding to an input of 60, 120 and 180 kJ. Clearly, these energies are much larger than those utilized in the standard ISO test, for example, but were chosen such that the range encompasses three possible accident scenarios: (i) an electrical breakdown in a robotic handling device operating at 410 V and 30 kW; (ii) the same in a remote platform at 75 kW; and (iii) a plasma torch operating at 720 kW and 230 V.



FIG. 12. Detail of gas-injection system and graphite-dust channel.

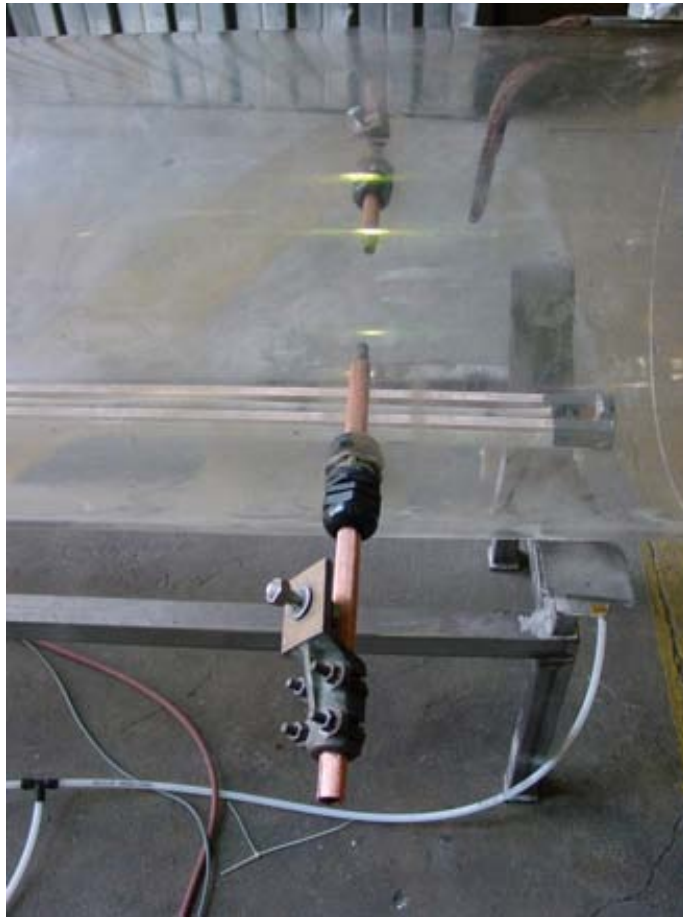


FIG. 13. Detail of electrodes used for ignition.

Indicative measurements of temperature and pressure within the apparatus as illustrated in Fig. 14 were effected in order to allow comparison of the nature of the pressure and temperature waves under different conditions.



FIG. 14. General view of CNPP apparatus in position at Les Renardières.

The progress of each test was recorded using a high speed camera system operating at 250 images per second: this has enabled some remarkable and convincing images of the relative performance of different dusts to be recorded.

A strict protocol was followed between tests. After each one, the apparatus was thoroughly cleaned and wiped out, with removal of all residual powder. The channels were then carefully re-filled with the appropriate amount of powder for the next test. For tests with graphite, this was generally 480 g. A new silver filament was attached to the electrodes, and the length of the tube beyond the electrodes was shielded with a polyester plaque. The filter was replaced if necessary. The opacimeter trajectory was checked to be 10 cm and the zero of optical density re-set.

Next, the voltage, intensity (current) and duration of the required electrical arc were set, the time of air injection to suspend the powder and the interval before ignition were pre-set, and the camera pre-trigger set, such that it would commence recording a few milliseconds before the ignition arc was struck. For the principle tests, 3.5 seconds were allowed for suspension before the arc was triggered, and the air injection was maintained for a further 3.5 seconds.

The apparatus as illustrated in Fig. 15 was initially calibrated with a fine wheat flour, 'Francine Fluide', using a 330 V arc, 5 kA current, a 10 ms arc, four seconds of suspension before striking the arc with the air injection maintained for a further three seconds — 1460 g flour was used (slightly under 2000 g.m^{-3} if all was suspended). In accordance with expectations, the discharge caused ignition of the flour, with propagation along the length of the tube with a pressure pulse sufficient to damage the filter system slightly. A comprehensive video record of this exists to illustrate that the apparatus responds positively to a significant deflagration and propagation of the flame, in any strongly explosible substance.



FIG. 15. Propagation of flame front in wheat flour in the CNPP/Les Renardières test, illustrating the expected performance of the test rig with a 'highly explosible' substance. Here the flame approaches the end of the tube having travelled a distance of approximately four metres.

A point of significance regarding the behaviour of the wheat flour was that the flame gained in intensity as it approached the 'open' end of the tube, indicating that it was receiving a better supply of oxygen at that time and, hence, that there was some oxygen deficiency within the tube during the ignition of the flour. A period of latency took place after the brightness of initial heat subsided: with graphite, this ended with complete extinction, whereas in flour tests it was followed by a renewal of

the combustion. This latency might be associated with a progressive deepening of oxidation within each particle, which was prevented in graphite by high thermal conductivity and lack of volatiles.

The principal results obtained using graphite powder are recorded in Table 4. In each case, a corresponding test utilizing the same ignition parameters was recorded with air alone. This was necessary for comparison purposes because the discharge at the electrodes was sufficient to vaporize some graphite, admixed with copper, to give a visible ball of flame in the vicinity of the electrodes. In the video records of which an example is given in *Appendix*, each image is therefore a composite showing the system at the same elapsed time with and without graphite.

At this stage of the studies, the graphite source was crushed unirradiated fuel-sleeve graphite from batches intended for either the Chinon or St. Laurent reactors.

Table 4. The principal results obtained using graphite powder

Test	Medium	Arc energy (kJ)	Duration of arc (ms)	Duration of incandescence (ms)	Maximum distance travelled by flame (m)
914	Air only	59.5	9.9	80	0.90
915	Air only	62.5	9.8	76	0.83
3006	Graphite	65.2	10.0	156	1.04
3007	Graphite	70.2	10.2	104	1.16
909	Air only	113	19.3	156	1.28
911	Air only	106	19.3	144	1.61
3004	Graphite	110	19.2	156	1.40
3005	Graphite	112	19.3	168	1.17
907	Air only	170	29.4	200	1.35
908	Air only	165	29.4	216	1.66
3002	Graphite	ND	29.4	508	1.91
3003	Graphite	164	29.4	500	2.25

As may be seen, the results are grouped by ignition energy, and shown alongside the corresponding results for air alone. This is an important comparison because the electrodes alone produce significant incandescence due to evaporation and oxidation of the graphite and copper, which moves along the tube. Thus, the results for graphite need to be viewed in comparison with this ‘graphite-free’ equivalent, and three sets of time-lapse photographs shown in the Appendix.

A further point of interpretation of this table is the final column — maximum distance travelled by flame. Generally, the observed flame travels a little further in the presence of the graphite. Since the graphite is oxidizable, and significant energy is initially transferred to the suspended material close to the electrodes, this is not surprising. However, inspection of the visual record then shows clearly that the flame front is slowed, and eventually extinguished with termination of oxidation, in contrast to the behaviour of the wheat flour illustrated earlier.

A final significant point is that the standard concentration of graphite used in the tests — equivalent to 647 g.m^{-3} if suspended with 100% efficiency, which is unlikely — greatly exceeds the measurable range of the opacimeters, from which no usable data were therefore recovered. Indeed, Ref. [10] records that the opacimeters were also an obstacle to combustion and retarded the propagation of the flame, so it was decided to remove them altogether once their unfailing saturation (guaranteeing a concentration of graphite dust in excess of 150 g.m^{-3}) and the general homogeneity of the dust suspension had been confirmed. By definition, this ‘confirmation’ must have been conducted with

a lesser amount of graphite dust. The specific graphite concentration chosen is not adequately explained in [10]. It lies on the shoulder of the ‘peak’ identified by the INERIS study, but not at a sufficiently high level to cover the apparently anomalous high result at 1250 g.m⁻³ which we have already challenged. It is assumed that the chosen concentration provided the best visual records, and this is important: the great value of this test is the absolute confirmation in a ‘real’ situation that a large scale graphite-dust deflagration is self-extinguishing whereas a ‘strongly explosible’ material like wheat flour clearly produced a ‘positive’ result sufficient to blow out the filter⁵ and cause (according to anecdotal reports) ‘a number of little fires’ on the floor area surrounding the apparatus.

It was also noted that the pressure signal was extremely weak, with changes of only a few millibars. Anecdotal remarks indicate a maximum pressure increase of 6.4 mbar for a 115 kJ ignition, accompanied by a sound ‘approximating to 55 Hz’ — in other words, a low-pitched ‘*whoomph*’ rather than a sharp report as from a detonation. Whilst this behaviour would be expected for a deflagration, there is reason to believe that this sound was associated with the destruction of fragments of the electrodes since it occurred in the absence of graphite, this being corroborated by the photographic evidence of the behaviour of graphite dusts within the tube and by its resonance being correlatable with the length of the tube. It was also noted anecdotally that there was no significant temperature change recorded at the surface of the tube in any of the tests.

Three sets of stills from the high speed photography were obtained, each corresponding to one zone of ignition energy from the above Table. The first set compares runs 914 and 3007, the second set 911 and 3005, and the final set 907 and 3002.

In each case, the evidence for the extinguishing of the flame front in the presence of graphite is unequivocal. The stills comparing runs 914 (air only, upper images) and 3007 (with graphite, lower images) are given as an example in the Appendix.

The conclusions of [10] in regard to this interpretation of this work may be summarized as follows:

- The zone of incandescence produced from the electrodes is of the same size in the reference tests with air alone as in the presence of graphite for the same energy input.
- In the presence of a graphite dust suspension, the graphite particles are initially heated by the electric arc and may reach temperatures higher than 1000°C: in opposition to this effect, the presence of the graphite may also suppress somewhat the visible emissions from the electrical arc.
- The incandescence within the graphite dust then expands in volume as a result of the heating (some surface oxidation of the hottest particles also occurs, making a further exothermic contribution, and this contributes to an extension of the duration of the visible incandescence).
- The incandescence within the graphite dust suspension does not produce energy sufficient to compensate for losses through conduction, convection and radiation: in consequence, the dust suspension cools and the incandescence is extinguished — this despite modest blowing of fresh air from beneath.
- Under the conditions of this experiment, there was no deflagration in the graphite dust.

Whilst this experiment, designed to allow reproducible testing conditions, was far from a ‘perfect’ replication of a realistic situation in decommissioning, the inability of such significant energy inputs to create a deflagration gives a large degree of support to the view of the present authors that there is no significant risk of encountering dust-deflagration issues in the course of decommissioning a graphite-moderated reactor.

⁵ In a number of cases, the filter was also blown out in the tests with graphite, presumably through the pressure wave produced from the electrical arc.

5. Conclusions

Extensive test programmes have been conducted by France and the United Kingdom, into the behaviour of nuclear-grade graphite dusts in the presence of an ignition source. These programmes have had common features which offer the chance to obtain independent confirmation of basic 'dust-explosion' parameters on a variety of samples drawn from graphites used in reactors now approaching decommissioning and have included innovative experiments intended at investigating specific practical situations relevant to the decommissioning of graphite-moderated nuclear plant. Account has also been taken of small amounts of relevant data from Italy and Japan.

The results obtained for basic explosion parameters have shown a high degree of conformity, confirming that pure graphite dusts are very weakly explosible under the conditions of an ISO standard or equivalent standard test. These standards require ignition of the material after suspension into a confined and known volume, utilizing chemical igniters of energy typically 10–20 kJ. Previously, such dusts had been reported as 'non-explosible' on the basis of older forms of apparatus employing much weaker ignition sources such as electrical sparks typically in the range of 10–100 J, and there is therefore no inconsistency in this altered definition. Standard methodologies such as the ISO test allow extremely useful comparisons between dusts of different composition but, in order to understand dust behaviour in a practical engineering situation, more sophisticated investigations are appropriate.

Basic 'explosion parameters' for nuclear-grade graphite dusts of the particle size distributions employed in these studies (intended to represent typical distributions of material within the reactor vessels) are as follows: minimum ignition energy: ~2 kJ over a range of practical concentrations; minimum explosible concentration: 60–125 g.m⁻³; maximum explosible concentration: poorly defined but >1500 g.m⁻³; maximum rate of pressure rise in standard test: 118–250 bar.s⁻¹; deflagration index: 14–61 bar.m.s⁻¹ (with the most probable value lying around 45 bar.m.s⁻¹): a value of deflagration index anywhere in this range classifies the material as very weakly explosible.

Additives and impurities generally reduce the potential 'explosibility' of the graphite dust, especially when the impurity is fully oxidized such as metal-oxide residues from other parts of a reactor circuit. Potential catalysts of thermal graphite oxidation, such as lead compounds, have no specific effect because the oxidation of the dust appears to be governed by the available supply of oxygen at the flame front rather than by the chemical kinetics of oxidation at surfaces. An exception to this general observation was iron powder as used in powder-cutting torches: this is extremely reactive as a dust and care needs to be taken to avoid any release into the reactor vessel if such technologies are used in decommissioning.

When a deflagration does occur with graphite dust, a significant amount of the dust remains unburned. UK work has shown that only particles with diameters less than around 5 µm participate in the dust deflagration, larger particles behaving as heat sinks and reducing the potential of the flame front to propagate. The same work also demonstrated that, except in freshly ground samples, smaller particles tend to agglomerate such that, in periods of 30–40 days, the potential reactivity of any sample is greatly reduced. Thus, the presence of fine particles would not be expected in dusts collected within reactors. Moisture also acts to reduce reactivity and to encourage agglomeration.

The behaviour of graphite dust in practical engineering situations has been investigated. These tests demonstrated that secondary explosions involving graphite dust are very difficult to initiate (using a methane-gas explosion as a primary driver), and that, in a pipeline situation with an extremely energetic ignition source (major electrical discharge), the potential deflagration in a suspended graphite-dust cloud was self-extinguishing. The suitability of these experimental configurations to demonstrate this lack of an effect for graphite dust was validated in both cases by substituting reactive maize or wheat flour, which then produced significant deflagrations.

Classically, the following conditions must be satisfied simultaneously in order for a dust explosion to occur:

- (a) The dust must be airborne.
- (b) An ignition source of sufficient energy must be present.
- (c) The dust must be combustible.
- (d) The atmosphere must support combustion.
- (e) The concentration must lie within the explosible range.
- (f) The particle size distribution must be optimized for flame propagation.

To this may be added the additional condition that, for a disruptive explosion to result, there must be confinement. It is clear that, for graphite dust, condition (e) is especially difficult to achieve in a practical decommissioning situation, since particles greater than about 5 µm in diameter tend to act as heat sinks, whilst condition (b) is only attainable with difficulty since the material is only very weakly ‘explosible’. In any practical decommissioning situation, it is relatively easy to ensure that at least one of these conditions is not present.

It is therefore concluded that the ‘risk’ of a dust explosion involving graphite dust during reactor decommissioning is extremely low and should not cause particular concern in planning a decommissioning strategy. It is, of course, prudent to eliminate any potential risk by eliminating one or more conditions from (7) in the course

ACKNOWLEDGEMENTS

G. Andrews, R. Phylaktou, the University of Leeds, UK
 W. Ingamells, M. Cross, for UKAEA, UK
 D. Roubineau, CNPP Vernon, France
 S. Cornet, S. Dupont, EdF R & D, Les Renardières, France
 C. Wood, for The EPRI Graphite Decommissioning Initiative, USA

This paper is published with the permission of UKAEA South (UK) and EdF CIDEN (France)

REFERENCES

- [1] FIELD, P., “Dust Explosions”, Handbook of Powder Technology (WILLIAMS, J.C., ALLEN, T., Eds), Elsevier 4 (1982).
- [2] Schriftenreihe des Hauptverbandes Gewerblich Berufsgenosschaften e.V., “Forschungsbericht Staubexplosionen, Brenn und Explosions Kenngrößen von Stauben”; Bonn (1980).
- [3] ISO 6184-1 “Explosion Protection Systems — Determination of Explosion Indices of Combustible Dusts in Air”, 1985 (also issued as European Standard EN 26184-1 [1991] and British Standard BS 6713-1 [1986] under the title “Explosion Protection Systems: Part 1; Method for Determination of Explosion Indices of Combustible Dusts in Air”); as amended February 1992: ISBN 0 580 15204 9.
- [4] ARNOLD, L., “Windscale 1957: Anatomy of a Nuclear Accident”, Macmillan (1992).
- [5] WICKHAM, A.J., INGAMELLS, W., “Evaluation of the Condition of the Graphite in the Fire-Damaged Zone of Windscale Pile No. 1”, paper presented to ‘Carbon 2006’, Aberdeen UK, July 2006.
- [6] AMARIGLIO, H., DUVAL, X., “Étude de la Combustion Catalytique du Graphite”, Carbon 4 (1966) 623–635.
- [7] S.I. 1769, 1956, “Dust — The Coal Mines (Precautions against Inflammable Dust) Regulations 1956”, Statutory Instrument 1956 No. 1769 (As varied by the Coal Mines (Precautions against Inflammable Dust) (Variation) Regulations 1960, S.I. 1960 No. 1738).
- [8] CARSON, D., “Etude de Risque Incendie-Explosion lié au Graphite UNGG — Caractérisation du Graphite”; INERIS, France, 14 November 2000.
- [9] ROUBINEAU, D., “Première Campagne: Approche Expérimentale: Résultats du Programme d’Essais Graphite EdF-CIDEN”; CNPP Report No. PE 03 6570, 8 January 2004.

- [10] ROUBINEAU, D., “Explosivité des poussières de graphite: Deuxième campagne d’essais concernant le risque incendie et explosion lors du démantèlement des centrales UNGG”; CNPP Report No. PE 03 6570-1, 14 March 2006.
- [11] CEA, “Evaluation de l’oxydation de l’empilement de graphite du réacteur Saint Laurent A1 après 50 ans de confinement”; CEA Technical Note CEA DTA/DIR.92-NT-04, 29th May 1992.
- [12] CEA, “Evaluation des risques de pyrophoricité des poussières de graphite déposées dans les piscines de stockage des chemises de graphite des éléments combustibles des centrales SLA1 et SLA2”; CEA Technical Note CEA DTA/DIR.96-NT-10, 5 January 1996.

Appendix

Stills from the high speed photography employed during the cnpp/edf flame-propagation study at Moret-sur-Loing (“Les Renardières”)

Tests 914 and 3007

For these tests, the ignition energies were 59.5 kJ (914, air only) and 70.2 kJ (3007, with graphite). In each case, the air-only result is the upper photograph. Images were obtained at intervals of 4 ms.







